Received: 13 September 2016 | Revised: 28 February 2017 | Accepted: 10 March 2017

DOI: 10.1002/ajpa.23213

RESEARCH ARTICLE

WILEY American Journal of PHYSICAL ANTHROPOLOGY

Quantification of the position and depth of the *flexor hallucis longus* groove in euarchontans, with implications for the evolution of primate positional behavior

Gabriel S. Yapuncich[1] | Erik R. Seiffert[2] | Doug M. Boyer[1]

[1]Department of Evolutionary Anthropology, Duke University, Durham, North Carolina

[2]Department of Cell and Neurobiology, Keck School of Medicine, University of Southern California, Los Angeles, California

Correspondence
Gabriel S. Yapuncich, Duke University, Department of Evolutionary Anthropology, Box 90383, Durham, NC.
Email: gabrielyapuncich@gmail.com

Funding information
NSF DDIG SBE; Grant numbers: 1028505, BCS 1540421, BCS 1317525, BCS 1231288, BCS 1440742, BCS 1552848, BCS 1440558; Leakey Grant; Wenner-Gren Grant; AAPA Professional Development Grant

Abstract

Objective: On the talus, the position and depth of the groove for the *flexor hallucis longus* tendon have been used to infer phylogenetic affinities and positional behaviors of fossil primates. This study quantifies aspects of the *flexor hallucis longus* groove (FHLG) to test if: (1) a lateral FHLG is a derived strepsirrhine feature, (2) a lateral FHLG reflects inverted and abducted foot postures, and (3) a deeper FHLG indicates a larger muscle.

Methods: We used linear measurements of microCT-generated models from a sample of euarchontans ($n = 378$ specimens, 125 species) to quantify FHLG position and depth. Data are analyzed with ANOVA, Ordinary and Phylogenetic Generalized Least Squares, and Bayesian Ancestral State Reconstruction (ASR).

Results: Extant strepsirrhines, adapiforms, plesiadapiforms, dermopterans, and *Ptilocercus* exhibit lateral FHLGs. Extant anthropoids, subfossil lemurs, and *Tupaia* have medial FHLGs. FHLGs of omomyiforms and basal fossil anthropoids are intermediate between those of strepsirrhines and extant anthropoids. FHLG position has few correlations with pedal inversion features. Relative FHLG depth is not significantly correlated with body mass. ASRs support a directional model for FHLG position and a random walk model for FHLG depth.

Conclusions: The prevalence of lateral FHLGs in many non-euprimates suggests a lateral FHLG is not a derived strepsirrhine feature. The lack of correlations with pedal inversion features suggests a lateral FHLG is not a sufficient indicator of strepsirrhine-like foot postures. Instead, a lateral FHLG may reduce the risk of tendon displacement in abducted foot postures on large diameter supports. A deep FHLG does not indicate a larger muscle, but likely reduces bowstringing during plantarflexion.

KEYWORDS
astragalus, flexor digitorum fibularis, prosimian, strepsirrhine, grasp-leaping, *Eosimias*, *Pondaungia*, *Purgatorius*

1 | INTRODUCTION

Because the talus (=astragalus) serves as the primary mechanical link between the leg and the foot, the bone's morphology strongly constrains a primate's positional behavior. The talus' functional responsibilities include promoting stability while transmitting forces generated by body mass and muscles, as well as permitting mobility at the talotibial, talofibular, talocalcaneal, and talonavicular joints. The bone's compactness and density increase the prevalence of tali in fossil assemblages. This combination of relative abundance and morphological complexity makes the talus a particularly useful skeletal element for generating functional and phylogenetic inferences. Variation in talar morphology has been used to distinguish living and fossil primate groups (Beard, Dagosto, Gebo, & Godinot, 1988; Beard, 1991; Covert, 1988; Dagosto, 1988; Gebo, 1986a, 1986b; Gebo, 1988; Gebo, 1993; Gebo, Dagosto, Beard, & Qi, 2001; Gebo, 2011; Lewis, 1980a,b,c; Morton, 1922,

1924), as well as to infer positional behaviors in fossil taxa (Boyer and Seiffert, 2013; Boyer, Seiffert, & Simons, 2010; Boyer, Yapuncich, Butler, Dunn, & Seiffert, 2015; Dagosto, 1983; Dunn et al., 2016; Gebo and Simons, 1987; Gebo, 1988; Gebo, Dagosto, Beard, & Ni, 2008; Gebo, Dagosto, Beard, Qi, & Wang, 2000; Gebo, Dagosto, & Rose, 1991; Gebo, Smith, & Dagosto, 2012; Marigó, Roig, Seiffert, Moyà-Solà, & Boyer, 2016; Marivaux et al., 2010; Marivaux et al., 2011; Seiffert and Simons, 2001; Seiffert, Costeur, & Boyer, 2015;).

Despite the extensive use of talar morphology in studies of primate evolution, many distinguishing features of the talus have rarely been put into a quantitative comparative framework (Boyer and Seiffert, 2013; Boyer et al., 2010; Boyer et al., 2015; Dagosto, 1988; Gebo, 2011; Rose, Chester, Dunn, Boyer, & Bloch, 2011). Further development of and increased access to new technologies such as micro-computed tomography (μCT), three-dimensional (3D) digital models, and online databases of digital surface models such as Morphosource.org (Boyer, Gunnell, Kaufman, & McGeary, 2017) have greatly augmented contemporary researchers' abilities to generate comprehensive comparative datasets and to quantify complex morphological features. For example, Boyer and Seiffert (2013) quantified the slope of the fibular facet in living and extinct primates, and revealed previously unappreciated variation within strepsirrhines and the earliest euprimates. Boyer et al. (2015) examined the size and shape of the medial tibial facet, confirming the dichotomous morphology of these features in "prosimians" and anthropoids, thereby garnering more evidence for the mechanical relationship between the relative size of this facet and the use of inverted foot postures.

The position of the groove for the tendon of the *flexor hallucis longus* (=*flexor digitorum fibularis*)[1] muscle, a plantarflexor of the foot and flexor of the digits (Gebo, 1993; Grand, 1967; Langdon, 1990), is another talar feature used to determine phylogenetic affinities of fossil primates, and to make inferences about their positional behaviors. Figure 1 highlights the paths of the tendons of three deep extrinsic plantarflexors of the foot (*flexor hallucis longus*, *flexor digitorum longus*, and *tibialis posterior*) and the position of the FHLG in *Nycticebus coucang* (DLC 1998f). The major goals of this study are similar to recent quantitative analyses of other prominent talar features (Boyer and Seiffert, 2013; Boyer et al., 2015): to quantify variation in *flexor hallucis longus* groove (FHLG) position and depth with digital models of tali representing a comprehensive sample of extant and extinct fossil euarchontans. Precise data on the variation of these features among euarchontans permits reassessment of their functional and phylogenetic significance, broadscale evolutionary patterns, and their correlations with other quantified talar features (e.g., orientation of the fibular facet and size and shape of the medial tibial facet).

The position of the groove for the tendon of *flexor hallucis longus* has most frequently been argued to distinguish extant strepsirrhines and adapiforms from extant haplorhines and omomyiforms (Beard et al., 1988; Dagosto, 1988; Gebo, 1986a, 1988, 1993, 2011). For extant haplorhines and omomyiforms, Gebo (1986a) states that "the flexor hallucis longus groove on the posterior trochlea lies in a midline position," while extant strepsirrhines and adapiforms, the groove's "position is lateral to the posterior trochlear [lateral tibial] facet" (pg. 424).

While initial morphological descriptions emphasized that the FHLG is lateral to the *posterior* trochlea in strepsirrhines and adapiforms (Beard et al., 1988; Covert, 1988; Dagosto, 1988; Gebo, 1988), subsequent researchers occasionally elide over this detail. For example, Kay, Ross, & Williams (1997) note the "lateral positioning of the groove for the flexor fibularis" (pg. 799) in strepsirrhines and adapiforms, and then state that "haplorhine features of the tali are a centrally positioned flexor hallucis groove and steep-sided talo-fibular facet" (pg. 801). The sporadic omission of what feature the FHLG is lateral to is important to highlight, as it alters interpretations of the groove's position. In extant strepsirrhines and adapiforms, the lateral tibial facet (LTF) runs at an angle across the posterior talus, so that the facet's dorsal aspect is lateral to its posterior or proximal aspect. This morphology is well illustrated by Dagosto et al. (2010; their Figure 4). In these cases, the FHLG may be in a midtrochlear position with respect to the dorsal aspect of the LTF, but the groove remains lateral to the LTF on the posterior aspect of the talar body. We developed our measurements for this study to reflect the original description of the position of the FHLG relative to the articular surface on the posterior part of the talus (see Methods).

1.1 | Functional considerations of FHLG position and depth

As with the slope of the fibular facet and the size and shape of the medial tibial facet, the predominant biomechanical explanation for observed variation in FHLG position has been distilled from the unique foot postures of strepsirrhines (Boyer and Seiffert, 2013; Boyer et al., 2015; Dagosto, 1983; Gebo, 1986a, 1993, 2011). Specifically, the lateral placement of the FHLG may facilitate frequent use of inverted and/or abducted foot postures on small-diameter and vertically oriented supports by maintaining the alignment of the FHLG and the tendon of the *flexor hallucis longus* (Gebo, 1986a, 1993). Gebo (2011, p. 325) summarized this proposed functional relationship:

> The mid-trochlear position of this groove [in haplorhines] suggests a foot posture that is less vertical oriented since an abducted, inverted grasping foot on a vertical substrate would place this tendon oblique to the lower leg and the flexor hallucis longus muscle . . . For strepsirrhines, an inverted foot grasping a vertical support maintains a straight path for this tendon from the lower leg to the foot making a lateral placement for the flexor groove advantageous in a vertical foot placement.

For primates, grasping a small-diameter and vertically oriented support with the foot requires a particular arrangement of multiple hind limb segments. In this posture, the thigh is flexed and abducted, the anatomical leg is flexed, rotated laterally and adducted, and the foot is dorsiflexed, inverted and abducted (Gebo, 1986a, 2011; Grand, 1967; see Boyer et al., 2015, their Figure 1). This configuration places the plantar surface of the foot in contact with the substrate, and allows

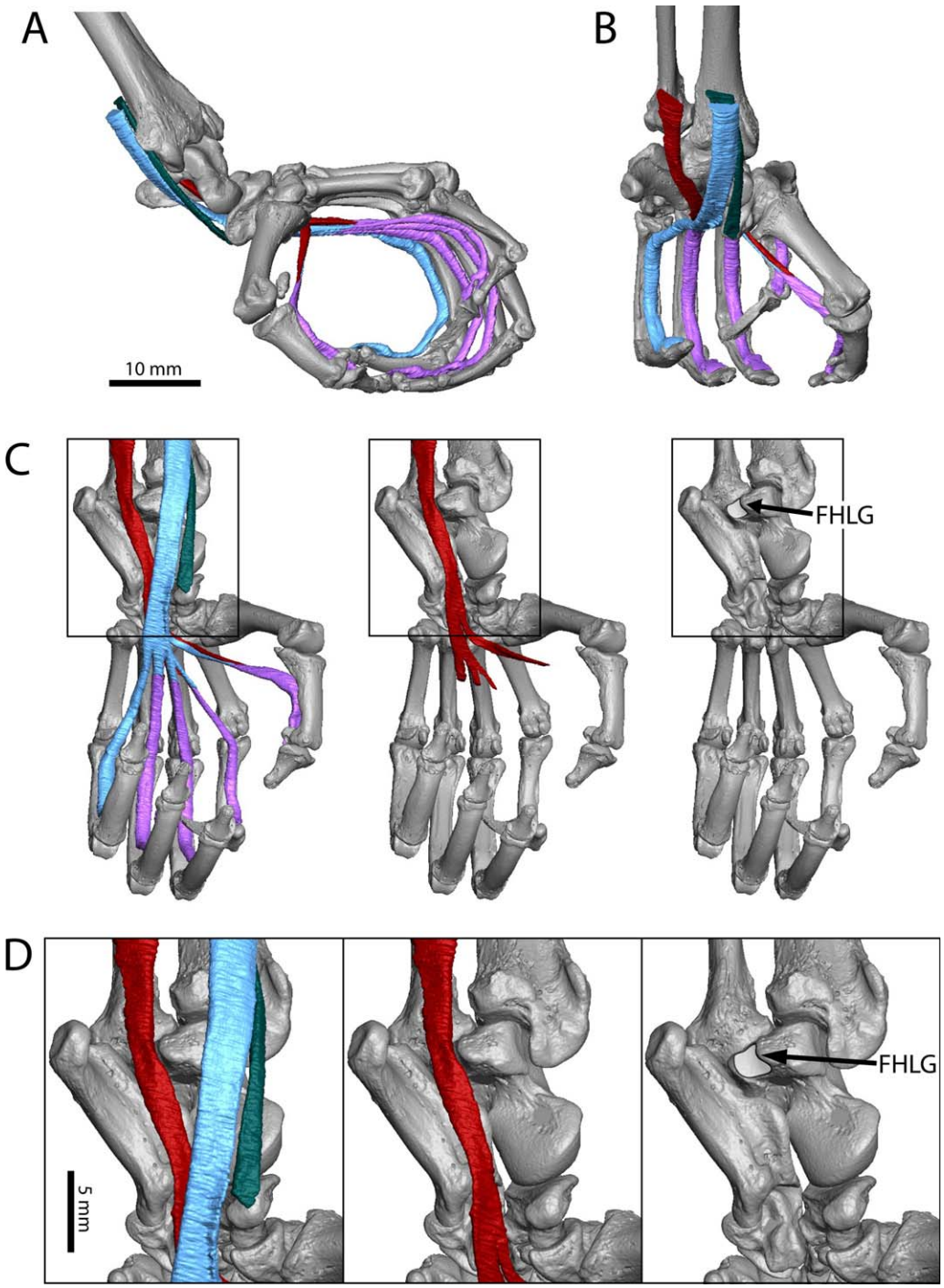

FIGURE 1 Tendons of the deep extrinsic plantarflexors in the foot of *Nycticebus coucang* (DLC 1998f). *Flexor hallucis longus* in red, *flexor digitorum longus* in light blue, and *tibialis posterior* in dark blue. Common tendons of *f. hallucis longus* and *f. digitorum longus* are shown in purple. Note that *f. hallucis longus* does not send a tendon to digit 5. (a) medial view; (b) posterior view; (c) plantar views with all three tendons (left), only *f. hallucis longus* (center), and groove for *f. hallucis longus* highlighted; and (d) close-up of three plantar views

oppositional forces generated by both hind limbs to support the animal's body mass (Gebo, 1986a). Under the alignment hypothesis detailed above, the laterally positioned FHLG observed among strepsirrhines (Figure 2a) provides a more direct path of the tendon of *flexor hallucis longus* around the posterolateral aspect of the talus. In anthropoids, infrequent use of small-diameter vertical supports likely reduces reliance on inverted and abducted foot postures (Boyer and Seiffert, 2013; Boyer et al., 2015; Gebo, 2011; Szalay and Dagosto, 1988), and thus permit a midtrochlear FHLG (Figure 2b) to maintain the position of the tendon. Finally, although tarsiers exhibit a midtrochlear FHLG (Figure 2c) and frequently do use small-diameter vertical supports (Niemitz, 1984; Roberts and Cunningham, 1986), several authors have

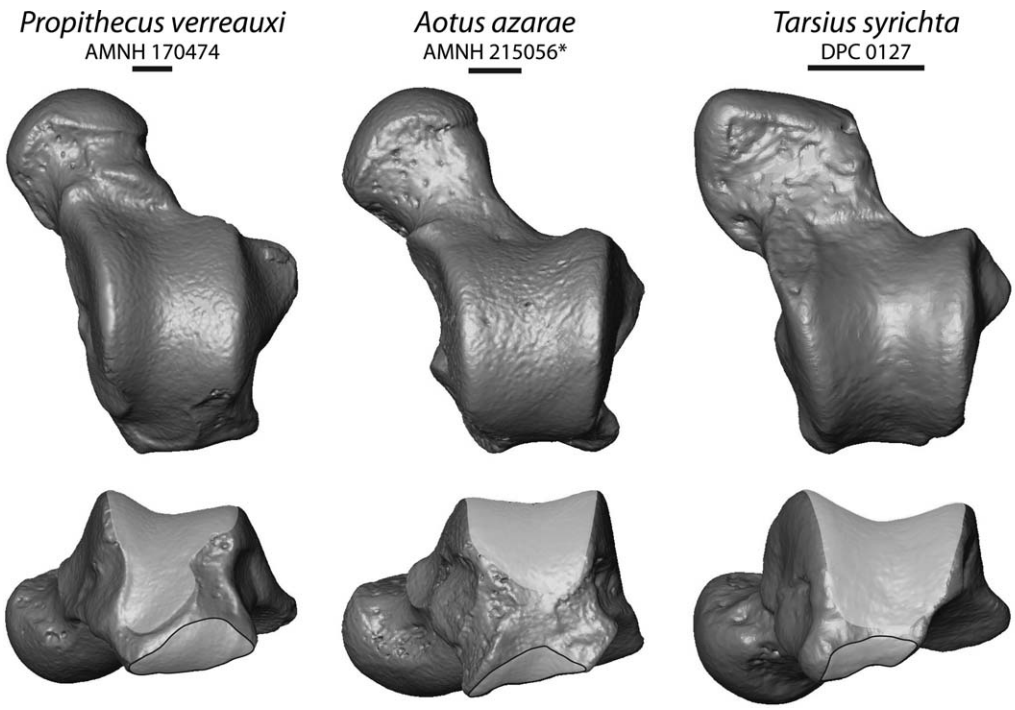

FIGURE 2 Examples of *flexor hallucis longus* groove morphology in a strepsirrhine and two haplorhine species. The lateral tibial facet is shaded; the FHLG is outlined. Views are dorsal (top) and posterior (bottom). Scale bars equal 2 mm. * indicates chirality has been reversed for consistency

argued that tarsiers have a unique suite of myological and osteological features that facilitate this positional behavior (e.g., Day and Iliffe, 1975; Gebo, 1987a, 2011; Jouffroy, Berge, & Niemitz, 1984). This alternative suite of features may provide explanation for the midtrochlear FHLG observed among tarsiers.

Beyond the groove's position, the size (anteroposterior depth and mediolateral breadth) of the FHLG has been linked to increased specialization for pedal grasping in primates (Chester, Bloch, Boyer, & Clemens, 2015; Seiffert et al., 2015; Szalay and Decker, 1974; Szalay and Drawhorn, 1980). Szalay and Decker (1974) noted the FHLG (on both the talus and the calcaneus) was relatively deeper in paromomyid plesiadapiforms compared to more basal eutherian taxa such as *Protungulatum* and *Procerberus*: "One cannot but infer that this flexor of the digits and plantar flexor of the foot might have been relatively more important in the earliest primates than in the known Cretaceous Eutheria, and/or there were movements performed tending to upset its alignment maintained by the groove." (p. 237). Similarly, the oldest known primate, *Purgatorius*, and micromomyid plesiadapiforms have "very large and mediolaterally wide" FHLGs, a morphology consistent with the expanded origination areas for the muscle on the fibula (Chester et al., 2015; p. 1490). For Szalay and Decker (1974) and Chester et al. (2015), the relative width and depth of the FHLG (presumably with consideration for the overall size of the talus) indicates a relatively larger *flexor hallucis longus*, which in turn suggests increased reliance on postures that require strong flexion of the pedal digits (though not necessarily hallucal grasping[2]). Finally, measuring FHLG depth in a sample of living and extinct strepsirrhines, Seiffert et al. (2015) proposed a link specifically between groove depth and strong pedal grasping in diverse foot postures; their results demonstrated that slow climbers and other species that engage in hind limb suspension have deeper FHLGs than leapers and more generalized pronograde quadrupeds.

1.2 | Evolutionary considerations of FHLG position

On the basis of comparisons to other eutherian mammals, researchers initially proposed that a laterally positioned FHLG was a derived condition that united extant strepsirrhines and adapiforms (Beard et al., 1988; Covert and Williams, 1994; Dagosto, 1988; Gebo, 1986a, 1988; Gebo et al., 1991; Kay et al., 1997). A midtrochlear FHLG was initially observed among euprimate outgroups, including scandentians, dermopterans, and plesiadapiforms (Beard et al., 1988; Gebo, 1986a, 1988).

This "classic" interpretation can be found in more recent publications as well. Gebo et al. (2008; p. 1001) affirm that a talus attributed to the adapiform *Adapoides* "has both of the classic strepsirhine talar characters: a laterally sloping talofibular facet and an offset posterior trochlear flexor hallucis longus groove." Describing the talar morphology of the asiadapids *Asiadapis* and *Marcgodinotius*, Rose et al. (2009; p. 397) note "The sloping fibular facet and offset flexor sulcus [=FHLG] present in the Vastan tali also indicate adapoid (and probably strepsirrhine) affinities." The talus of *Afradapis* "exhibits a number of features that are observable in crown strepsirrhines and adapiform primates, including a groove for the tendon of the flexor fibularis that is proximolaterally positioned" (Boyer et al., 2010; p. 389). Marivaux et al. (2011; p. 452) describe two species of azibiids as displaying "a suite of derived morphological characteristics, which are otherwise found only in adapiforms and strepsirrhines. These features include. . .a lateral position on

the posterior trochlea of the groove for the *flexor hallucis longus* muscle." In the adapiform *Caenopithecus*, "the proximal tapering of the [lateral tibial] facet allows for a capacious groove for the tendon of the flexor fibularis muscle, which is situated lateral to the lateral tibial facet, as in all known adapiforms and crown strepsirrhines" (Seiffert et al., 2015; p. 15). In all of these studies, a laterally positioned FHLG is used to diagnose strepsirrhine affinities of fossils, implying that the FHLG is a strepsirrhine synapomorphy.

Despite the prevalence of the classic interpretation, there have been alternative interpretations of the primitive and derived conditions of FHLG position. Because of the lateral position of the FHLG in paromomyid plesiadapiforms and dermopterans, Beard (1991) suggested a lateral FHLG as a synapomorphy of Primatomorpha (Primates + Dermoptera); the lateral FHLG position in paromomyids and dermopterans was further emphasized by Dagosto and Gebo (1994). If the lateral position of the FHLG is indeed primitive for euprimates, then a midtrochlear FHLG could potentially support the monophyly of omomyiforms, tarsiers, and anthropoids. To assess the phylogenetic affinities of isolated haplorhine tarsals attributed to *Eosimias* from the middle Eocene Shanghuang fissure fillings in China, Gebo et al. (2000) performed cladistic analysis of 11 tarsal characters, and revised the classic interpretation of FHLG position, by proposing a midtrochlear FHLG was instead a synapomorphy of Haplorhini (along with increased distal length of the calcaneus, relatively short heel, and a steep-sided talofibular facet with a plantar lip). Gebo et al. (2001) included more isolated Shanghuang tarsals attributed to haplorhines, repeated the analyses, and came to a similar conclusion regarding the polarity of FHLG position.

Both analyses by Gebo et al. (2000, 2001) utilize a composite outgroup, consisting of character states shared by scandentians, dermopterans, and plesiadapiforms. FHLG position is coded as "lateral to trochlea" in the outgroup (Gebo et al., 2001; their Table 12), and the authors state "these taxa differ insignificantly in the expression of these tarsal traits" (Gebo et al., 2001; p. 105). However, there is considerable variation in how FHLG position has been described in these taxa, particularly among plesiadapiforms. Initial descriptions noted that *Plesiadapis* had a midtrochlear FHLG position (Gebo, 1986a), and that "converting the foot bones of *Plesiadapis* into those of *Cantius*" would require several modifications, including shifting "the position of the flexor hallucis longus groove on the posterior talar trochlea" (Gebo, 1988; p. 35). Dagosto (1988; p. 48) stated that "plesiadapiforms exhibit a range of morphologies" for FHLG position: in *Plesiadapis tricuspidens*, the groove is lateral and plantar on the posterior trochlea, while in *Nannodectes gidleyi*, the groove is primarily plantar. As noted above, Beard (1991) and Dagosto and Gebo (1994) noted the lateral FHLG position of paromomyids and dermopterans. The described diversity in FHLG position among euprimate outgroups is difficult to reconcile with the assertion that FHLG position of dermopterans, scandentians, and plesiadapiforms differs "insignificantly" (Gebo et al., 2000, 2001), and underscores the importance of quantifying the feature in a more comprehensive sample.

The description of NMMP 39, an isolated talus from the Pondaung Formation of Myanmar and now tentatively attributed to *Pondaungia*, by Marivaux et al. (2003) provides an excellent example of the ambiguity regarding the polarity of FHLG position. We focus on this study not to highlight particular flaws, but rather to demonstrate the pervasiveness of the classic interpretation of FHLG position (Beard et al., 1988; Gebo, 1986, 1988) despite more recent reinterpretations (Gebo et al., 2000, 2001). Marivaux et al. (2003; p. 13177) state that "all known Eocene adapiforms have a derived talar morphology" that includes "a flexor fibularis groove that is laterally positioned on the trochlea," and that NMMP 39 "lacks these adapiform talar synapomorphies." The authors then argue that although certain talar features exhibited by anthropoids (including a midtrochlear FHLG) would seem to represent the ancestral euprimate condition, "because they occur in most likely outgroups to Primates (Scandentia, Dermoptera, and Plesiadapiformes)," these features are in fact reversals from the primitive primate condition, since Gebo et al. (2001) "clearly establish[ed] that these tarsal characteristics are actually anthropoid apomorphies" (Marivaux et al., 2003, p. 13177). However, Gebo et al. (2000, 2001) only suggested a dorsally limited talocrural facet as an anthropoid apomorphy. Both a steep-sided talofibular facet and a midtrochlear FHLG position were interpreted as haplorhine synapomorphies (Gebo et al., 2000, 2001) as these features are observed in omomyiforms, tarsiers, and anthropoids. To maintain the classic interpretation of FHLG position (i.e., a lateral FHLG position is a derived strepsirrhine feature and that euprimate outgroups exhibit a midtrochlear FHLG), Marivaux et al. (2003) have to make the difficult argument that lateral and midtrochlear FHLG positions are both derived morphologies (in strepsirrhines and anthropoids respectively).

Marivaux et al. (2003) conducted their own phylogenetic analysis with a matrix largely based on that of Gebo et al. (2000, 2001), adding one new character (development of the medial cotylar fossa) and four new taxa (*Proteopithecus*, *Catopithecus*, *Aegyptopithecus*, and NMMP 39). A composite of scandentians, dermopterans, and plesiadapiforms was again used as the outgroup, but the FHLG position for the outgroup was recoded from "lateral to trochlea" (as in Gebo et al., 2000, 2001) to "central to trochlea" (Marivaux et al., 2003; their Table 2). This character change complicates the claim that a midtrochlear FHLG position is a derived anthropoid character that can reveal shared evolutionary history exclusive to anthropoids and amphipithecids, since a midtrochlear FHLG is shared by anthropoids, omomyiforms, NMMP 39, and the composite outgroup. In this case, it would seem more parsimonious to interpret the midtrochlear FHLG position as a retention of the ancestral euarchontan condition.

1.3 | Hypotheses and predictions

Despite its frequent reference in studies of primate talar morphology, there is a large amount of ambiguity surrounding the functional and evolutionary significance of the position of the FHLG. Some of the confusion likely stems from an apparent lack of consensus on the morphological condition in euprimate outgroups, which have been described as exhibiting both midtrochlear FHLGs (Gebo, 1986a, 1988; Marivaux et al., 2003) and laterally positioned FHLGs (Beard, 1991; Dagosto, 1988; Dagosto and Gebo, 1994; Gebo et al., 2000, 2001). If

some euprimate outgroups do exhibit laterally positioned FHLGs, then the predominant functional explanation for the feature—alignment of the groove and the tendon of the *flexor hallucis longus* in inverted and abducted foot postures—becomes less plausible, since no euprimate outgroup has been suggested or observed to utilize strepsirrhine-like pedal grasping on small-diameter and vertically oriented supports. Many researchers continue to treat a laterally positioned FHLG as a synapomorphy of strepsirrhines (Boyer et al., 2010; Gebo et al., 2008; Marivaux et al., 2011; Rose et al., 2009; Seiffert et al., 2015), but, as mentioned above, arguments have been made that a midtrochlear FHLG is derived in haplorhines (Gebo et al., 2000, 2001) or in anthropoids (Marivaux et al., 2003).

There has been less discussion of the phylogenetic significance of the depth of the FHLG, but the feature has been functionally linked to increased reliance on pedal (not necessarily hallucal) grasping (Bloch, Silcox, Boyer, & Sargis, 2007; Chester et al., 2015; Seiffert et al., 2015; Szalay and Decker, 1974; Szalay and Drawhorn, 1980). A deeper groove may accommodate a relatively larger tendon (presumably attached to a relatively larger *flexor hallucis longus*) or prevent the tendon from slipping out of the FHLG. Though these functional interpretations of FHLG depth are intuitively appealing, they have not been tested with broad euarchontan-wide comparative datasets, thorough quantification, and modern phylogenetic comparative methods.

Our hypotheses and predictions for the position and depth of the FHLG are the following:

H1. The strepsirrhine-like FHLG position of adapiforms is a synapomorphy reflecting behavioral changes along the strepsirrhine stem lineage [i.e., the "classic" interpretation of FHLG polarity originally suggested by Gebo (1986a, 1988) and Beard et al. (1988)].

P1a. FHLG positions of stem primates (plesiadapiforms) will differ from those of strepsirrhines.

P1b. FHLG positions of extant primate outgroups (dermopterans and scandentians) will differ from those of strepsirrhines.

H2. Adapiforms utilized substrates more like living strepsirrhines, whereas early anthropoids utilized substrates more typical of living anthropoids.

P2a. Adapiforms will exhibit FHLG positions similar to those of extant strepsirrhines.

P2b. Fossil anthropoids will exhibit FHLG positions similar to those of extant anthropoids.

H3. Because of habitually abducted and inverted foot postures, strepsirrhines have more laterally positioned FHLGs than haplorhines (Gebo, 1986a, 1988, 2011).

P3a. As fibular facet angle may indicate habitual inversion of the foot (Boyer and Seiffert, 2013), FHLG position will correlate with fibular facet angle.

P3b. As the size and shape of the medial tibial facet (MTF) may also indicate habitual inversion of the foot (Boyer et al., 2015), FHLG position will correlate with MTF size and shape.

P3c. Because larger-bodied euarchontans may more frequently encounter relatively small substrates that require more highly abducted and inverted foot postures (Boyer and Seiffert, 2013; Dagosto, 1988; Toussaint, Herrel, Ross, Auard, & Pouydebat, 2015), there will be a significant relationship between body mass and FHLG position. FHLGs will be more laterally positioned among large-bodied euarchontans.

H4. FHLG depth is associated with an increased reliance on pedal grasping. Increased groove depth permits the passage of a tendon of a relatively larger *flexor hallucis longus* (Bloch et al., 2007; Chester et al., 2015; Szalay and Decker, 1974; Szalay and Drawhorn, 1980).

P4. Provided *flexor hallucis longus* follows the same slight positive allometric pattern recovered by Muchlinski, Snodgrass, & Terranova (2012) for overall muscle mass in primates, FHLG depth will correlate with body mass (i.e., larger taxa should have deeper grooves).

2 | MATERIALS

2.1 | Sample

The sample for this study largely overlaps with the samples used by Boyer and Seiffert (2013) and Boyer et al. (2015). Because of the variable preservation of the margins of the FHLG in fossil specimens, this study's sample differs slightly from that of Boyer et al. (2015). In total, we included 378 individuals representing 125 extant and extinct euarchontan species (Tables 1 and 2). Our fossil sample is comprehensive with respect to previous perspectives on FHLG including all plesiadapiforms discussed by previous authors, as well as a diverse sample of omomyiforms and adapiforms, the enigmatic NMMP 39 (*Pondaungia*?), *Eosimias*, and subfossil lemuriforms.

All FHLG measurements were taken on 3D digital surface models (all available on Morphosource.org), which were created with a variety of scanning modalities (associated with each specimen on Morphosource.org). The majority of the sample was CT-scanned at Stony Brook University (using a ScancoMedical VivaCT 75 scanner, a ScancoMedical μCT40 scanner, or a medical CT scanner), at the Microscopy and Imaging Facility of American Museum of Natural History (Phoenix v/tome/x s240), at the Shared Microscopy and Instrumentation Facility of Duke University (Nikon XTH 225 CT), or at the Institut des Sciences de l'Evolution de Montpellier (SkyScan in vivo 1076). Specimens of *Nasalis*, *Gorilla*, *Pan*, and *Pongo* were scanned at the Ohio University μCT Facility with a GE eXplore Locus SP machine. Most specimens were scanned at a resolution of 39 microns or less, though the highest resolutions were 3–5 μm for the smallest fossil specimens. Some 3D models were generated using a Cyberware 3D laser scanner, including *Homo* (from New York medical collection at AMNH), *Hoolock*, and one *Symphalangus* (AMNH 106584).

2.2 | Institutional abbreviations

AMNH, American Museum of Natural History, New York, NY; CGM, Egyptian Geological Museum, Cairo, Egypt; DLC, Duke Lemur Center, Durham, NC; DPC, Duke Lemur Center Division of Fossil Primates,

TABLE 1 Mean computed indices, standard deviations (SD), and ranges for extant taxa

Taxon	*n*	FHLG Position	SD	Range	FHLG Ellipse	SD	Range
Hominidae							
Gorilla gorilla	5	−0.86	0.07	−0.97, −0.79	0.98	0.19	0.75, 1.20
Homo sapiens	5	−0.91	0.09	−1.03, −0.80	0.94	0.27	0.53, 1.18
Pan troglodytes	6	−0.72	0.08	−0.83, −0.60	1.00	0.20	0.77, 1.33
Pongo pygmaeus	5	−0.84	0.10	−0.94, −0.71	0.68	0.17	0.51, 0.94
Hylobatidae							
Hoolock hoolock	7	−0.80	0.06	−0.88, −0.71	1.72	0.36	1.35, 2.38
Hylobates lar	7	−0.73	0.09	−0.90, −0.60	1.30	0.42	0.70, 1.94
Symphalangus syndactylus	2	−0.64	0.07	−0.69, −0.59	1.48	0.38	1.28, 1.82
Cercopithecoidea							
Macaca fascicularis	4	−0.85	0.07	−0.91, −0.77	1.34	0.28	1.00, 1.64
Macaca nemestrina	4	−0.76	0.07	−0.82, −0.67	1.38	0.16	1.19, 1.56
Nasalis larvatus	4	−0.85	0.17	−1.06, −0.71	1.69	0.28	1.37, 2.06
Presbytis melalophos	1	−1.06	–	–	1.53	–	–
Trachypithecus cristata	3	−0.86	0.03	−0.89, −0.83	1.27	0.04	1.24, 1.31
Trachypithecus obscurus	1	−0.79	–	–	1.31	–	–
Platyrrhini							
Alouatta caraya	6	−0.73	0.03	−0.79, −0.69	0.77	0.40	0.43, 1.49
Ateles belzebuth	1	−0.80	–	–	1.30	–	–
Ateles fusciceps	1	−0.82	–	–	1.02	–	–
Ateles geoffroyi	4	−0.81	0.09	−0.90, −0.71	1.32	0.16	1.19, 1.52
Brachyteles arachnoides	1	−0.73	–	-	0.77	–	–
Lagothrix lagotricha	5	−0.76	0.05	−0.81, −0.68	0.41	0.31	−0.08, 0.64
Callitrichinae							
Callimico goeldii	6	−0.82	0.03	−0.89, −0.80	0.79	0.10	0.64, 0.90
Callithrix jacchus	4	−0.80	0.07	−0.90, −0.73	0.19	0.09	0.06, 0.26
Callithrix penicillata	2	−0.85	0.00	−0.85	0.01	0.11	−0.07, 0.08
Callithrix pygmaea	6	−0.73	0.08	−0.85, −0.67	0.12	0.24	−0.07, 0.47
Leontopithecus rosalia	4	−0.75	0.04	−0.78, −0.69	0.36	0.04	0.31, 0.41
Saguinus midas	3	−0.82	0.05	−0.88, −0.79	0.11	0.07	0.05, 0.19
Saguinus mystax	2	−0.71	0.02	−0.73, −0.70	0.35	0.26	0.19, 0.56
Saguinus oedipus	1	−0.71	–	–	0.68	–	–
Cebinae							
Aotus azarae	2	−0.71	0.00	−0.71, −0.70	1.23	0.37	1.00, 1.53
Aotus infulatus	1	−0.77	–	–	1.45	–	–
Aotus nancymaae	1	−0.71	–	–	0.86	–	–
Aotus trivirgatus	2	−0.73	0.08	−0.78, −0.67	1.02	0.19	0.90, 1.17
Cebus apella	6	−0.73	0.06	−0.80, −0.66	1.30	0.22	1.06, 1.57

(Continues)

TABLE 1 (Continued)

Taxon	*n*	FHLG Position	SD	Range	FHLG Ellipse	SD	Range
Saimiri boliviensis	4	−0.76	0.04	−0.81, −0.73	1.16	0.26	0.98, 1.55
Saimiri sciureus	2	−0.76	0.00	−0.76	1.25	0.32	1.06, 1.51
Pithecinae							
Cacajao calvus	3	−0.76	0.01	−0.78, −0.76	0.99	0.25	0.85, 1.29
Callicebus donacophilus	3	−0.76	0.03	−0.79, −0.74	1.17	0.26	0.94, 1.46
Callicebus moloch	3	−0.75	0.04	−0.80, −0.72	1.09	0.37	0.76, 1.50
Chiropotes sp.	4	−0.73	0.04	−0.78, −0.69	0.50	0.12	0.35, 0.63
Pithecia sp.	3	−0.75	0.03	−0.77, −0.73	0.64	0.30	0.43, 0.98
Tarsiidae							
Tarsius bancanus	2	−0.85	0.01	−0.85, −0.84	1.02	0.17	0.90, 1.15
Tarsius syrichta	4	−0.85	0.02	−0.87, −0.82	1.13	0.37	0.65, 1.37
Tarsius tarsier	2	−0.76	0.06	−0.81, −0.72	0.74	0.10	0.67, 0.81
Cheirogaleiidae							
Cheirogaleus major	1	−0.18	–	–	1.03	–	–
Cheirogaleus medius	3	−0.13	0.06	−0.18, −0.06	0.80	0.09	0.73, 0.90
Microcebus griseorufus	10	−0.18	0.13	−0.47, 0.02	1.34	0.37	1.13, 2.08
Mirza coquereli	2	−0.48	0.19	−0.62, −0.35	1.34	0.10	1.27, 1.42
Phaner furcifer	3	−0.47	0.10	−0.56, −0.36	1.00	0.22	0.79, 1.24
Lepilemuridae							
Lepilemur mustelinus	6	−0.45	0.12	−0.60, −0.32	2.07	0.48	1.56, 2.60
Daubentoniidae							
Daubentonia madagascariensis	3	−0.40	0.07	−0.47, −0.34	0.98	0.13	0.91, 1.14
Indriidae							
Avahi laniger	3	−0.29	0.16	−0.47, −0.18	2.56	1.94	1.90, 5.51
Indri indri	3	−0.37	0.12	−0.50, −0.26	1.53	0.46	1.15, 2.06
Propithecus diadema	1	−0.34	–	–	1.67	–	–
Propithecus verreauxi	7	−0.34	0.06	−0.43, −0.23	2.57	0.57	1.90, 3.32
Lemuridae							
Eulemur albifrons	1	−0.41	–	–	1.70	–	–
Eulemur collaris	3	−0.44	0.11	−0.50, −0.31	1.49	0.15	1.41, 1.68
Eulemur fulvus	3	−0.43	0.07	−0.51, −0.38	1.30	0.16	1.19, 1.48
Eulemur mongoz	2	−0.49	0.01	−0.50, −0.49	1.09	0.09	1.03, 1.16
Hapalemur griseus	3	−0.44	0.07	−0.51, −0.38	1.46	0.17	1.30, 1.63
Lemur catta	2	−0.34	0.09	−0.41, −0.28	1.65	0.14	1.55, 1.75
Prolemur simus	4	−0.46	0.08	−0.57, −0.40	1.58	0.62	1.25, 2.57
Varecia variegata	4	−0.41	0.06	−0.50, −0.37	1.01	0.08	0.92, 1.11
Galagidae							
Euoticus elegantulus	2	−0.37	0.13	−0.46, −0.27	1.13	0.03	1.11, 1.15

(Continues)

TABLE 1 (Continued)

Taxon	*n*	FHLG Position	SD	Range	FHLG Ellipse	SD	Range
Galago moholi	1	−0.65	–	–	1.71	–	–
Galago senegalensis	4	−0.59	0.03	−0.63, −0.56	1.22	0.23	0.99, 1.50
Galagoides demidoff	6	−0.52	0.13	−0.65, −0.27	1.35	0.20	1.16, 1.69
Otolemur crassicaudatus	5	−0.53	0.01	−0.53, −0.52	1.87	0.21	1.60, 2.12
Lorisidae							
Arctocebus calabarensis	2	−0.15	0.09	−0.21, −0.09	0.71	0.10	0.64, 0.78
Loris tardigradus	3	−0.20	0.12	−0.34, −0.12	0.51	0.09	0.42, 0.61
Nycticebus coucang	4	−0.32	0.15	−0.44, −0.13	0.43	0.10	0.32, 0.57
Perodicticus potto	6	−0.01	0.23	−0.33, 0.33	0.62	0.17	0.36, 0.88
Euarchonta							
Cynocephalidae	5	−0.46	0.12	−0.60, −0.33	0.55	0.24	0.35, 0.95
Ptilocercus lowii	3	−0.05	0.54	−0.38, 0.57	0.74	0.16	0.56, 0.87
Tupaia sp.	9	−0.95	0.05	−1.04, −0.89	0.36	0.14	0.22, 0.71

Individual raw measurements are available in Supporting Information Table S1.

Durham, NC; CM, Carnegie Museum of Natural History, Pittsburgh, PA; GU, H.N.B. Garhwal University, Srinagar, Uttarakhand, India; HTB, Cleveland Museum of Natural History, Hamann-Todd non-human primate osteological collection, Cleveland, OH; ISE-M, Institut des Sciences de l'Evolution de Montpellier, Montpellier, France; IRSNB, Institut Royal des Sciences Naturelles de Belgique, Brussels, Belgium; IVPP, Institute of Vertebrate Paleontology and Paleoanthropology, Chinese Academy of Sciences, Beijing, China; MACN, Museo Nacional de Ciencias Naturales, Buenos Aires, Argentina; MCZ, Museum of Comparative Zoology, Harvard University, Cambridge, MA; MNHN, Muséum National d'Histoire Naturelle, Paris, France; NMB, Naturhistorisches Museum Basel, Basel, Switzerland; NMMP, National Museum of Myanmar Primates, Yangon, Myanmar; NMNH, Smithsonian Institution National Museum of Natural History, Washington, DC; NYCEP, New York Consortium in Evolutionary Primatology, New York, NY; SBU, Stony Brook University, Stony Brook, NY; SDNHM, San Diego Natural History Museum, San Diego, CA; UCM, University of Colorado Museum of Natural History, Boulder, CO; UF, University of Florida, Florida Museum of Natural History, Gainesville, FL; UM, University of Michigan, Ann Arbor, MI; USGS, United States Geological Survey, Denver, CO; UNSM, University of Nebraska Science Museum, Lincoln, NE; USNM, United States National Museum, Smithsonian Institute, Washington, DC.

3 | METHODS

3.1 | Measurements

Using a combination of three linear measurements, two indices were computed for this study (Figure 3), which quantify the lateral extent and the shape of the FHLG. All measurements were taken using the 2D measurement tool in Avizo 8.0 (Visualization Systems, 2014) by a single observer (GSY). First, in Avizo, a series of landmarks were placed along the lateral rim of the trochlea (Figure 3a). Next, the talus was oriented with the dorsal aspect of the trochlea parallel with the viewing plane. We then rotated the talus about its anteroposterior and dorsoplantar axes so that a line would pass through the projections of the lateral rim landmarks onto the viewing plane (Figure 3b). This line (R1) served as the primary reference axis for subsequent measurements. When R1 was established, the talus was rotated dorsoplantarly until the main axis of the FHLG was orthogonal to the viewing plane (Figure 3c). This procedure effectively causes the observer to look along the path of the tendon of the *flexor hallucis longus* muscle. The dorsoplantar rotation was always conducted using the trackball tool in Avizo, which only permits rotation a single plane, so the lateral rim of the talus did not deviate from R1. Finally, once the talus was oriented properly, a secondary reference axis (R2) was created, passing through the most posterior points of the lateral and medial margins of the FHLG (Figure 3c)

When the talus was properly oriented and both reference axes were created, three measurements were taken (Figure 3c,d):

- FHLGLateral measures the distance from the lateral margin of the FHLG to R1 along R2.
- FHLGMedial measures the distance from the medial margin of the FHLG to R1 along R2.
- FHLGDepth measures the maximum orthogonal distance between R2 and the FHLG.

Negative distances were possible if the FHLG was positioned entirely lateral to R1 (resulting in negative FHLGMedial values) or entirely medial to R1 (negative FHLGLateral values). FHLGLateral and FHLGMedial were summed to generate FHLGTotal, a measure of the total width of the FHLG.

TABLE 2 Mean computed indices, standard deviations (SD), and ranges for extinct taxa

Higher taxon	Taxon	*n*	FHLG Position	SD	Range	FHLG Ellipse	SD	Range
Anthropoidea: *incertae sedis* & stem								
Eosimiidae	*Eosimias sinensis*	3	−0.24	0.32	−0.54, 0.10	1.55	0.10	1.47, 1.66
incertae sedis	"Protoanthropoid" IVPP 12306	1	−0.66	–	–	1.30	–	–
incertae sedis	*Pondaungia* (?) NMMP 39	1	−1.01	–	–	1.43	–	–
Parapithecidae	Parapithecidae	5	−0.89	0.05	−0.92, −0.82	1.77	0.24	1.51, 2.18
Parapithecidae	*Proteopithecus sylviae*	1	−0.64	–	–	1.29	–	–
Catarrhini								
Hominoidea	*Australopithecus afarensis* AL-288	1	−0.79	–	–	1.13	–	–
Hominoidea	*Homo sp.* ER 1464	1	−0.92	–	–	1.43	–	–
Propliopithecidae	*Aegyptopithecus zeuxis*	1	−0.59	–	–	1.13	–	–
Oligopithecidae	*Catopithecus browni*	1	−0.49	–	–	0.84	–	–
Platyrrhini								
incertae sedis	*Cebupithecia sarmientoi*	1	−0.70	–	–	1.01	–	–
incertae sedis	*Dolichocebus gaimanensis*	1	−0.62	–	–	0.52	–	–
Cebinae	*Neosaimiri fieldsi*	1	−0.71	–	–	1.13	–	–
incertae sedis	*Proteropithecia neuquensis*	1	−0.69	–	–	1.51	–	–
Omomyiformes								
Microchoerinae	*Necrolemur antiquus*	4	−0.57	0.10	−0.67, −0.44	1.75	0.18	1.57, 1.99
Omomyidae	*Absarokius* sp.	1	−0.53	–	–	1.68	–	–
Omomyidae	*Anemorhysis* sp.	4	−0.54	0.18	−0.73, −0.29	1.40	0.22	1.10, 1.56
Omomyidae	*Hemiacodon gracilis*	4	−0.74	0.14	−0.94, −0.65	1.77	0.76	1.29, 3.09
Omomyidae	*Omomys carteri*	4	−0.79	0.03	−0.84, −0.77	1.76	0.26	1.54, 2.14
Omomyidae	*Ourayia uintensis*	2	−0.70	0.14	−0.80, −0.60	1.63	0.32	1.38, 1.84
Omomyidae	*Shoshonius* sp.	3	−0.55	0.10	−0.67, −0.47	1.50	0.49	1.27, 2.13
Omomyidae	*Steinius* sp.	4	−0.67	0.11	−0.73, −0.51	1.62	0.21	1.41, 1.89
Omomyidae	*Teilhardina belgica*	2	−0.60	0.02	−0.61, −0.58	1.65	0.70	1.16, 2.15
Omomyidae	*Teilhardina brandti*	1	−0.46	–	–	1.51	–	–
Omomyidae	*Tetonius homunculus*	3	−0.59	0.15	−0.77, −0.50	1.62	0.39	1.15, 1.89
Omomyidae	*Vastanomys major* GU 800	1	−0.63	–	–	1.26	–	–
Omomyidae	*Washakius* sp.	3	−0.56	0.04	−0.59, −0.51	1.88	0.21	1.66, 2.02
Lemuriformes								
Megaladapidae	*Megaladapis* sp.	6	−0.70	0.08	−0.84, −0.63	0.07	0.51	−0.27, 1.10
Archaeolemuridae	*Archaeolemur edwardsi*	8	−0.71	0.09	−0.90, −0.59	1.20	0.48	0.66, 1.88
Paleopropithecidae	*Babakotia radofilai*	2	−0.61	0.07	−0.66, −0.56	−0.08	0.02	−0.10, −0.07
Paleopropithecidae	*Palaeopropithecus* sp.	4	−0.51	0.09	−0.61, −0.41	0.63	0.19	0.45, 0.90
Adapiformes								
Adapidae	*Adapis parisiensis*	7	−0.42	0.11	−0.57, −0.22	0.93	0.30	0.57, 1.31
Adapidae	*Leptadapis magnus*	2	−0.20	0.49	−0.55, 0.14	0.64	0.12	0.62, 0.79

(Continues)

TABLE 2 (Continued)

Higher taxon	Taxon	*n*	FHLG Position	SD	Range	FHLG Ellipse	SD	Range
Asiadapinae	*Asiadapis cambayensis* GU 747	1	0.08	–	–	0.95	–	–
Asiadapinae	*Marcgodinotius indicus*	2	−0.07	0.18	−0.20, 0.05	1.27	0.40	0.98, 1.55
Caenopithecinae	*Afradapis longicristatus*	1	−0.35	–	–	0.67	–	–
Caenopithecinae	*Caenopithecus lemuroides*	1	−0.41	–	–	0.69	–	–
Notharctidae	*Anchomomys frontanyensis*	3	−0.28	0.09	−0.37, −0.20	1.34	0.23	1.12, 1.56
Notharctidae	*Cantius abditus*	2	−0.05	0.25	−0.22, 0.13	1.33	0.03	1.31, 1.35
Notharctidae	*Cantius mckennai*	1	−0.07	–	–	1.06	–	–
Notharctidae	*Cantius ralstoni*	2	−0.07	0.19	−0.20, 0.07	1.60	0.31	1.42, 1.86
Notharctidae	*Cantius trigonodus*	2	−0.44	0.18	−0.57, −0.31	1.28	0.08	1.23, 1.34
Notharctidae	*Djebelemur martinezi*	1	−0.28	–	–	1.74	–	–
Notharctidae	*Notharctus* sp.	9	−0.30	0.16	−0.56, −0.07	1.93	0.21	1.54, 2.18
Notharctidae	*Notharctus venticolus*	2	−0.52	0.12	−0.60, −0.43	1.56	0.57	1.28, 2.08
Notharctidae	*Smilodectes gracilis*	2	−0.64	0.03	−0.66, −0.62	1.50	0.66	1.13, 2.07
Plesiadapiformes								
Carpoleststidae	*Carpolestes simpsoni*	1	−0.88	–	–	1.17	–	–
Paromomyidae	*Ignacius graybullianus*	1	−0.41	–	–	1.03	–	–
Plesiadapidae	*Nannodectes gidleyi*	1	−0.33	–	–	1.27	–	–
Plesiadapidae	*Plesiadapis cookei*	1	−0.28	–	–	0.80	–	–
Plesiadapidae	*Plesiadapis rex*	1	−0.14	–	–	0.89	–	–
Purgatoriidae	*Purgatorius* sp.	3	−0.26	0.20	−0.44, −0.03	0.91	0.08	0.86, 1.00
Saxonellidae	*Saxonella* sp.	1	−0.15	–	–	1.36	–	–

Individual raw measurements are available in Supporting Information Table S1.

With these three measures, two indices were generated. After their computation, all indices were natural-log transformed. The relative position of the FHLG was quantified with the following formula:

$$\ln[\text{FHLGTotal}/(\text{FHLGMedial} + \text{FHLGTotal})] = \text{FHLG Position}$$

Specimens with more medially positioned FHLGs have lower ratios, while higher ratios indicate more laterally positioned FHLGs. If FHLGMedial and FHLGLateral were subequal, the specimen would have FHLG Position value of −0.42 (=ln[0.66]).

The shape of the FHLG was quantified with the following formula:

$$\ln[(\text{FHLGTotal}/2)/\text{FHLGDepth}] = \text{FHLG Ellipse}$$

This ratio models the FHLG as an ellipse, and compares the semi-major axis (FHLGTotal/2) to the semi-minor axis (FHLGDepth). Specimens with a mediolaterally narrow but anteroposterior deep FHLGs have low ratios, while higher ratios indicate mediolaterally wide but anteroposteriorly shallow FHLGs. For a specimen in which the FHLG is a perfect semi-circle, the FHLG ellipse value would be 0 (=ln[1]). FHLG Ellipse is similar to the contour measure of the FHLG in Seiffert et al. (2015), but while their measure quantifies the shape of the FHLG at the distal outlet of the tendon's path, our measure quantifies the shape of the proximal inlet of the tendon. One *Avahi* specimen (USNM 83652) had a convex FHLG, so FHLGDepth had a negative value. In this case, FHLG Depth was altered *post hoc* to 0.01, creating a very high positive FHLG Ellipse value.[3]

3.2 | Additional measurements

Hypothesis 1 generates predictions about the covariation of FHLG position, fibular facet angle (FFa), and the size and shape of the MTF. The majority of FFa values come directly from Boyer and Seiffert (2013); other FFa values and the majority of MTF values come from Boyer et al. (2015). FFa or MTF measures for additional specimens were computed using the methods described in Boyer and Seiffert (2013) or Boyer et al. (2015), respectively.

3.3 | Traditional statistical analyses

3.3.1 | Measurement error

To evaluate the degree of intraobserver measurement error in the data, we repeated the three FHLG measurements described above on 130 individuals. On each specimen, we repeated the three FHLG linear

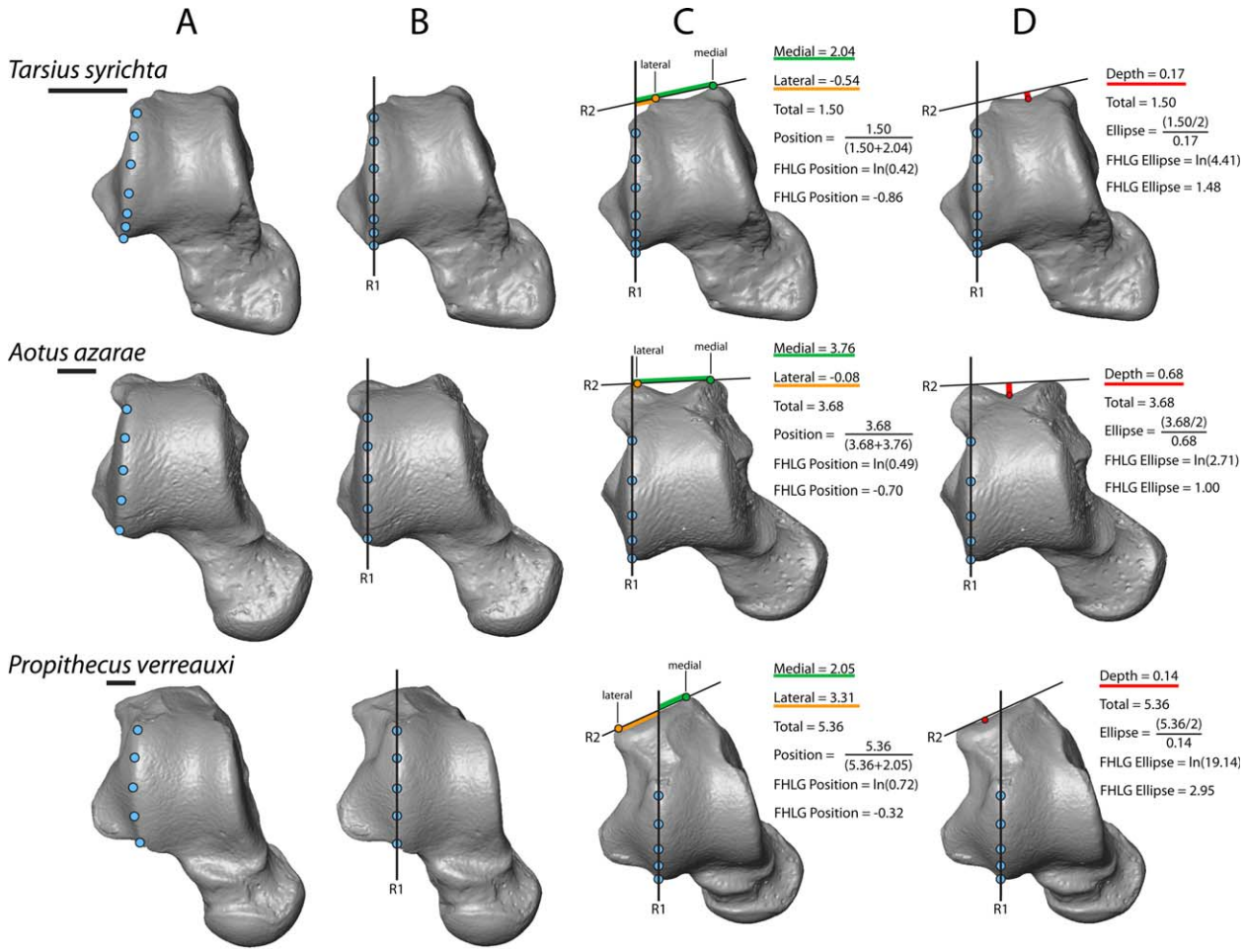

FIGURE 3 Linear measurements and computation of indices used to quantify FHLG position and relative depth in three primate taxa. (a) Landmarks (blue circles) are placed along the lateral trochlear rim. (b) A reference axis (R1) is drawn through the lateral rim landmarks. (c) The specimen is rotated in the plane of R1 so the FHLG is oblique to the viewing plane. Landmarks are placed on the medial- and lateralmost margins of the FHLG, and a second reference axis (R2) is drawn through these landmarks. Measurements are taken from the medial and lateral margins of the FHLG along R2 to R1. (d) Maximum depth of the FHLG is measured perpendicular to R2. Scale bars equal 2 mm

measurements on separate days so memory of previous measurements was unlikely. The variables of interest for this study (FHLG Position and FHLG Ellipse) were then computed from each set of replicate measurements. Error rates for both FFa and MTF measurements have been previously reported in Boyer and Seiffert (2013) and Boyer et al. (2015) respectively. To quantify error in the FHLG variables, we computed percentage error (PE) of the three replicates (White and Folkens, 2010). PE was calculated by (1) taking the absolute value of the difference between each replicate and the mean of all three replicates, (2) computing the mean of these deviations, (3) dividing the mean deviation by the mean measurement value, and multiplying this result by 100.

3.3.2 | Regressions of FHLG indices against body mass

Both FHLG position and FHLG Ellipse are dimensionless ratios with the potential to be "size free" variables. However, if there is a biomechanical basis for the position or depth of the FHLG, both variables may scale allometrically (i.e., exhibit a nonzero slope) relative to body mass (Boyer, Seiffert, Gladman, & Bloch, 2013a; 2015). To check for potential allometric trends, we performed phylogenetic generalized least squares (PGLS) and ordinary least squares (OLS) regressions of FHLG Position and FHLG Ellipse on the natural logarithm of species mean body mass. All regressions were initially conducted using PGLS in the *caper* package (Orme et al., 2012) in R. If Pagel's lambda did not differ significantly from 0 (indicating a lack of significant phylogenetic autocorrelation) or if the relationship was non-significant, then OLS regression was implemented. This regression protocol follows Yapuncich and Boyer (2014) and Boyer et al. (2015).

For PGLS regressions, species mean values were computed for all extant taxa in our sample (Supporting Information Table S1) and regressed against species mean body mass weighted by the sex and subspecific attribution of individual specimens. Sex- and subspecies-specific mean body masses were taken from the literature. Most primate body masses came from Smith and Jungers (1997), except *Microcebus griseorufus* (Rasoazanabary, 2010), *Prolemur simus* (Tacutu et al., 2013), and *Phaner furcifer* (Smith et al., 2003). Nonprimate euarchontan body masses came from Smith et al. (2003). Individuals of unknown

sex were assigned a body mass representing the average of male and female values for species with <20% sexual dimorphism ($n = 52$). A few extant specimens ($n = 11$) were of unknown sex and represented species with >20% sexual dimorphism; female body masses were used for these specimens. PGLS regressions were conducted with *caper* (Orme et al., 2012) in R. The phylogenetic tree used for this analysis was downloaded from the 10K trees website, version 3.0 (Arnold, Matthews, & Nunn, 2010) and edited in Mesquite (Maddison and Maddison, 2011) to include non-primate euarchontans. Branch lengths for dermopterans and scandentians came from Janečka et al. (2007) and Roberts, Lanier, Sargis, & Olson (2011) respectively. The tree is provided in the supporting documentation (Supporting Information, Tree S1).

OLS regression was conducted in PAST 3.07 (Hammer, Harper, & Ryan, 2001). In these analyses, in order to account for high levels of sexual size dimorphism in some anthropoid species, FHLG Position, FHLG Ellipse, and natural-log body mass were averaged into sex-specific means when species displayed greater than 20% sexual size dimorphism (computed as |ln[male body mass] - ln[female body mass]|) (Yapuncich, Gladman, & Boyer, 2015).

3.3.3 | ANOVAs of FHLG indices by clade

Because morphological differences in FHLG position have primarily been noted between anthropoids and strepsirrhines (Dagosto, 1988; Gebo, 1986, 1988, 1993, 2011), we used one-way analysis of variance (ANOVA) in PAST 3.07 (Hammer et al., 2001) to test several predictions of our hypotheses. Though it may seem counterintuitive, we suspect that ANOVA is more appropriate than Phylogenetic ANOVA when phylogenetic affinity is hypothesized to explain a large amount of observed morphological differences (Boyer et al., 2015). When functional similarities (such as similar diets) are largely responsible for observed morphological differences, and phylogenetic affinity is a potentially confounding factor, then Phylogenetic ANOVA with PGLS is clearly more appropriate (Winchester et al., 2014). The structure of our hypotheses and predictions meets the former rather than the latter conditions.

Species means were used for all ANOVAs in order to control for different sample sizes within species. Species means were compiled into taxonomic families, and ANOVAs were first performed at the family level within the primary clades of interest (anthropoids and strepsirrhines). If families were not significantly different from each other, species mean values within those families were combined into higher taxonomic groups. The final FHLG Position ANOVA compared seven groups; the final FHLG Ellipse ANOVA compared nine groups. The results section below provides more details on the combined taxonomic groups.

3.3.4 | Regression of FHLG position against fibular facet angle

If both the position of the FHLG and fibular facet angle reflect the frequent use of inverted and abducted foot postures, then there should be a significant correlation between FHLG Position and FFa. To test this relationship, we used PGLS regression with species mean data, including fossil specimens (Tables 1 and 2). The phylogenetic tree was nearly identical to the expanded tree of Boyer et al. (2015, their Tree2a.nex), with six additional taxa (*Brachyteles arachnoides*, *Nannodectes gidleyi*, *Neosaimiri fieldsi*, *Phaner furcifer*, *Purgatorius* sp., and *Saxonella* sp.). This new, more comprehensive tree is available in the supporting documentation (Supplementary Information, Tree S2). The process for adding these taxa is detailed below. PGLS regressions were conducted with *caper* (Orme et al., 2012) in R. Regressions were performed separately for eight euarchontan groups (group membership indicated in Table S2 of Supporting Information).

3.3.5 | Regression of FHLG position against MTF variables

If both the position of the FHLG and the size and shape of the medial tibial facet reflect frequent use of inverted and abducted foot postures, than there should be a significant correlation between FHLG Position and the MTF measures of Boyer et al. (2015). To test this relationship, rather than analyzing the relationship between each MTF variable and FHLG position, we computed the first principal component of three MTF measurements from Boyer et al. (2015): the ratio of MTF area to ectal facet area ($\ln[(MTFa^{1/2})/(EFa^{1/2})]$, the ratio of MTF perimeter to MTF area ($\ln[(MTF\text{-}Perimeter)/(MTFa^{1/2})]$, and a ratio quantifying the dorsoplantar extent of the MTF ($\ln[(MTH1)/(MTH2)]$. As noted by Boyer et al. (2015), the first principal component may more completely capture the morphological differences described qualitatively by previous researchers (e.g., Dagosto, 1990; Gebo, 1986). Principal component analysis was performed on the correlation matrix of the species mean values of these three variables in PAST 3.07 (Hammer et al., 2001). PGLS regressions were conducted with *caper* (Orme et al., 2012) in R. The same phylogenetic tree was used for these regressions as the fibular facet angle regressions above (Tree S2 in Supporting Information). As above, regressions were performed separately for eight euarchontan groups (Table S2 in Supporting Information).

3.4 | Phylogenetic framework and ancestral state reconstruction

Phylogenetic methods used here closely follow those employed previously by Boyer and Seiffert (2013), Boyer et al. (2013a), and Boyer et al. (2015). The phylogenetic tree of living and extinct primates that was used for ancestral state reconstructions was assembled using Matrix Representation with Parsimony (MRP), and combined topological information from the "core" tree of Paleogene primates used by Boyer et al. (2015), the molecular phylogenies of extant euarchontans recovered by Springer et al. (2012) and Janečka et al. (2007), the basal fossil euarchontan tree of Bloch et al. (2007), omomyiform phylogenies of Tornow (2008) and Rose et al. (2011), the notharctine phylogeny of Gunnell (2002), the phylogeny of living and extinct platyrrhines generated by Kay (2015), and the hominin phylogeny of Strait and Grine (2004). Taxa not present in the tree of Boyer et al. (2015) include *Caenopithecus* [originally present in their "core" tree but pruned for the analysis of medial tibial facet size and shape, as the tarsals of that species had not yet been described by Seiffert et al. (2015)]; the plesiadapiforms *Nannodectes*, *Purgatorius*, and *Saxonella* [from Bloch et al. (2007), with relationships within Plesiadapoidea on the basis of Boyer,

Scott, & Fox (2012)]; the middle Miocene platyrrhine *Neosaimiri*, present in the tree of Kay (2015); and the extant lemuriform *Phaner* and extant platyrrhine anthropoid *Brachyteles*, both present in the molecular phylogeny of primates published by Springer et al. (2012). Three other terminal taxa that were present in the supertree of Boyer et al. (2015) were pruned for ancestral state reconstruction as they could not be measured for the FHLG variables (*Pelycodus*, *Homo habilis*, and KNM-ER 813). Time-scaling of the final tree used the same approach as that employed by Boyer et al. (2015).

Also as in Boyer and Seiffert (2013), Boyer et al. (2013a), and Boyer et al. (2015), ancestral state reconstructions were performed using the program BayesTraits version 2 (Pagel and Meade, 2013). We first ran 10,050,000-generation Markov chain Monte Carlo (MCMC) analyses for each combination of model (random walk or random walk with a directional trend) and scaling parameter (delta, kappa, lambda, or none) and used Bayes factor comparisons to determine which combination best fit the evolution of FHLG Position and FHLG Ellipse on our time-scaled supertree, based on the harmonic mean in the final generation of each analysis. We then used the model files output by initial MCMC analysis of the preferred model and scaling parameter in longer (20,050,000 generation) MCMC analyses for ancestral reconstructions at selected nodes. The means and 95% highest posterior density intervals for ancestral estimates at each node were calculated in Tracer v1.5 (Rambaut and Drummond, 2009), with the first 50,000 generations discarded as burn-in. We also tested whether the inclusion of plesiadapiforms as paraphyletic with respect to crown primates—a result that has not been recovered by all recent phylogenetic analyses of living and extinct Euarchonta (e.g., Ni et al., 2013)—biased our results by pruning these species from the supertree and running model tests and ancestral state reconstructions as described above.

4 | RESULTS

Species means, standard deviations, and ranges of FHLG Position and FHLG Ellipse are shown in Table 1 for extant taxa and Table 2 for extinct taxa. All individual measurements used to compute these indices can be found in Table S1 of the Supporting Information.

4.1 | Measurement error

For both FHLG indices, intraobserver measurement error was lower than the recommended 5% threshold (White and Folkens, 2010). FHLG Position has an average percent error of 2.77%, while FHLG Ellipse has an average percent error of 3.86%.

4.2 | Regression of FHLG indices against body mass

For FHLG Position, PGLS regressions of extant taxa reveal significantly non-zero Pagel's lambda (indicating phylogenetic autocorrelation in variable error structure) in four groups: euarchontans, primates, prosimians, and strepsirrhines (Table 3). A significant correlation between FHLG Position and body mass was found only among anthropoids and lemuriforms (Table 3). The correlation was inverse in both cases,

TABLE 3 Phylogenetic generalized least squares (PGLS) and ordinary least squares (OLS) regressions of FHLG Position and body mass

Sample	Dependent	Independent	Method	*n*	Slope	Slope 95% CI	Intercept	Intercept 95% CI	r^2	*p*	Lambda	Lambda 95% CI	Allometry
Euarchontans	FHLG Position	lnBM	PGLS	73	−0.011	(−0.042, 0.021)	−0.469	(−0.745, −0.193)	0.006	0.510	0.990	(0.946, NA)	–
Primates			PGLS	70	−0.007	(−0.037, 0.024)	−0.528	(−0.789, −0.267)	0.003	0.663	0.981	(0.904, 1.000)	–
Haplorhines			OLS	48	−0.009	(−0.021, 0.002)	−0.711	(−0.796, −0.626)	0.052	0.119	–	–	–
Anthropoids			**OLS**	**45**	**−0.015**	**(−0.026, −0.004)**	**−0.661**	**(−0.744, −0.571)**	**0.112**	*	–	–	**Negative**
Platyrrhines			OLS	29	0.000	(−0.017, 0.014)	−0.757	(−0.864, −0.635)	0.000	0.992	–	–	–
Catarrhines			OLS	16	−0.010	(−0.051, 0.023)	−0.721	(−1.054, −0.304)	0.015	0.650	–	–	–
Prosimians			PGLS	31	0.010	(−0.046, 0.066)	−0.547	(−0.963, −0.132)	0.005	0.717	0.995	(0.772, NA)	–
Strepsirrhines			PGLS	28	−0.004	(−0.058, 0.051)	−0.320	(−0.733, 0.093)	0.001	0.893	0.957	(0.491, NA)	–
Lemuriforms			**OLS**	**21**	**−0.043**	**(−0.099, −0.015)**	**−0.064**	**(−0.260, 0.368)**	**0.232**	*	–	–	**Negative**
Lorisiforms			OLS	9	0.106	(−0.104, 0.275)	−0.984	(−1.991, 0.229)	0.199	0.228	–	–	–

Bold text indicates significant relationships. Tree used for PGLS available in Supporting Information Tree S1. $^{*}p < 0.05$, $^{**}p < 0.01$, $^{***}p < 0.001$.

indicating that larger taxa have FHLGs that are more medially positioned (i.e., more "haplorhine-like") than smaller taxa. For FHLG Ellipse, PGLS regressions of extant taxa reveal significant phylogenetic autocorrelation in seven groups: euarchontans, primates, haplorhines, anthropoids, platyrrhines, prosimians, and strepsirrhines (Table 4). A significant negative correlation was found between FHLG Ellipse and body mass among catarrhines (Table 4), indicating that larger taxa have relatively shallow FHLGs compared to smaller taxa.

4.3 | ANOVAs of FHLG indices by clade

Average intraspecific range in FHLG Position (Figure 4) is only 14% of the total observed range of the entire sample. ANOVAs and *post hoc* comparisons of major clades and grades (Figure 5) at the level of species means reveal significant differences between several groups (Table 5). Among strepsirrhines, major *post hoc* differences arise due to galagids having a more medially positioned FHLG, while lorises have a more laterally positioned FHLG than the other strepsirrhine groups (Figure 5a, Table 5). There is broad overlap among anthropoid groups, and ANOVAs and *post hoc* comparisons reveal few significant differences. Cercopithecoids are the only examined group that is statistically differentiated (from hylobatids and cebids) in having more medially placed grooves (Figure 5b, Table 5).

Comparisons among all major euarchontan groups (Figure 5c,d, Table 5) reveal a number of interesting differences. To improve the power of the combined analysis, we consolidated groups that were not significantly different from one another. Strepsirrhines were represented by galagids, lorisids, and lemuriforms; anthropoids were represented by cercopithecoids and non-cercopithecoid anthropoids. The combined analysis (Figure 5c,d) recovers differences between strepsirrhines and tarsiers as well as strepsirrhines and anthropoids (Table 5). There are no significant differences between non-primate euarchontans and any primate group when *Tupaia*, *Ptilocercus*, and dermopterans are considered together as "non-primate euarchontans" (Table 5). However, while *Ptilocercus* and dermopterans have laterally positioned FHLGs, tupaiids have much more medially positioned FHLGs. ANOVAs and *post hoc* comparison tests reveal that when these non-primate euarchontans are separated, there is no significant difference between *Ptilocercus* + dermopterans and strepsirrhines, but significant differences between *Ptilocercus* + dermopterans and tarsiers as well as anthropoids (Table 5).

Average intraspecific range in FHLG Ellipse (Figure 6) is only 10% of the total observed range of the entire sample. For FHLG Ellipse, ANOVAs and *post hoc* comparisons of major clades and grades (Figure 7) at the level of species means also reveal significant differences between several groups (Table 6). Among strepsirrhines, the major *post hoc* differences arise due to indriids having extremely high FHLG Ellipse values (and therefore shallow grooves) compared to other groups examined, while lorises have extremely low values (and therefore deep grooves) (Figure 7a, Table 6). All other strepsirrhines have FHLGs of intermediate depth. Among anthropoids, hylobatids and cercopithecoids are distinctive in their high values, callitrichids are distinctive in

TABLE 4 Phylogenetic generalized least squares (PGLS) and ordinary least squares (OLS) regressions of FHLG Ellipse and body mass

Sample	Dependent	Independent	Method	*n*	Slope	Slope 95% CI	Intercept	Intercept 95% CI	r^2	*p*	Lambda	Lambda 95% CI	Allometry
Euarchontans	FHLG Ellipse	lnBM	PGLS	73	0.062	(−0.037, 0.162)	0.465	(−0.363, 1.294)	0.022	0.216	0.925	(0.777, 0.977)	–
Primates			PGLS	70	0.061	(−0.043, 0.165)	0.668	(−0.207, 1.543)	0.020	0.248	0.918	(0.760, 0.975)	–
Haplorhines			PGLS	42	0.088	(−0.045, 0.220)	0.066	(−0.733, 1.549)	0.043	0.188	0.941	(0.755, 0.993)	–
Anthropoids			PGLS	39	0.096	(−0.054, 0.245)	0.074	(−1.108, 1.644)	0.044	0.202	0.928	(0.710, 0.993)	–
Platyrrhines			PGLS	26	0.185	(−0.029, 0.399)	−0.499	(−2.090, 1.092)	0.117	0.087	0.852	(0.401, 0.995)	–
Catarrhines			**OLS**	**16**	**−0.151**	**(−0.259, −0.033)**	**2.718**	**(1.562, 3.720)**	**0.320**	*	–	–	**Negative**
Prosimians			PGLS	31	0.044	(−0.124, 0.213)	0.823	(−0.354, 2.001)	0.010	0.593	0.837	(0.218, 0.973)	–
Strepsirrhines			PGLS	28	0.036	(−0.147, 0.220)	0.911	(−0.442, 2.263)	0.006	0.688	0.840	(0.265, 0.975)	–
Lemuriforms			OLS	21	0.096	(−0.069, 0.228)	0.911	(−0.070, 2.024)	0.036	0.413	–	–	–
Lorisiforms			OLS	9	−0.113	(−0.640, 0.464)	1.715	(−1.471, 4.843)	0.039	0.608	–	–	–

Bold text indicates significant relationships. Tree used for PGLS available in Supporting Information Tree S1. $^{*}p < 0.05$, $^{**}p < 0.01$, $^{***}p < 0.001$.

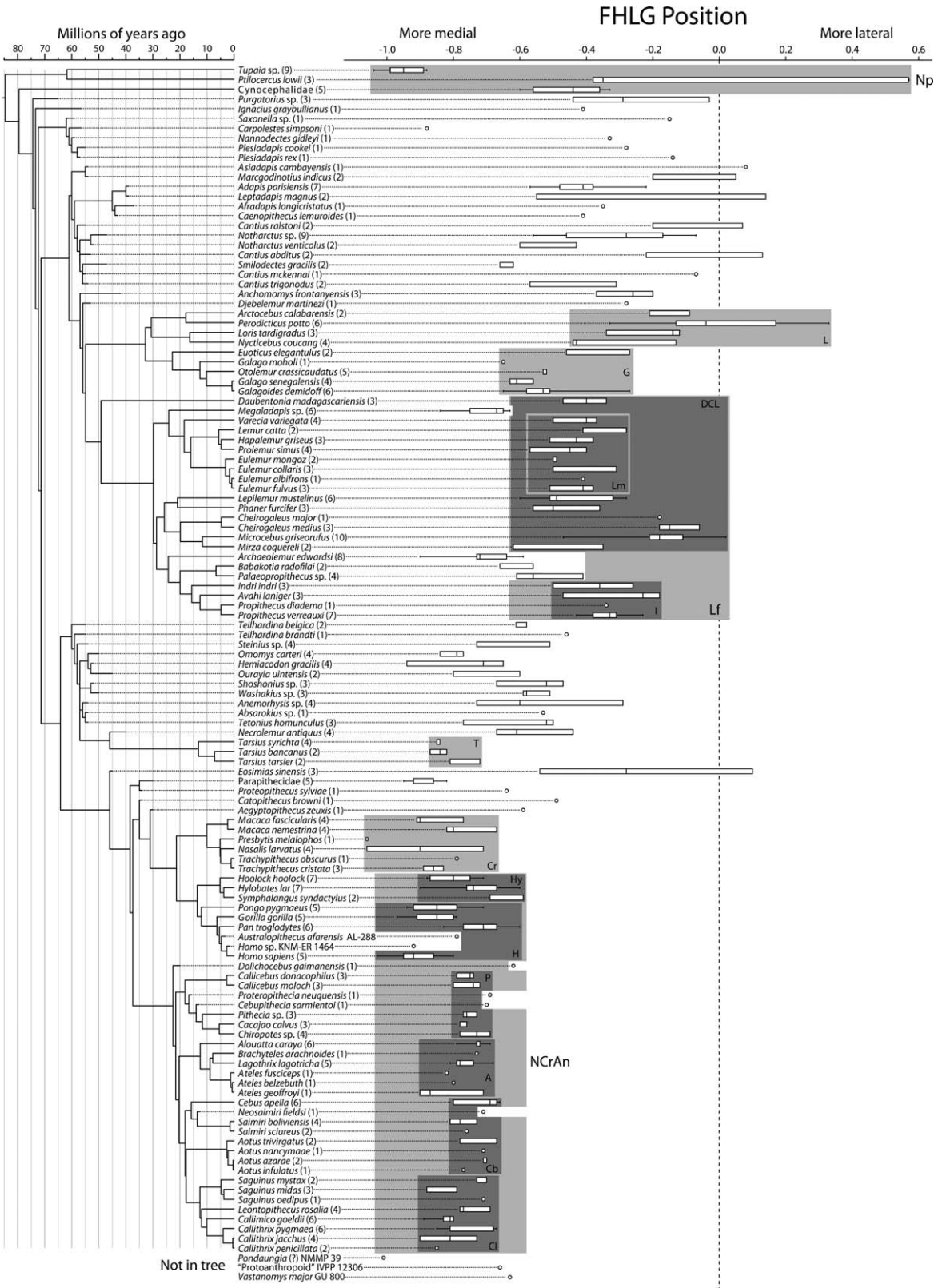

FIGURE 4 Boxplots of FHLG Position with phylogenetic tree showing all included taxa. Boxes include 25–75% quartiles; horizontal lines in boxes indicate species means; whiskers extend to the farthest points <1.5 times the interquartile range. Gray boxes indicate groups of extant species used in within-strepsirrhine and within-haplorhine ANOVAs (Figure 5a,b, Table 5) or within-Euarchonta ANOVAs (Figure 5c, Table 5). Abbreviations for taxonomic groups are given in text and Figure 5 caption

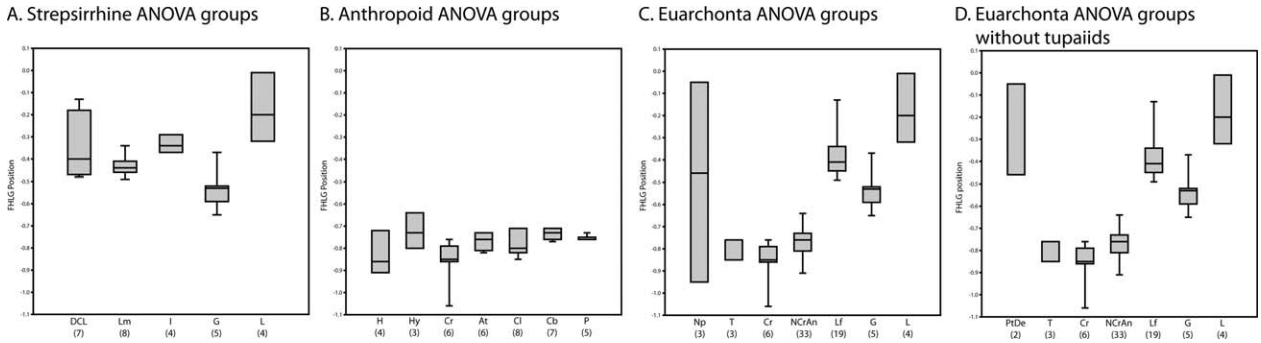

FIGURE 5 Boxplots of group means for FHLG Position compared with ANOVA and reported in Table 5. Number in parentheses indicates number of species in each group. Abbreviations are: DCL, *Daubentonia* + cheirogaleids + lepilemurids; Lm, lemurids; I, indriids; G, galagids; L, lorisids; H, hominids; Hy, hylobatids; Cr, cercopithecoids; At, atelids; Cl, callitrichines; Cb, cebines/aotines; P, pithecines; Np, non-primates; T, tarsiers; NCrAn, non-cercopithecoid anthropoids; Lf, lemuriforms; PtDe, *Ptilocercus* + dermopterans

their low values, and hominids and other platyrrhines have intermediate values (Figure 7b, Table 6).

As with FHLG Position, before making comparisons among all major euarchontan groups, we first consolidated groups that were not significantly different from one another on the basis of previous analyses. Strepsirrhines were represented by indriids, lorisids, and a group containing all other strepsirrhines. Anthropoids were represented by callitrichines, noncallitrichine platyrrhines (cebines, pithecines, and atelines), hominids, and nonhominid catarrhines (hylobatids and cercopithecoids). These groups were then compared against each other, a tarsier group, and a nonprimate euarchontan group. The combined analysis reveals that non-primate euarchontans, callitrichids and lorises share low FHLG Ellipse values, while indriids have the highest values (and shallowest grooves) among euarchontans (Figure 7c, Table 6). Unlike FHLG Position there is no clear strepsirrhine-haplorhine divide in the values. Furthermore, there is low variance among nonprimate euarchontans.

4.4 | Regression of FHLG position against fibular facet angle

Plotting FHLG Position against fibular facet angle for all extant and extinct euarchontan taxa suggests a significant and positive relationship between the two variables (Figure 8) and that taxa with higher fibular facet angles also have more laterally positioned FHLGs. However, PGLS regressions reveal that there is only a significant correlation between FHLG Position and FFa among strepsirrhines (Table 7), and in this group, there is an inverse relationship between the two variables, which is *opposite* the broader (and the expected) pattern. In strepsirrhines, as FFa increases (i.e., the angle between the fibular and lateral tibial facets becomes more obtuse), FHLG becomes more medially positioned. The significance of this relationship disappears when large-bodied subfossil lemurs are excluded; indicating the inclusion of subfossil lemurs drives the recovery of a significant and negative correlation of FFa and FHLG position. These taxa are unusual among strepsirrhines in their large body masses, high FFas, and medially positioned FHLGs. However, though the relationship is not significant without subfossils, the trend remains inverse. Small-bodied cheirogaleids such as *Microcebus* have steepest fibular facet angles and very laterally positioned FHLGs.

4.5 | Regression of FHLG position against MTF variables

The first principal component (PC1) of the three MTF variables from Boyer et al. (2015) has an eigenvalue of 2.31 and represents 77% of the variance. Loadings indicate that the variables are roughly equally represented: −0.8676 for ln[(MTFa$^{1/2}$)/(EFa$^{1/2}$)], 0.8242 for ln[(MTF-Perimeter)/(MTFa$^{1/2}$)], and 0.9374 for ln[(MTH1)/(MTH2)]. However, no significant relationships were recovered between FHLG Position and the first principal component of the MTF variables (Table 8).

4.6 | Position of fossil taxa

Figure 9 illustrates the variation of FHLG Position and FHLG Ellipse among some notable extant and extinct taxa.

As a group, plesiadapiforms have more laterally placed (i.e., more strepsirrhine-like) FHLGs (Figure 4), and are also similar to cynocephalids and *Ptilocercus*. *Carpolestes simpsoni* is a notable exception; in this case, the measurements may have been affected by poor preservation of UM 101963. Plesiadapiforms generally have shallower FHLGs (as gauged by FHLG Ellipse) than those of cynocephalids and scandentians (Figure 6), confirming qualitative assessments of Chester et al. (2015). However, FHLG Ellipse in extant nonprimate euarchontans is generally not outside the range of extant and fossil primates.

Adapiforms are consistently strepsirrhine-like in their FHLG position, and are, for the most part, strongly differentiated from extant haplorhines (Figure 4), though values for the notharctines *Notharctus venticolus*, *Cantius trigonodus*, and particularly *Smilodectes* fall well within the range seen in omomyiforms and early fossil anthropoids. There is no clear pattern to the variation seen within adapiforms except that the earlier occurring and potentially more basal taxa (i.e., *Asiadapis*, *Marcgodinotius*, *Cantius*) tend to have the most laterally positioned FHLGs. Notharctids appear to have the shallowest grooves, while adapines, caenopithecines, and asiadapids have the deepest

TABLE 5 ANOVA and post hoc comparison tests for FHLG position

ANOVA	Strepsirrhine	Anthropoid	Combined1	Combined2
df (B,W)	4,23	6,32	6,66	6,65
MSE (B,W)	0.08, 0.01	0.01, 0.00	0.54, 0.01	0.58,0.01
F	7.53	3.42	41.32	69.01
p(same)	***	**	***	***
Tukey's Q	DCL/Lm	H/Hy	Np/T	PtDe/T
	0.56	0.10	***	***
	DCL/I	H/Cr	Np/Cr	PtDe/Cr
	1.00	0.99	***	***
	DCL/G	H/At	Np/NCrAn	PtDe/NCrAn
	*	0.75	***	***
	DCL/L	H/Cl	Np/Lf	PtDe/Lf
	0.15	0.73	0.67	0.47
	Lm/I	H/Cb	Np/G	PtDe/G
	0.63	0.22	1.00	***
	Lm/G	H/P	Np/L	PtDe/L
	0.52	0.36	***	0.80
	Lm/L	Hy/Cr	T/Cr	T/Cr
	**	*	1.00	0.99
	I/G	Hy/At	T/NCrAn	T/NCrAn
	*	0.83	0.99	0.97
	I/L	Hy/Cl	T/Lf	T/Lf
	0.12	1.00	***	***
	G/L	Hy/Cb	T/G	T/G
	***	1.00	***	***
		Hy/P	T/L	T/L
		0.99	***	***
		Cr/At	Cr/NCrAn	Cr/NCrAn
		0.30	0.83	0.69
		Cr/Cl	Cr/Lf	Cr/Lf
		0.29	***	***
		Cr/Cb	Cr/G	Cr/G
		*	***	***
		Cr/P	Cr/L	Cr/L
		0.09	***	***
		At/Cl	NCrAn/Lf	NCrAn/Lf
		1.00	***	***
		At/Cb	NCrAn/G	NCrAn/G
		0.96	*	***
		At/P	NCrAn/L	NCrAn/L
		0.99	***	***
		Cl/Cb	Lf/G	Lf/G
		0.97	0.28	0.12
		Cl/P	Lf/L	Lf/L
		1.00	0.09	*
		Cb/P	G/L	G/L
		1.00	***	***

Group abbreviations are given in Figure 5 caption. $^{*}p < 0.05$, $^{**}p < 0.01$, $^{***}p < 0.001$.

grooves (Figure 6). All values for FHLG depth are within the range of extant strepsirrhines and overlap extensively with extant haplorhines.

Omomyiforms tend to have more medially positioned FHLGs. However, a number of species include individuals with quite laterally positioned grooves, including *Teilhardina brandti* (as suggested by Boyer and Seiffert, 2013), *Steinius*, *Shoshonius*, *Washakius*, *Anemorhysis*, *Absarokius*, *Tetonius*, and *Necrolemur* (Figure 4). *Omomys*, *Hemiacodon*, and *Ourayia* all have more medially positioned (i.e., more haplorhine-like) grooves. Omomyiforms tend to have FHLG Ellipse values within (but towards the high end of) the adapiform range, making omomyiforms most similar to notharctids among adapiforms. With the exception of one specimen of *Hemiacodon* (AMNH 12613), omomyiforms are within the range of non-indriid lemuriforms for FHLG Ellipse. The recently described talus GU 800 attributed to *Vastanomys major* (Dunn et al., 2016) has a higher (more lateral) FHLG Position value than almost all extant anthropoids, but is well within the range of omomyiforms.

Given earlier descriptions of *Eosimias* (Gebo et al., 2000, 2001) and its status as a possible basal stem anthropoid, the strepsirrhine-like values for its FHLG Position are surprising (Figure 4), though higher values are not unusual among early anthropoids. *Catopithecus browni*, a putative early catarrhine from the L-41 locality in the Fayum Depression of Egypt has a more laterally positioned FHLG than any extant haplorhine, and the undoubted stem catarrhine *Aegyptopithecus zeuxis* has an FHLG that is more laterally placed than any extant anthropoid. Furthermore, the probable stem platyrrhine *Dolichocebus gaimanensis* (Kay, 2015; Kay et al., 2008) has a more laterally placed FHLG than any extant platyrrhine. In strong contrast to the pattern of laterally placed FHLGs in early anthropoids, NMMP-39 (?*Pondaungia*) has a notably medially-placed FHLG, being more medially positioned than almost all extant euarchontans, with the exceptions of *Homo sapiens*, the cercopithecoids *Nasalis* and *Presbytis*, and *Tupaia*. All other examined fossil anthropoids plot within the range of extant anthropoids for FHLG Position, including the "protoanthropoid" from Shanghuang. FHLG Ellipse values are not notable for any fossil anthropoid, as all examined taxa fall within the range of extant anthropoids (Figure 6).

The subfossil lemurs *Megaladapis* and *Archaeolemur* have strongly medial FHLGs, and are thus surprisingly haplorhine-like, whereas the

FIGURE 6 Boxplots of FHLG Ellipse with phylogenetic tree showing all included taxa. Boxes include 25–75% quartiles; horizontal lines in boxes indicate species means; whiskers extend to the farthest points <1.5 times the interquartile range. Gray boxes indicate groups of species used in within-strepsirrhine and within-haplorhine ANOVAs (Figure 7a,b, Table 6) or within-Euarchonta ANOVAs (Figure 7c, Table 6). Abbreviations for taxonomic groups are given in text and Figure 7 caption

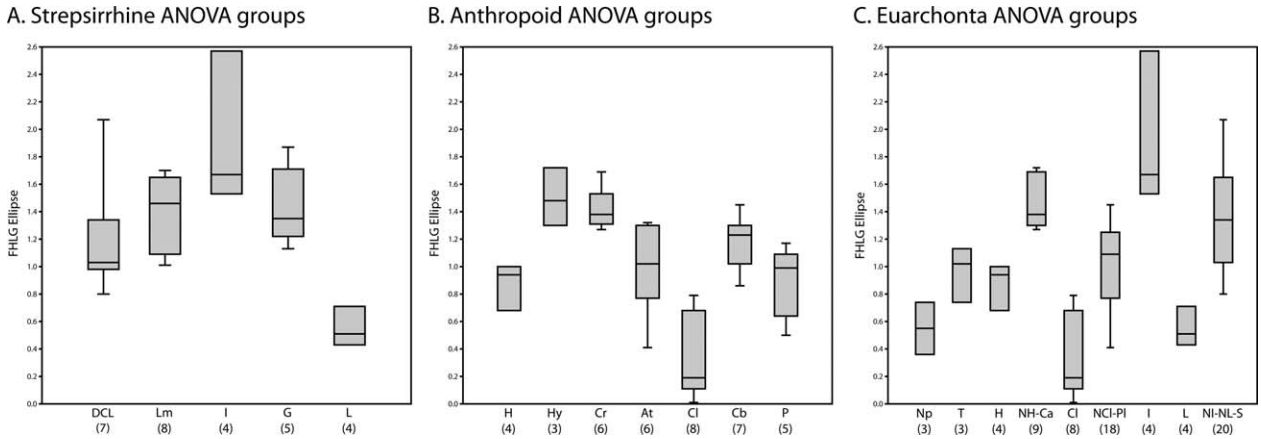

FIGURE 7 Boxplots of group means for FHLG Ellipse compared with ANOVA and reported in Table 6. Number in parentheses indicates number of species in each group. Abbreviations are: DCL, *Daubentonia* + cheirogaleids + lepilemurids; Lm, lemurids; I, indriids; G, galagids; L, lorisids; H, hominids; Hy, hylobatids; Cr, cercopithecoids; At, atelids; Cl, callitrichines; Cb, cebines/aotines; P, pithecines; Np, non-primates; T, tarsiers; NH-Ca, non-hominid catarrhines; NCl-Pl, non-callitrichine platyrrhines; NI-NL-S, non-indriid and non-lorisid strepsirrhines

sloth lemurs *Babakotia* and *Palaeopropithecus* are more securely in the range of modern strepsirrhines (Figure 4). In contrast, for FHLG Ellipse, *Megaladapis* and the sloth lemurs have exceptionally deep grooves, while *Archaeolemur* is more similar to extant strepsirrhines in groove depth (Figure 6).

4.7 | Modeling character evolution and ancestral state reconstruction

Different evolutionary models are preferred for the two FHLG indices (Table 9). Excluding plesiadapiforms from the phylogeny does not change the preferred evolutionary model for either index (Table S4 in Supporting Information). FHLG Position shows a strong directional trend, and is preferred over a random walk model for each phylogenetic scaling parameter; the delta scaling parameter returned the highest harmonic mean likelihood in the final generation and was employed for ancestral reconstructions. The distribution of FHLG Ellipse values is better described by a random walk model, with the kappa scaling parameter only weakly favored over the lambda parameter; the former was used in ancestral reconstructions.

Trends revealed by ancestral state reconstructions reflect what might be surmised from qualitative outgroup assessments (Table 10, Figure 10). The directional trend detected in the FHLG position variable contributes to the reconstruction of a strongly lateral position at basal nodes in Euarchonta, with the ancestral Euprimate being unequivocally strepsirrhine-like in this feature. Multiple higher-level primate clades are reconstructed as having evolved more medially positioned FHLGs in parallel; for instance, the ancestral crown haplorhine is effectively strepsirrhine-like in its FHLG position, and only later do tarsiers and anthropoids independently shift to more medial FHLG positions. Presumably due to the relatively lateral positions seen in basal fossil forms (*Eosimias*, *Catopithecus*, *Aegyptopithecus*, and *Dolichocebus*), platyrrhines, catarrhines, and parapithecoids are reconstructed as independently evolving medially positioned FHLGs from an ancestor that had a more laterally positioned FHLG. Similar independent trends are seen in lemuriforms, lorisiforms, and adapiforms. For FHLG Ellipse, the tree as a whole does not exhibit directionality, but the branch leading from the ancestral euarchontan to the ancestor of extant primates is strongly directional, showing a change from deeper FHLGs to more shallow FHLGs (Table 10, Figure 10). Among strepsirrhines, three separate clades (galagids, indriids, and lemurids) appear to have developed shallower grooves independently, while platyrrhines, lorisids, and adapids re-evolved deeper grooves, in a reversal back to conditions otherwise seen only in basal euarchontans (Table 10, Figure 10).

5 | DISCUSSION AND CONCLUSIONS

5.1 | Evolutionary considerations of FHLG position

As previously suggested (Beard et al., 1988; Dagosto, 1988; Gebo, 1986, 1988), strepsirrhines have FHLGs that are significantly more laterally positioned than anthropoids and tarsiers. However, according to our measurements, strepsirrhines do not have significantly more laterally positioned FHLGs than plesiadapiforms, dermopterans or ptilocercid tree shrews. These observations complicate the classic interpretation of a laterally positioned FHLG as a derived strepsirrhine feature (Beard et al., 1988; Covert and Williams, 1994; Dagosto, 1988; Gebo, 1986a, 1988; Gebo et al., 1991; Kay et al., 1997). On the basis of our analyses, the crown euarchontan likely exhibited a laterally positioned FHLG, and certain euarchontan lineages (anthropoids, tarsiiforms, and tupaiids) evolved a medially positioned FHLG in parallel. Compared to the crown primate node, the crown haplorhine is reconstructed as having a relatively more medially positioned FHLG, but the groove still remains quite lateral (indeed, the position is comparable to many extant strepsirrhines). It is therefore difficult to claim a medially positioned FHLG as a definite haplorhine synapomorphy. Nonetheless, development of a medially positioned FHLG does appear to be a tendency of both haplorhine lineages (i.e., tarsiiforms and anthropoids).

Though patterns within fossil groups are complex (Figure 4), extinct species generally provide additional support for the lateral

TABLE 6 ANOVA and post hoc comparison tests for FHLG ellipse

ANOVA	Strepsirrhine	Anthropoid	Combined1
df (B,W)	4,23	6,32	8,64
MSE (B,W)	1.20, 0.13	0.96, 0.06	1.68, 0.09
F	9.44	15.22	19.09
p(same)	***	***	***
Tukey's Q	DCL/Lm	H/Hy	Np/T
	0.91	**	0.40
	DCL/I	H/Cr	Np/I
	**	*	***
	DCL/G	H/At	Np/L
	0.83	1.00	1.00
	DCL/L	H/Cl	Np/NI-NL-S
	0.05	*	***
	Lm/I	H/Cb	Np/H
	*	0.57	0.62
	Lm/G	H/P	Np/NH-Ca
	1.00	1.00	***
	Lm/L	Hy/Cr	Np/Cl
	**	1.00	0.95
	I/G	Hy/At	Np/NCl-Pl
	0.07	*	0.25
	I/L	Hy/Cl	T/I
	***	***	***
	G/L	Hy/Cb	T/L
	***	0.42	0.46
		Hy/P	T/NI-NL-S
		0.01	0.47
		Cr/At	T/H
		0.06	1.00
		Cr/Cl	T/NH-Ca
		***	0.20
		Cr/Cb	T/Cl
		0.74	*
		Cr/P	T/NCl-Pl
		*	1.00
		At/Cl	I/L
		**	***
		At/Cb	I/NI-NL-S
		0.69	**
		At/P	I/H
		1.00	***
		Cl/Cb	I/NH-Ca
		***	*
		Cl/P	I/Cl
		*	***
		Cb/P	I/NCl-Pl
		0.48	***
			L/NI-NL-S
			***
			L/H
			0.69
			L/NH-Ca
			***
			L/Cl
			0.93
			L/NCl-Pl
			0.30
			NI-NL-S/H
			0.27
			NI-NL-S/NH-Ca
			1.00
			NI-NL-S/Cl
			***
			NI-NL-S/NCl-Pl
			0.65
			H/NH-Ca
			0.10
			H/Cl
			0.07
			H/NCl-Pl
			1.00
			NH-Ca/Cl
			***
			NH-Ca/NCl-Pl
			0.34
			Cl/NCl-Pl
			**

Group abbreviations are given in Figure 7 caption. $^{*}p < 0.05$, $^{**}p < 0.01$, $^{***}p < 0.001$.

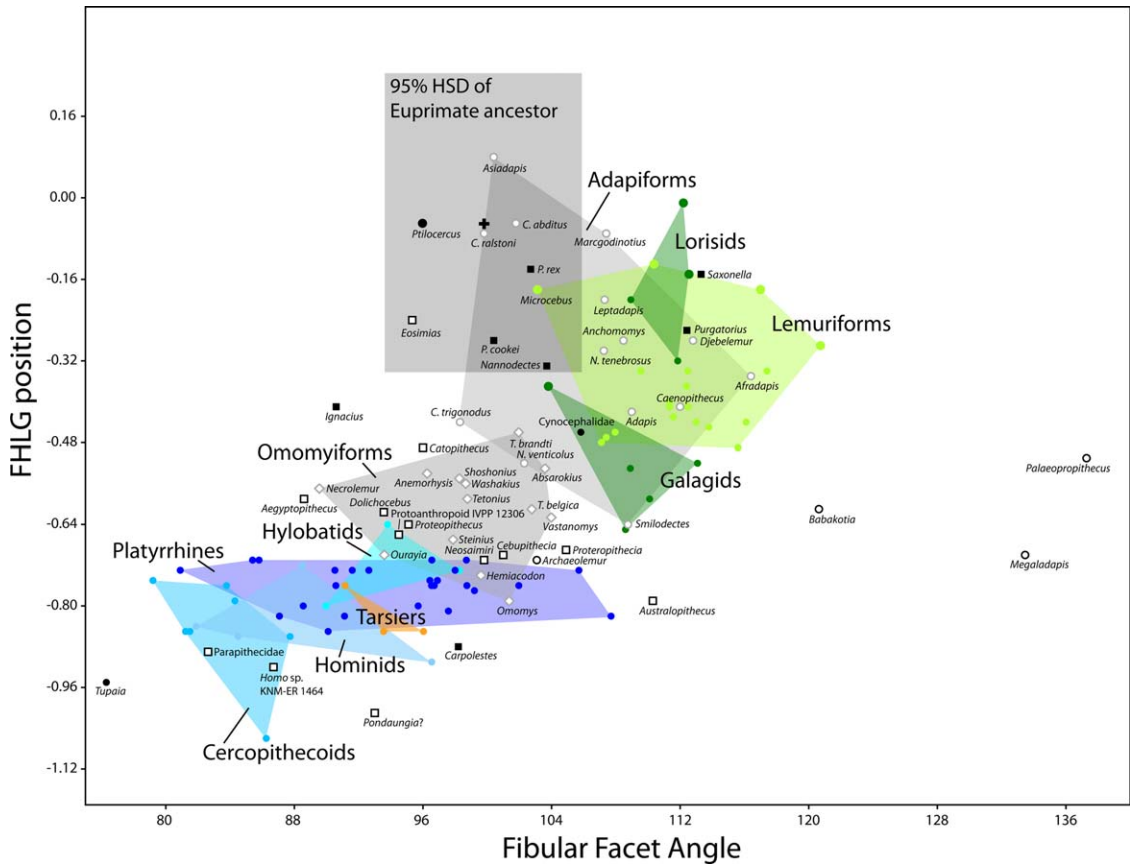

FIGURE 8 Plot of species mean values of fibular facet angle and FHLG Position. Although there appears to be a positive correlation between these two variables, phylogenetic generalized least squares does not recover a significant relationship for all euarchontans (Table 7). A significant negative relationship was recovered within strepsirrhines (Table 7). The bold cross represents the mean value for the euprimate ancestral node, and the gray box indicates the 95% Bayesian highest probability density interval for the ancestral values of both variables. ASR for fibular facet angle was taken from Boyer et al. (2015). Black circles indicate non-primate euarchontans; black open squares, fossil anthropoids; black open circles, subfossil lemurs. All other groups are labeled. Note that many fossil taxa are represented by a single individual (Table 3), and may display a greater level of variance than extant species

position of the FHLG being primitive within Euarchonta, Euprimates, and Haplorhini. Lateral placement of the FHLG at crown Haplorhini is an unexpected result, but is supported by the presence of a laterally positioned FHLG in stem anthropoids (*Eosimias*), as well as basal crown anthropoids (*Catopithecus*, *Aegyptopithecus*, *Dolichocebus*), and basal omomyiforms such as *Teilhardina brandti*. These observations suggest

TABLE 7 Phylogenetic generalized least squares (PGLS) regressions between FHLG position and fibular facet angle (FFa)

Sample	Dependent	Independent	Method	*n*	Slope	Slope 95% CI	Intercept	Intercept 95% CI	r^2	*p*	Lambda	Lambda 95% CI
Euarchontans	FHLG Position	FFa	PGLS	122	0.00	(−0.003, 0.006)	−0.49	(−1.041, 0.064)	0.00	0.58	1.00	(0.927, NA)
Primates			PGLS	119	0.00	(−0.004, 0.005)	−0.39	(−0.847, 0.101)	0.00	0.77	1.00	(0.974, NA)
Euprimates			PGLS	112	0.00	(−0.005, 0.003)	−0.21	(−0.683, 0.266)	0.00	0.50	1.00	(0.949, NA)
Haplorhines			PGLS	65	0.00	(−0.002, 0.006)	−0.72	(−1.107, −0.331)	0.02	0.24	1.00	(0.964, NA)
Strepsirrhines			**PGLS**	**47**	**−0.01**	**(−0.021, −0.002)**	**1.01**	**(0.012, 2.015)**	**0.12**	*	**0.98**	**(0.601, NA)**
Anthropoids			PGLS	50	0.00	(−0.001, 0.006)	−0.50	(−0.861, −0.136)	0.03	0.21	0.99	(0.951, NA)
Prosimians			PGLS	62	−0.01	(−0.016, 0.000)	0.42	(−0.428, 1.259)	0.06	0.06	0.90	(0.638, 0.996)
Platyrrhines			PGLS	30	0.00	(−0.005, 0.002)	−0.54	(−0.865, −0.211)	0.02	0.43	0.91	(0.655, 0.985)
Lemuriforms			PGLS	23	0.00	(−0.009, 0.005)	−0.21	(−1.034, 0.605)	0.02	0.56	1.00	(0.872, NA)

Bold text indicates significant relationships. Tree used for PGLS available in Supporting Information Tree S2. $^*p < 0.05$, $^{**}p < 0.01$, $^{***}p < 0.001$.

TABLE 8 Phylogenetic generalized least squares (PGLS) regressions between FHLG position and first principal component score of medial tibial facet morphology (MTF PC1)

Sample	Dependent	Independent	Method	*n*	Slope	Slope 95% CI	Intercept	Intercept 95% CI	r^2	*p*	Lambda	Lambda 95% CI
Euarchontans	FHLG Position	MTF PC1	PGLS	119	−0.03	(−0.058, 0.002)	−0.34	(−0.657, −0.015)	0.03	0.06	1.00	(0.966, NA)
Primates			PGLS	116	−0.03	(−0.056, 0.003)	−0.29	(−0.481, −0.107)	0.03	0.08	1.00	(0.976, NA)
Euprimates			PGLS	109	0.00	(−0.029, 0.031)	−0.36	(−0.576, −0.138)	0.00	0.96	1.00	(0.968, NA)
Haplorhines			PGLS	64	−0.01	(−0.030, 0.028)	−0.51	(−0.664, −0.354)	0.00	0.95	1.00	(0.968, NA)
Strepsirrhines			PGLS	45	0.01	(−0.061, 0.078)	−0.19	(−0.362, −0.017)	0.00	0.81	1.00	(0.846, NA)
Anthropoids			PGLS	49	−0.01	(−0.036, 0.025)	−0.27	(−0.347, −0.189)	0.00	0.72	1.00	(0.960, NA)
Prosimians			PGLS	60	0.00	(−0.058, 0.065)	−0.38	(−0.622, −0.142)	0.00	0.91	0.97	(0.791, NA)
Platyrrhines			OLS	29	0.01	(−0.033, 0.034)	−0.76	(−0.779, −0.700)	0.01	0.63	–	–
Lemuriforms			PGLS	23	−0.03	(−0.073, 0.009)	−0.47	(−0.702, −0.232)	0.11	0.12	1.00	(0.905, NA)

Bold text indicates significant relationships. Tree used for PGLS available in Supporting Information Tree S2. $^{*}p < 0.05$, $^{**}p < 0.01$, $^{***}p < 0.001$.

that anthropoids and tarsiiforms evolved a medially positioned FHLG in parallel from ancestors that were more strepsirrhine-like in this feature.

5.2 | Functional interpretations of FHLG position

The primary hypothesis for the functional significance of a laterally positioned FHLG is its correlation with inverted and abducted foot postures on small diameter vertical supports, best exemplified by extant strepsirrhines (Gebo, 1986a; 1988, 2011). We predicted that laterally positioned FHLGs would be observed in taxa with larger fibular facet angles (P3a), expanded medial tibial facets (P3b), and larger body masses (P3c), as these factors may correlate with habitual use of inverted and abducted foot postures. However, regressions of FHLG Position against these three features provide no support for a relationship between a laterally positioned FHLG and strepsirrhine-like inverted and abducted foot postures.

Considering that strepsirrhines are not the only euarchontans that exhibit a laterally positioned FHLG, it is perhaps not surprising that our analyses do not support a functional relationship between FHLG position and strepsirrhine-like foot postures. While all strepsirrhines (with the exception of certain subfossil lemuriforms) have laterally positioned FHLGs, dermopterans, ptilocercids, *Eosimias*, and all plesiadapiforms (except *Carpolestes*) exhibit a similar FHLG morphology. Dermopterans and many plesiadapiforms use (or have been argued to use [Beard, 1991; Boyer and Bloch, 2008]) large diameter vertical supports. Being particularly small-bodied (~42.5g [Smith et al., 2003]), ptilocercids likely more frequently encounter relatively large diameter supports, and first-hand accounts by Le Gros Clark (1927) describe *Ptilocercus* as being perfectly adept on flat vertical surfaces via claw clinging. On large diameter vertical supports, increased abduction of the foot increases the central angle subtended by the pedal distal phalanges (Cartmill, 1985; Gebo, 1986a), and improves the grip by increasing the component of the adduction force that is normal to the points of contact (Cartmill, 1985). When the foot is dorsiflexed, abduction of the foot at the talocrural joint will rotate the FHLG medially. Eventually, a large degree of abduction will compromise the FHLG's ability to serve as a trochlea in the line of action of the FHL tendon. Thus, a more lateral position may maintain the FHLG's ability to resist forces of the FHL tendon while the foot is dorsiflexed and abducted (Figure 11). This functional interpretation for lateral positioning of the FHLG is largely in accord with that proposed by Gebo (1986a; 1993, 2011), but emphasizes the importance of abducted foot postures on vertical supports, rather than strepsirrhine-like abducted and inverted foot postures.

Decoupling the movements and morphological indicators of abduction and inversion as well as considering the relationship between body size and relative substrate size helps resolve why our results do not support our predictions. Recent functional interpretations for both fibular facet angle (Boyer and Seiffert, 2013) and medial tibial facet morphology (Boyer et al., 2015) focus primarily on inversion, not abduction, at the talocrural joint. Provided these functional interpretations are correct, the absence of a significant relationship between FHLG Position and medial tibial facet morphology is not surprising.

Furthermore, although we recover significant relationships between FHLG Position and FFa among strepsirrhines (Table 7), the direction of the correlation is opposite our prediction (i.e., as fibular facet angle increases, the FHLG becomes more medially positioned). However, it seems likely that the relationship between FFa and FHLG Position is complicated by correlations with body size: Boyer and Seiffert (2013) recover significant positive allometric relationships between body size proxies and fibular facet angle among platyrrhines, strepsirrhines, and lemuriforms (i.e., fibular facet angle becomes more obtuse as body size increases), while we recover negative allometric relationships between body mass and FHLG Position in anthropoids and lemuriforms (i.e., the FHLG becomes more medially positioned as body size increases) (Table 3). Small-bodied taxa (e.g., *Microcebus* and *Saguinus*) tend to exhibit both steeper fibular facets and more laterally positioned FHLGs, while large-bodied taxa (e.g., *Propithecus* and *Ateles*)

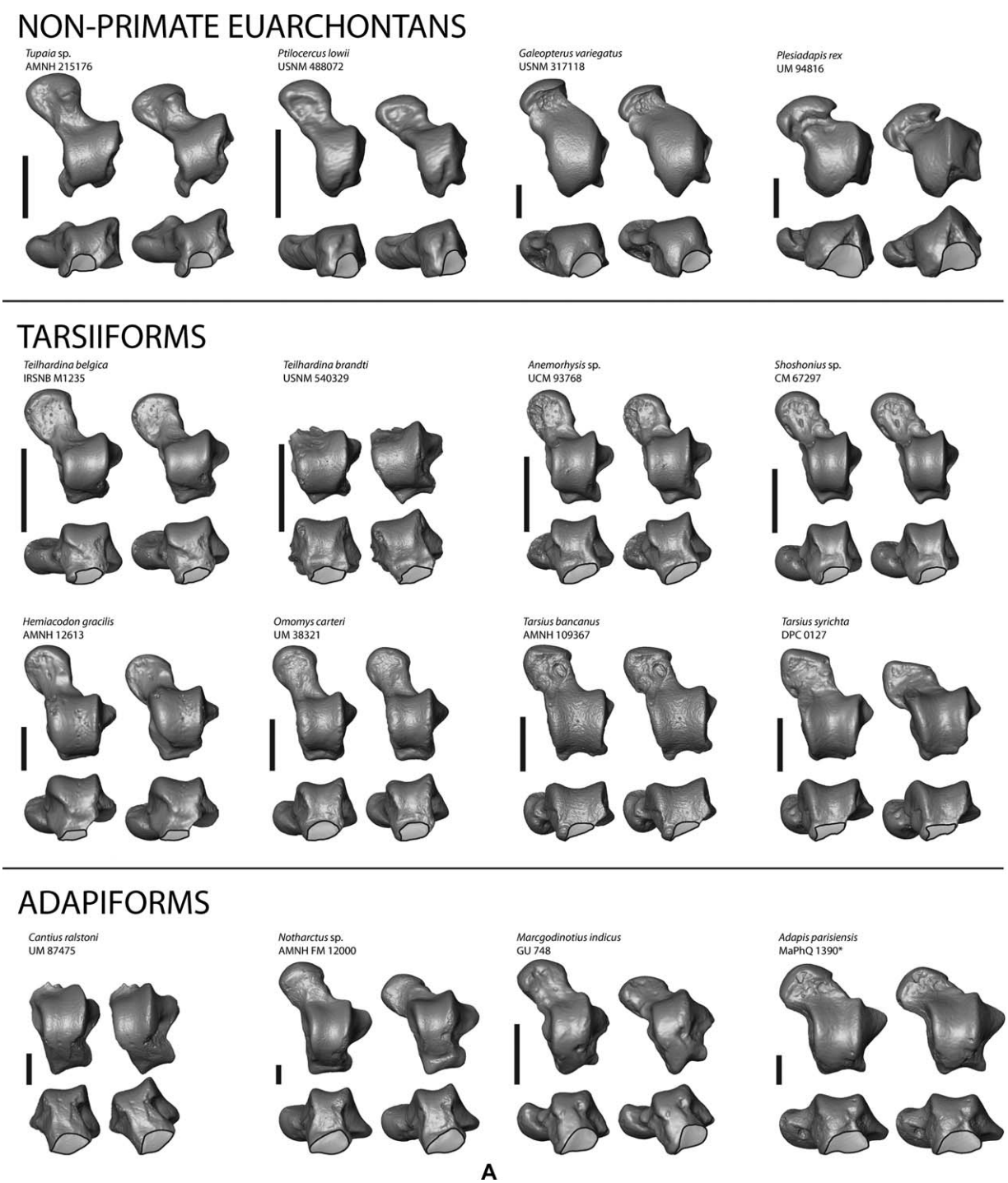

FIGURE 9 Comparative plates of select extant and extinct euarchontan species showing FHLG morphology. (a) noneuprimate euarchontans, tarsiiforms, and adapiforms. (b) lorisiforms, lemuriforms, and subfossil lemurs. (c) extant and fossil anthropoids. Clockwise, the views for each specimen are dorsal, aligned to reference axis through lateral trochlear rim, FHLG aligned to path of tendon, and posterior. * indicates chirality has been reversed for consistency. Scale bars equal 3 mm

tend to exhibit more obtuse fibular facets and more medially positioned FHLGs. We feel this combination of features can be best explained by considering abduction and inversion separately, and that relatively large diameter supports increase abduction and decrease inversion of the foot in small-bodied taxa.

The proposed functional relationship between these four variables (body size, fibular facet angle, medial tibial facet morphology, and FHLG position) matches the observed talar morphology of cheirogaleids well: small body size may increase the use of abducted foot postures (reflected by an extremely lateral FHLG position) while

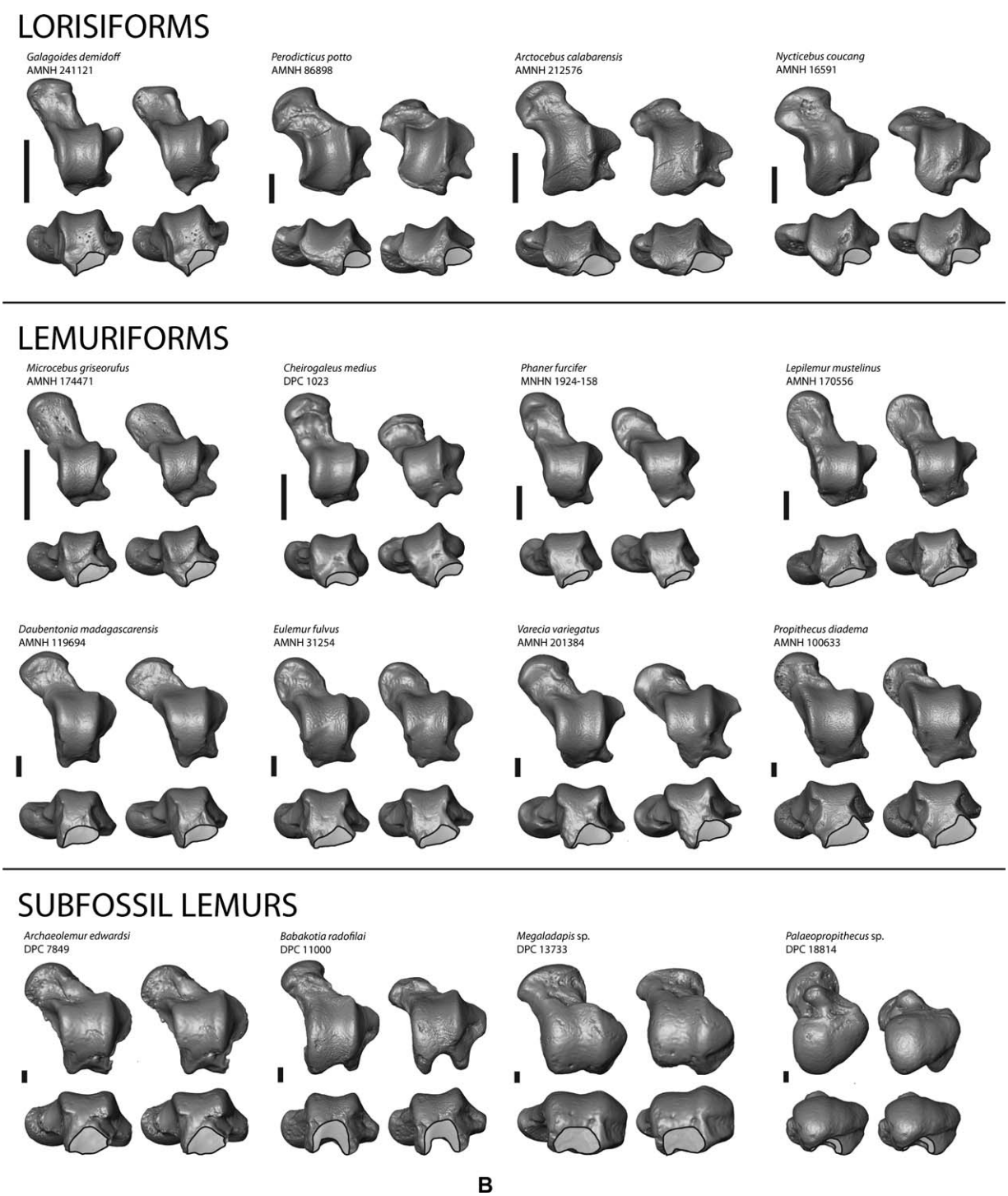

FIGURE 9 (Continued)

decreasing the use of inverted foot postures (reflected by a steep fibular facet angle [Boyer and Seiffert, 2013] and a relatively small medial tibial facet [Boyer et al., 2015]). While several studies examine the relationship between substrate size and gait kinematics of cheirogaleids (e.g., Stevens, 2008; Shapiro, Kemp, & Young, 2016), we know of no studies that examine cheirogaleid foot posture and the degree of inversion or abduction on a variety of substrate sizes. However, Gebo (1989) measured joint mobility in several tarsal joints, including the degree of abduction and adduction at the talocrural joint. In his study, cheirogaleids exhibited the second greatest range of motion (lorisids, which also have very laterally positioned FHLGs, displayed the most abduction-adduction). Our proposed relationship is also bolstered by a

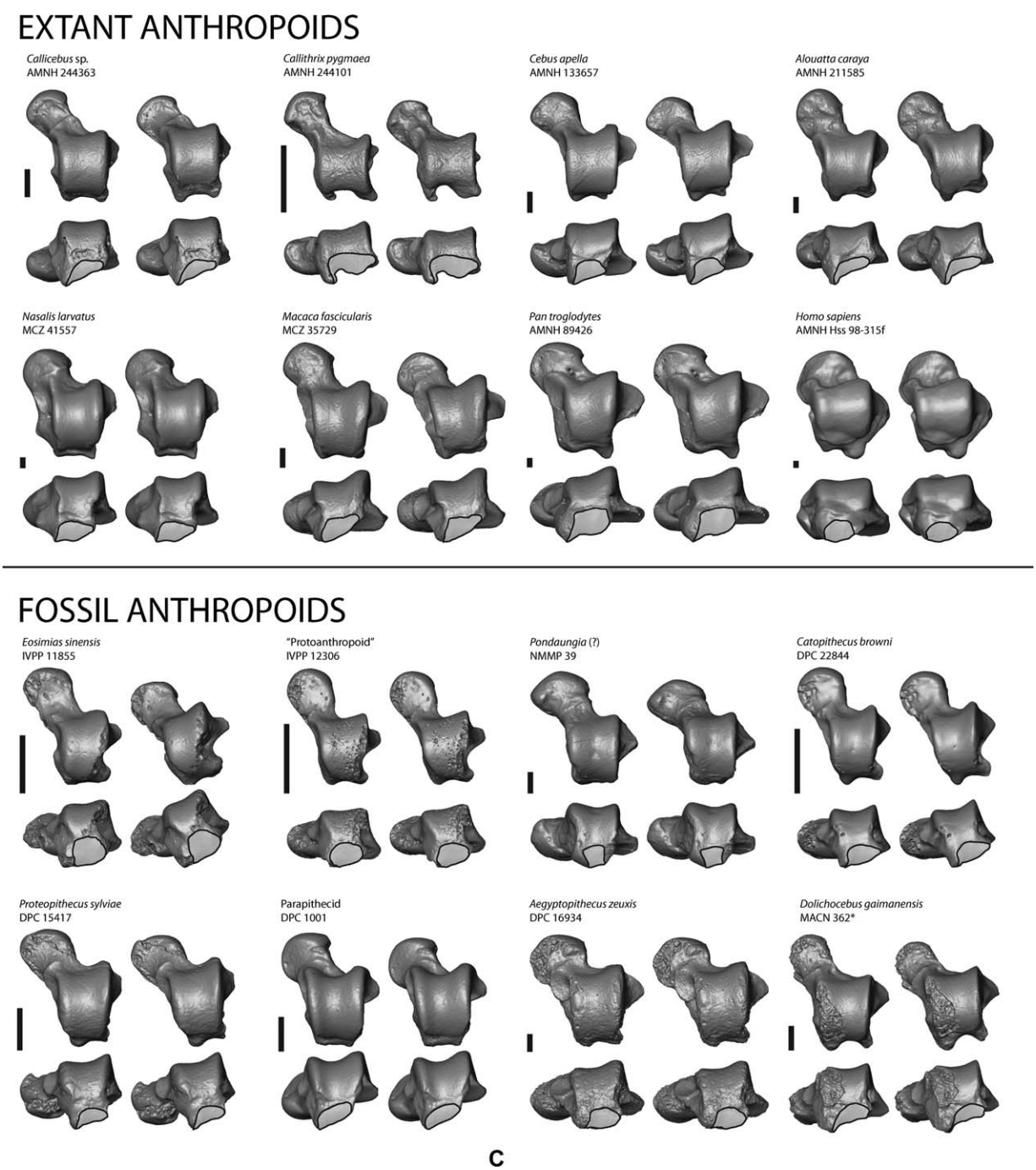

FIGURE 9 (Continued)

similar combination of talar features in other small-bodied euarchontans such as *Ptilocercus* and *Eosimias* which are not phylogenetically close to cheirogaleids.

The relationships between fibular facet angle, medial tibial facet morphology, and FHLG position become more evident when these three quantified variables are visualized with principal components analysis (Figure 12). When generated from the correlation matrix of FFa, MTF PC1, and FHLG Position, the first principal component explains 67.9% of the total variance; PC1 is strongly positively correlated with FFa (0.85) and FHLG Position (0.82) and strongly negatively correlated with MTF PC1 (-0.80). The second principal component explains 18.2% of the total variance, and is moderately correlated with MTF PC1 (0.58) and FHLG Position (0.45), and weakly correlated with FFa (0.11).

The PCA plot highlights the importance of considering FHLG position in overall talar morphology, as taxonomic groups are well differentiated from one another. While the bivariate plot of fibular facet angle to relative MTF area presented by Boyer et al. (2015, their Figure 11) separates extant haplorhines and strepsirrhines, there is substantial overlap between plesiadapiforms and anthropoids. When FHLG

TABLE 9 Mean estimates and 95% highest probability density intervals of ancestral state reconstructions of select nodes

		FHLG position			FHLG ellipse		
Node	Node #	Mean	Lower	Upper	Mean	Lower	Upper
Crown Scandentia	1	−0.023	−0.569	0.568	0.668	0.119	1.237
Crown Primatomorpha	2	0.309	−0.291	0.911	0.864	0.411	1.308
Purgatorius + crown Primates	3	0.019	−0.321	0.348	0.997	0.629	1.353
Paromomyidae + crown Primates	4	−0.012	−0.324	0.292	1.081	0.730	1.429
Plesiadapoidea + crown Primates	5	−0.035	−0.314	0.269	1.177	0.825	1.526
Saxonella + Plesiadapoidea	6	−0.271	−0.413	−0.119	1.242	0.956	1.541
Euprimates (crown Primates)	7	−0.051	−0.341	0.244	1.253	0.883	1.633
Adapiformes + crown Strepsirrhini	8	−0.073	−0.254	0.115	1.288	0.953	1.634
Anchomomys + crown Strepsirrhini	9	−0.151	−0.329	0.027	1.391	1.057	1.734
Djebelemur + crown Strepsirrhini	10	−0.170	−0.332	−0.011	1.450	1.130	1.760
Crown Strepsirrhini	11	−0.162	−0.343	0.028	1.345	0.964	1.731
Crown Lemuriformes	12	−0.184	−0.438	0.080	1.211	0.762	1.692
Crown Lemuriformes excl. *Daubentonia*	13	−0.300	−0.480	−0.120	1.097	0.666	1.510
Archaeolemuridae + Indrioidea	14	−0.350	−0.528	−0.176	1.183	0.774	1.592
Crown Indrioidea	15	−0.350	−0.516	−0.187	1.203	0.787	1.613
Crown Indriidae	16	−0.321	−0.472	−0.164	1.598	1.204	1.979
Propithecus + *Avahi*	17	−0.307	−0.457	−0.162	1.956	1.572	2.339
Propithecus	18	−0.324	−0.434	−0.217	2.073	1.758	2.391
Lepilemuridae + Cheirogaleidae	19	−0.286	−0.460	−0.109	1.233	0.827	1.642
Crown Cheirogaleidae	20	−0.241	−0.420	−0.061	1.184	0.767	1.618
Microcebus + *Mirza*	21	−0.278	−0.443	−0.124	1.281	0.904	1.671
Megaladapis + Lemuridae	22	−0.361	−0.544	−0.174	0.901	0.466	1.328
Crown Lemuridae	23	−0.362	−0.523	−0.187	1.084	0.676	1.500
Lemuridae excl. *Varecia*	24	−0.368	−0.533	−0.209	1.227	0.821	1.633
Lemur-Prolemur-Hapalemur	25	−0.389	−0.494	−0.288	1.491	1.168	1.814
Eulemur	26	−0.439	−0.521	−0.356	1.278	0.991	1.583
Crown Lorisiformes	27	−0.164	−0.380	0.065	1.063	0.595	1.517
Crown Lorisidae	28	−0.143	−0.363	0.079	0.903	0.447	1.360
Crown Galagidae	29	−0.314	−0.529	−0.114	1.247	0.783	1.696
Crown Galagidae excl. *Euoticus*	30	−0.492	−0.633	−0.349	1.545	1.183	1.917
Asiadapinae	31	0.005	−0.079	0.086	1.134	0.914	1.356
Adapidae + Notharctidae	32	−0.097	−0.240	0.055	1.260	0.957	1.575
Adapidae	33	−0.339	−0.456	−0.219	0.836	0.525	1.151
Caenopithecinae	34	−0.370	−0.460	−0.281	0.747	0.492	1.002
Adapinae	35	−0.309	−0.379	−0.244	0.795	0.572	1.010
Notharctidae	36	−0.116	−0.239	0.005	1.376	1.111	1.642
Notharctidae excl. *C. ralstoni*	37	−0.163	−0.266	−0.059	1.365	1.128	1.604
Notharctidae excl. *Notharctus* and basal *Cantius*	38	−0.195	−0.279	−0.108	1.261	1.052	1.474

(Continues)

TABLE 9 (Continued)

Node	Node #	FHLG position			FHLG ellipse		
		Mean	Lower	Upper	Mean	Lower	Upper
Crown Haplorhini	39	−0.287	−0.542	−0.034	1.435	1.047	1.813
Tarsiiformes	40	−0.463	−0.623	−0.306	1.558	1.263	1.871
Tarsiiformes excl. *Steinius* and *Teilhardina*	41	−0.537	−0.644	−0.431	1.604	1.370	1.849
Microchoerinae + Tarsiidae	42	−0.557	−0.749	−0.353	1.583	1.201	1.970
Eosimias + crown Anthropoidea	43	−0.267	−0.366	−0.167	1.469	1.190	1.757
Parapithecoidea + crown Anthropoidea	44	−0.513	−0.635	−0.388	1.247	0.926	1.578
Parapithecoidea	45	−0.646	−0.726	−0.564	1.383	1.122	1.629
Crown Anthropoidea	46	−0.512	−0.637	−0.394	1.101	0.777	1.437
Catopithecus + Catarrhini	47	−0.504	−0.582	−0.424	0.976	0.715	1.235
Aegyptopithecus + Catarrhini	48	−0.578	−0.661	−0.498	1.102	0.832	1.363
Crown Catarrhini	49	−0.689	−0.857	−0.523	1.206	0.801	1.620
Crown Hominoidea	50	−0.728	−0.869	−0.596	1.174	0.778	1.543
Crown Hominidae	51	−0.745	−0.879	−0.614	1.052	0.702	1.432
Crown Homininae	52	−0.792	−0.882	−0.703	1.054	0.751	1.370
Pan + *Homo*	53	−0.794	−0.869	−0.719	1.080	0.800	1.356
Australopithecus + *Homo*	54	−0.810	−0.875	−0.746	1.129	0.880	1.371
Crown Cercopithecoidea	55	−0.802	−0.940	−0.667	1.364	0.991	1.748
Dolichocebus + crown Platyrrhini	56	−0.621	−0.718	−0.521	0.805	0.507	1.110
Crown Pitheciidae	57	−0.667	−0.767	−0.569	1.132	0.804	1.451
Proteropithecia + crown Pitheciinae	58	−0.680	−0.752	−0.615	1.266	1.014	1.522
Cebupithecia + crown Pitheciinae	59	−0.693	−0.761	−0.625	1.041	0.791	1.299
Crown Atelidae + crown Cebidae	60	−0.644	−0.756	−0.536	0.900	0.570	1.240
Crown Atelidae	61	−0.693	−0.828	−0.556	0.840	0.469	1.214
Cebus + *Saimiri*	62	−0.680	−0.786	−0.572	1.060	0.725	1.387
Crown Callitrichidae	63	−0.701	−0.820	−0.582	0.584	0.249	0.943

Reconstructions based on values in Tables 1 and 2. Phylogenetic tree available in Supporting Information Tree S2. Supporting Information Table S3 provides node value estimates for phylogeny excluding plesiadapiforms. Supporting Information Figure S1 indicates node numbers.

position is included, the level of taxonomic separation achieved with only three quantified features is rather remarkable, and is a testament to the original descriptions of talar morphological variation within primates (e.g., Beard et al., 1988; Covert, 1988; Dagosto, 1988; Gebo, 1986, 1988). Plesiadapiforms and non-euprimate euarchontans (except *Tupaia* sp.) are well separated from both haplorhines and strepsirrhines. The similarities of these taxa suggest that this region of the morphospace would likely encapsulate the ancestral euarchontan morphotype (ASRs for the root node of our phylogeny [=ancestral euarchontan] were not available for all variables). The potential position of the ancestral euprimate is less obvious, as the earliest euprimates represented by tarsal elements (*Teilhardina* sp. and *Cantius ralstoni*) are separated from the non-euprimate euarchontan group. However, when the ASR values for the ancestral euprimate are plotted in the morphospace of Figure 12, the mean value for the ancestral euprimate falls within the non-euprimate euarchontan polygon, near *Ptilocercus lowii*, *Purgatorius* sp., and *Eosimias sinensis*. Among primates, cheirogaleids are separated from other extant lemuriforms and plot between noneuprimate euarchontans and adapiforms. Adapiforms overlap substantially with extant strepsirrhines, while omomyiforms are intermediate between extant haplorhines and strepsirrhines. Implications for several fossil taxa are also discussed further below.

While there are other unique characteristics of euprimate pedal grasping (i.e., nail-bearing digits and a strongly divergent hallux), these features do not appear to be correlated with FHLG position based on the patterns of variation in euprimate outgroups and within euprimates. Among euprimates, *flexor hallucis longus* most frequently inserts into the distal phalanges of the hallux and the third and fourth rays (Langdon, 1990). Provided this typical insertion pattern holds for other euarchontans, abducted foot postures could potentially improve the

TABLE 10 Estimated marginal likelihoods for different evolutionary models and scaling parameters

Variable	Scaling parameter	Directional model Harmonic mean	Random walk Harmonic mean
FHLG position	None	39.071	36.208
	Delta	**53.679**	50.541
	Kappa	44.694	41.102
	Lambda	37.582	32.271
FHLG ellipse	None	−62.121	−61.496
	Delta	−64.131	−61.496
	Kappa	−61.935	**−56.383**
	Lambda	−57.719	−57.156

Bold text indicates model and scaling parameter with highest likelihood. Results for phylogeny excluding plesiadapiforms can be found in Supporting Information Table S4.

grip of both claw-bearing (dermopterans, scandentians, plesiadapiforms, callitrichines, and *Euoticus*) and nail-bearing taxa (all other euprimates). The lateral position of the FHLG in dermopterans, ptilocercids, and most plesiadapiforms also suggests that hallucal grasping is not a prerequisite for a laterally positioned FHLG.

Tarsiers, which both uses vertical postures (sometimes on large diameter supports) and have a medially positioned FHLG, seem to refute the proposed link between abducted foot postures and FHLG position. However, tarsiers have a number of unique morphological features that restrict mobility at the upper and lower ankle joints yet increase mobility at other hind limb joints. Most obviously, tarsiers are unique among living euarchontans in having a fused distal tibia and fibula, which likely limits abduction at the talocrural joint. Additionally, Jouffroy et al. (1984) emphasize that, in tarsiers, a symmetrical talar trochlea and a flat calcaneocuboid joint reduce mobility in the proximal tarsus (i.e., from the talocrural to the transverse tarsal joint). Thus, Jouffroy et al. (1984) argue these joints function primarily in a parasagittal plane, with little to no lateral deviation. Also noting the flat calcaneocuboid joint in tarsiers, Gebo (1987a) suggested that much of the rotational mobility of the tarsier foot was achieved by movement at the proximal and distal ends of the navicular, while the calcaneus remained stationary. Increased mobility at the talonavicular and naviculocuneiform joints may reduce the amount of mobility required at the upper and lower ankle joints. Finally, tarsiers have additional osteological features that may increase capacity for greater lateral rotation at the knee joint (White and Gebo, 2004) and greater abduction at the hip (Anemone, 1990). Thus, though ankle mobility is restricted to dorsi- and plantarflexion, tarsiers may be capable of abduction of the foot through increased lateral rotation of the hind limb at the knee and hip, obviating the need for a laterally positioned FHLG.

Though appealing, the preceding interpretation is complicated by the observation that galagos, which lack tarsier-like specializations (Schultz, 1963; Gebo, 1987a), have a more medially positioned FHLG than other strepsirrhines. However, galagos and tarsiers do both exhibit extreme elongation of the navicular and distal calcaneus (Boyer et al. 2013a; Hall-Craggs, 1965; Moyà-Solà, Köhler, Alba, & Roig, 2012). It is possible that an elongate distal calcaneus and navicular reduce the demands for abduction (in degrees of outward rotation), since a relatively longer foot can subtend a greater arc around a substrate of a given diameter while incurring less outward angular rotation (abduction). The lateral FHLG position of *Euoticus*, the needle-clawed bushbaby, is exceptional among galagos, but this taxon also has unique feeding behavior, frequently claw-clinging on large diameter vertical supports to access exudates (Charles-Dominique, 1977). If vertical postures require greater foot abduction, then the morphology of *Euoticus* also supports a relationship between abduction and lateral positioning

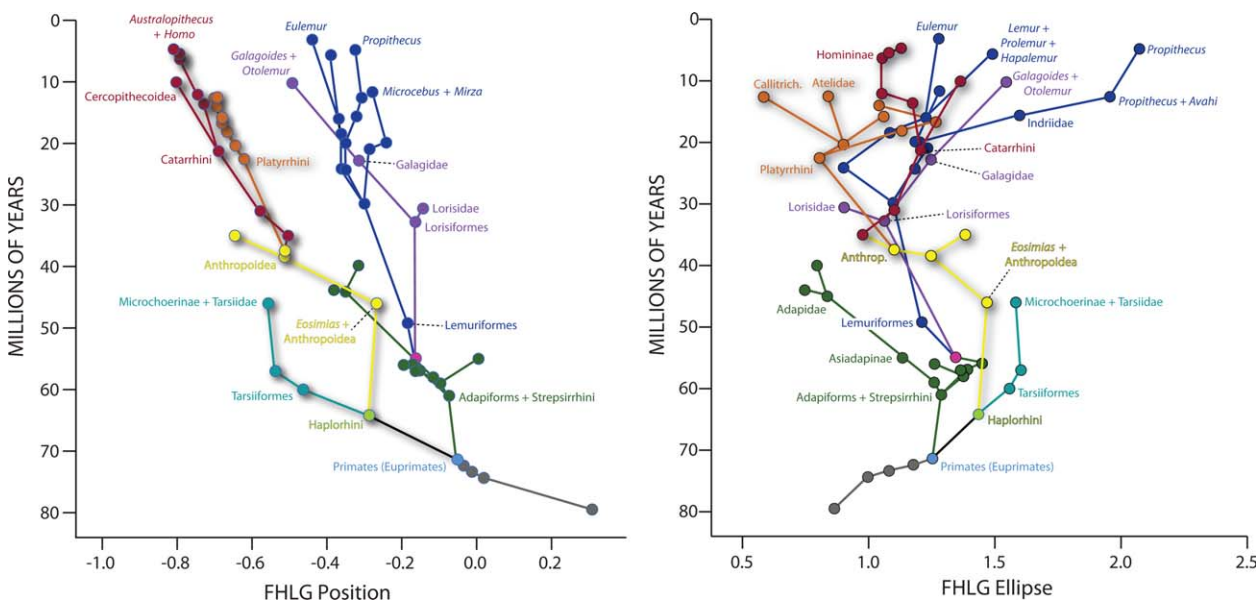

FIGURE 10 Ancestral state reconstruction of FHLG position (A) and FHLG Ellipse (B) for select nodes of the euarchontan tree. Mean estimates and confidence intervals are presented in Table 9

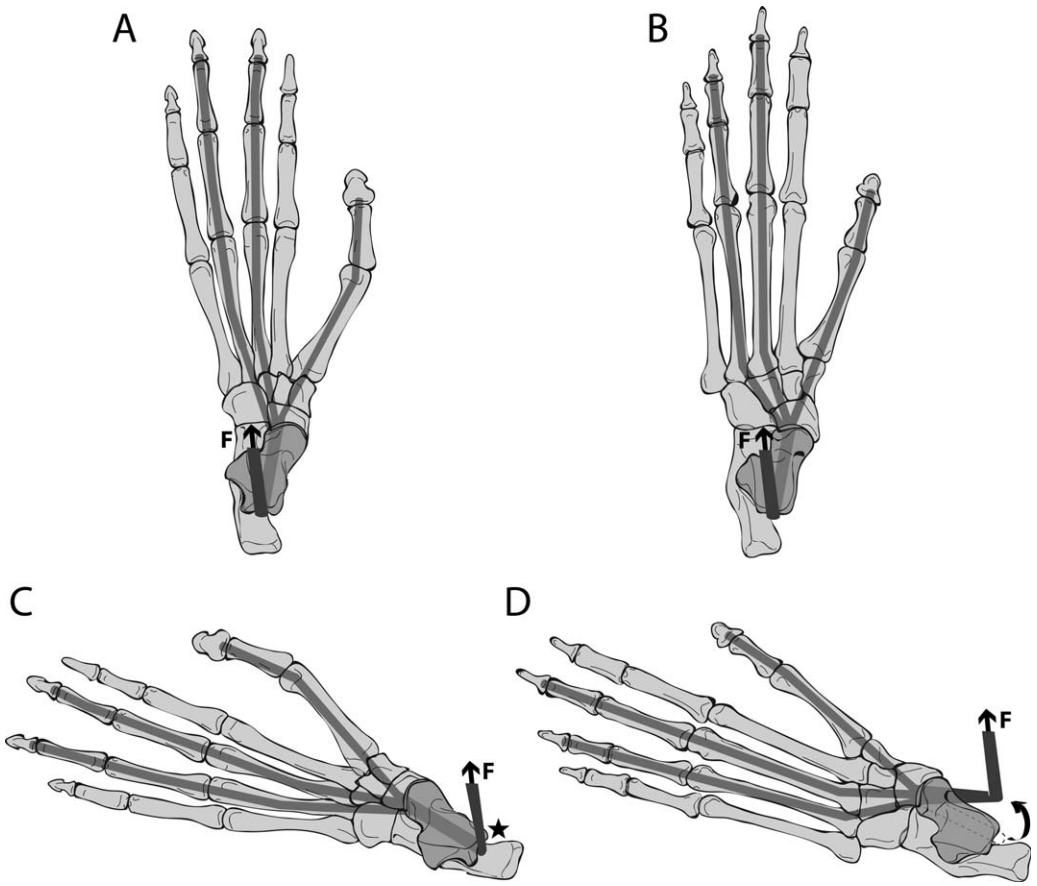

FIGURE 11 Functional interpretation of FHLG position. (a) neutral foot position in *Varecia*, (b) neutral position in *Macaca*, (c) abducted foot position in *Varecia*, (d) abducted foot position in *Macaca*. A laterally positioned FHLG faces posterolaterally in a neutral position (a), so that as the foot becomes highly abducted, the groove is still buttressed on its medial aspect (indicated by the star in c). A medially positioned FHLG faces posteriorly in a neutral position (b), so that as the foot becomes highly abducted, the tendon may become displaced medially (indicated by the arrow in d). Dark gray lines indicate paths of the *flexor hallucis longus* tendons, and insertion patterns follow Langdon (1990). Arrow indicated by F shows direction of force generated by the *flexor hallucis longus*. Tibia and fibula are not shown for simplicity, and abduction has been exaggerated at the talocrural joint. Drawing of *Varecia* foot modified from Boyer et al. (2007)

of the FHLG. *Euoticus* is also the sister taxon of all other extant galagids (Pozzi et al., 2014) and plesiomorphically retains less distal calcaneal elongation (relative to body mass) than any other galagid (Boyer et al., 2013a), potentially requiring greater abduction on large vertical supports than that required by galagids with more elongate distal calcaneus and navicular.

Although there is a large amount of diversity within the clade (e.g., Dunn, Sybalsky, Conroy & Rasmussen, 2006; Gunnell and Rose, 2002; Tornow, 2008), omomyiforms are generally small-bodied taxa (<500 g) that have been compared favorably with cheirogaleids (Cartmill, 1972, 1975; Dagosto, Gebo, & Beard, 1999; Gebo, 1987a, 2011), which would suggest that omomyiforms should have laterally positioned FHLGs. However, it is possible that increased rotational mobility at other hind limb joints and/or elongation of the foot may also explain why the omomyiforms in our sample exhibit fairly medially positioned FHLGs. For example, the prominence of tibial intercondylar spines of some omomyiforms resemble *Tarsius* and strepsirrhines: White and Gebo (2004) describe a specimen attributed to *Hemiacodon* as having a "very reduced medial spine relative to the lateral" (p. 300), while Dunn et al. (2006) note that *Ourayia* has a single intercondylar spine. Additionally, although omomyiforms do not exhibit tarsier-like elongation of the navicular and distal calcaneus (Boyer et al., 2013a), they achieve an elongate foot through the lengthening of other pedal elements. Several authors have described elongated cuboids and cuneiforms in omomyiforms (Anemone and Covert, 2000; Gebo, 1987a; Szalay, 1976). Ni et al. (2013) showed that the basal haplorhine/omomyiform *Archicebus* has elongated metatarsals. Gebo, Smith, Dagosto, & Smith (2015) described the first metatarsal of *Teilhardina*, and showed this bone to be much longer relative to body mass than in *Microcebus berthae*. Given that *Teilhardina brandti* has a laterally positioned FHLG and that the calcaneus (and presumably other tarsals) become more elongate over the course of omomyiform evolution (Boyer et al., 2013a), it seems reasonable to suggest that evolutionary increases in foot length reduce the demands incurred by abduction at the talocrural joint early in omomyiform evolution, and subsequently permit medial migration of the FHLG. Future discoveries of associated omomyiform tarsals and metatarsals would allow this hypothesis to be tested.

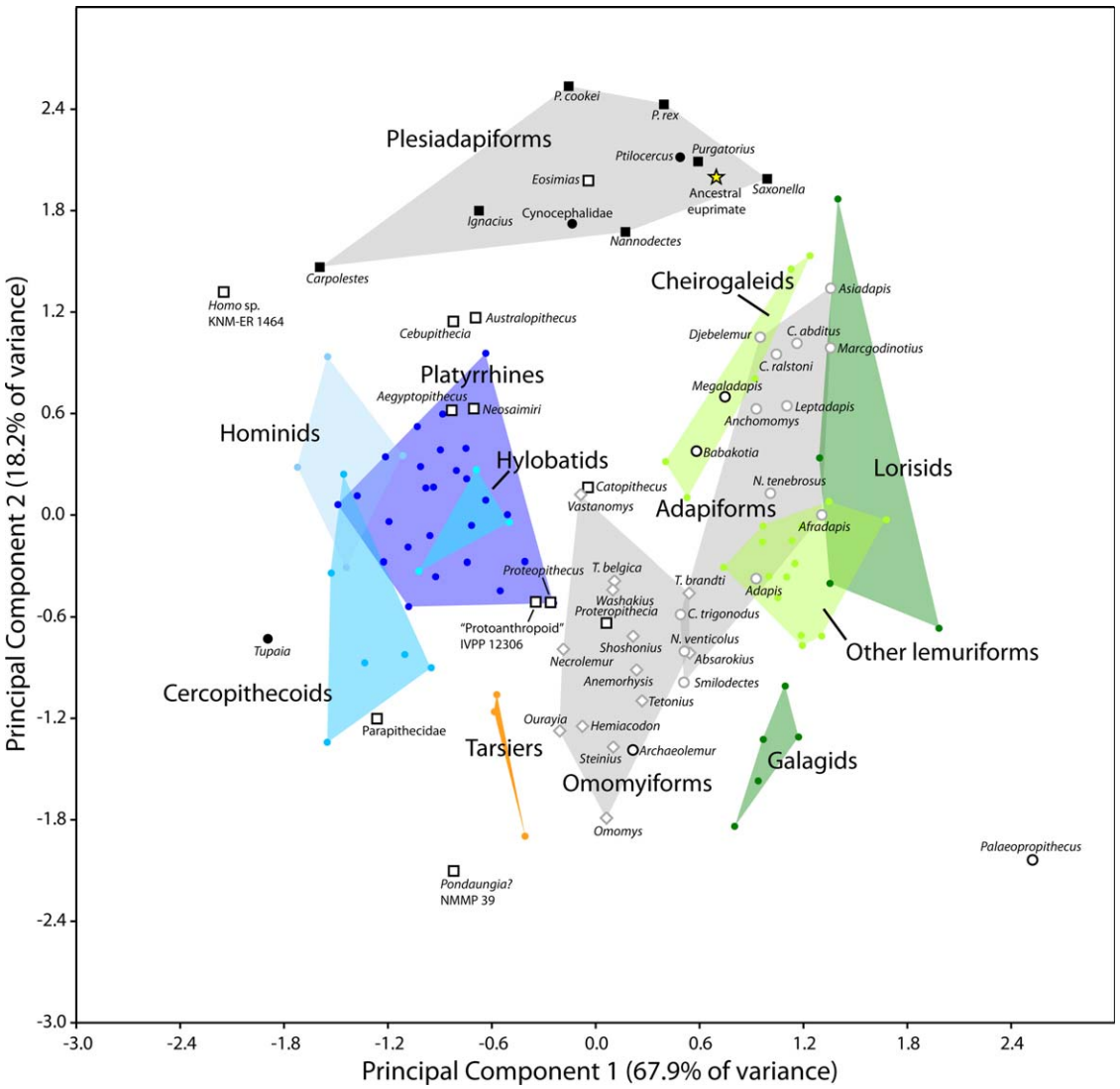

FIGURE 12 Principal components analysis of FHLG Position, fibular facet angle, and medial tibial facet morphology (the first principal component of three MTF variables in Boyer et al., 2015). Black circles indicate non-primate euarchontans; black open squares, fossil anthropoids; black open circles, subfossil lemurs; yellow star, mean value for euprimate ancestral node. All other groups are labeled

5.3 | Functional interpretations of FHLG depth

With the assumption that a deeper groove may accommodate a relatively larger tendon arising from a relatively larger *flexor hallucis longus* muscle, it was hypothesized that increased FHLG depth is an adaptation for increased reliance on pedal grasping (Bloch et al., 2007; Chester et al., 2015; Szalay and Decker, 1974; Szalay and Drawhorn, 1980). Our study allows evaluation of this hypothesis and its assumed mechanism. We predicted that FHLG depth, as measured by FHLG Ellipse, would increase and be positively correlated with body mass, provided that muscle mass scales with slight positive allometry relative to body mass in primates (Muchlinski et al., 2012).[4] However, we recovered a significant relationship only among catarrhines, and the scaling coefficient was opposite our prediction (larger taxa have relatively shallower FHLGs). Additionally, though lorisids exhibit some of the deepest FHLGs and indriids exhibit the shallowest, the *flexor hallucis longus* is a relatively larger muscle in indriids (24% of the total mass of the extrinsic muscles of the foot) than in lorisids (only 16%) (Gebo and Dagosto, 1988). On the basis of these observations, it is difficult to conclude that a deeper FHLG indicates a relatively larger *flexor hallucis longus* muscle per se. This decoupling of an osteological feature and its associated musculature is similar to the lack of correlation between the size of the peroneal process of the first metatarsal and the size of the *peroneus longus* (Argot, 2002; Boyer, Patel, Larson, & Stern, 2007; Gebo, 1987a, 2011; Sargis, Boyer, Bloch, & Silcox, 2007), and serves as an important reminder that seemingly intuitive relationships between osteological and myological structures should be verified among extant taxa before functional interpretations are applied to fossils.

Both Szalay and Decker (1974) and Seiffert et al. (2015) suggest a deeper FHLG may help maintain the tendon's placement in the groove while engaged in certain foot postures, particularly hind limb suspension. By our metric, taxa with the deepest FHLGs include scandentians, dermopterans, lorisids, callitrichines, the adapines *Adapis* and

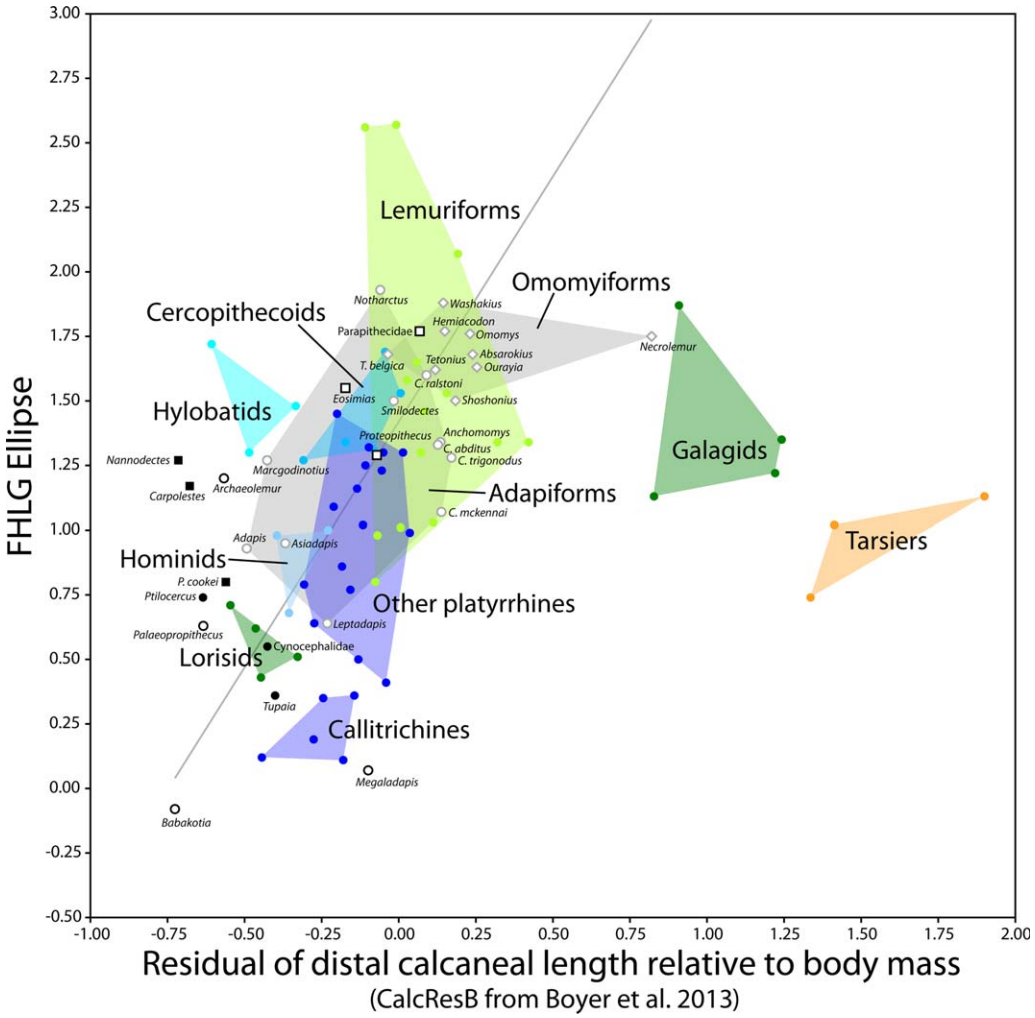

FIGURE 13 Plot of species mean values for Residual B (a measure of distal calcaneal elongation relative to body mass from Boyer et al., 2013a) and FHLG Ellipse. Phylogenetic generalized least squares regression recovers a significant positive relationship when all taxa are included ($n = 89$ species). Gray line indicates RMA regression of all taxa except tarsiers and galagids ($n = 82$ species) (FHLG Ellipse = 0.53*ResB – 0.75; $r^2 = 0.25$; $p < 0.001$). Black circles indicate non-primate euarchontans; black open squares, fossil anthropoids; black open circles, subfossil lemurs. All other groups are labeled. Note that measurements for extant taxa where taken on tali and calcanei of the same individual, the same is not true for fossil taxa

Leptadapis, the caenopithecines *Afradapis* and *Caenopithecus*, and the subfossil lemuriforms *Megaladapis*, *Babakotia*, and *Palaeopropithecus*. These taxa are similar to those with deep FHLGs as measured by Seiffert et al. (2015), and many engage (or have been argued to engage) in occasional or habitual hind limb suspension. Seiffert et al. (2015) argue that the extreme plantarflexion during hind limb suspension increases the possibility of plantar bowstringing of the *flexor hallucis longus* tendon, and a deeper FHLG mitigates this potential biomechanical failure. While callitrichines are not suspensory, they frequently adopt orthograde postures on large vertical supports, utilizing claws (or claw-like nails) to cling to the substrate. In these postures, increasing the depth of the FHLG would increase the possible range of abduction before the tendon slips from its groove (Figure 11). The prominent medial tubercle of callitrichines (Figure 9c) would provide additional protection against high shearing stresses induced by the FHL tendon, and is similar to the strongly developed medial wall of the FHLG in lorises and *Babakotia* (Figure 9b) (Seiffert et al., 2015).

Ancestral state reconstructions (Table 9, Figure 10) suggest that a deep groove was characteristic of basal euarchontans that lacked a large, grasping hallux. Because *flexor hallucis longus* inserts on multiple pedal rays, this may reflect strong digital flexion used to cling to vertical supports, as Beard (1991) and Boyer and Bloch (2008) suggest for several plesiadapiform taxa. The groove was shallow in the ancestral euprimate, which may indicate an increased propensity for leaping. Within strepsirrhines, depth increases in the groove may reflect powerful hallucal grasping in diverse foot postures (including hind limb suspension). With the exception of callitrichines, all anthropoids with a relatively deep groove engage in hind limb suspension (i.e., *Pongo*, *Pithecia*, *Lagothrix*). The deep groove in callitrichines may represent a reversal toward the ancestral euarchontan condition in order to meet biomechanical demands induced by claw-clinging on large diameter vertical supports via strong digital flexion.

While deep FHLGs are associated with strong pedal grasping in diverse foot postures, a shallow FHLG appears to characterize taxa

that are, or are presumed to be, specialized leapers. Our metric indicates that indriids and lepilemurids have almost no appreciable FHLG (one *Avahi* individual has a convex "groove") (Table 1, Figure 6). The tali of many omomyids also exhibit shallow FHLGs, though the FHLGs of tarsiers are not particularly shallow. To test the relationship between FHLG depth and leaping propensity in more detail, we used PGLS to examine the correlation between FHLG Ellipse and the residuals calculated from a regression of absolute distal calcaneal length against body mass (Boyer et al., 2013a; Res B in their Tables 1 and 2) for the 89 euarchontan taxa represented in both studies. In these taxa, the relationship was significant (FHLG Ellipse = 0.34[SE ± 0.17]*ResB + 1.21 [SE ± 0.33], $p = 0.0478$, lambda = 0.964; 95% CI = 0.855–0.997), and indicates that as the distal calcaneus becomes increasingly elongated (relative to body mass), FHLG depth decreases (Figure 13).

A notable exception to the relationship between FHLG depth and calcaneal elongation are tarsiers and galagos, taxa with extremely elongated calcanei but without particularly shallow FHLGs (Figure 13). Both tarsiers and galagos are specialized tarsifulcrumating[5] leapers that generate a large amount of propulsive force through deep and powerful plantarflexion at the talocrural joint. In contrast, indriids and lepilemurids (both of which exhibit very shallow FHLGs) generate most propulsive force at the hip and do not appear to use the foot as a propulsive lever (Demes et al., 1996; though Boyer et al. [2013a] show that many species in these groups still elongate calcanei for their body size). Excursion angles at the talocrural joint for *Galago moholi* (132° ± 8°) and *Otolemur garnetti* (100° ± 9°) (Demes and Günther, 1989) are much higher than the *combined* excursion angles of the ankle, intertarsal, and metatarsophalangeal joints in indriids (<90°) (Demes et al., 1996). Therefore, while leaping from vertical supports, indriids do not combine powerful pedal grasping with the degree of plantarflexion seen in tarsifulcrumating leapers. If a shallow groove increases the possibility that the FHL tendon could bowstring during deep plantarflexion, we would not expect tarsiers and galagos to exhibit notably shallow FHLGs.

It is also plausible that soft tissue structures such as the flexor retinaculum could stabilize the FHL tendon in those taxa with shallow FHLGs, but this does not appear to be the case in indriids or lepilemurids. Gebo's (1986b) description of the flexor retinacula in prosimians does not suggest that indriids have particularly robust flexor retinacula relative to other taxa (though indriids do have an additional *extensor* retinacular band [Gebo, 1986b; Gebo and Dagosto, 1988]). It seems more likely that indriids limit the risk of bowstringing of the FHL tendon by avoiding deep plantarflexion at the talocrural joint.

Finally, while deep grooves appear to be associated with suspensory postures, we do not interpret these results as evidence that indriids (or other taxa with shallow FHLGs) are incapable of a powerful pedal grasp in diverse foot postures. For example, both Gebo (1986b; 1987b) and Meldrum, Dagosto, & White (1997) observe the adoption of suspensory postures by *Propithecus*. However, relative to other taxa in their samples, suspension by *Propithecus* is infrequent (5% of locomotor bouts in Gebo [1987b] and 6.5% of locomotor bouts in Meldrum et al. [1997]). Further, among possible suspensory postures (quadrupedal, tripedal, bipedal, or bimanual), *Propithecus* uses bipedal suspension less frequently than *Varecia variegata*, *Eulemur fulvus*, or *Eulemur rubriventer* (Meldrum et al., 1997). Meldrum et al. (1997) also make the important point that taxa that engage in hind limb suspension can achieve the posture through the different proximate mechanisms (i.e., unlike *Varecia*, neither *Daubentonia* nor *Cercopithecus* exhibit full plantarflexion at the talocrural joint during hind limb suspension). Evaluating the degree of plantarflexion during hind limb suspension would be a worthwhile test of the proposed functional relationship between FHLG depth and suspensory postures.

5.4 | Implications for particular fossils

This study provided a large amount of new high fidelity quantitative comparative data on a variety of fossils. These data present an opportunity to revisit discussions about phylogenetic affinities and functional morphology for certain species. Though we are cautious to interpret broader evolutionary patterns from a single postcranial element, we also discuss the implications of this study for various scenarios concerning the adaptive origins of euprimates.

5.4.1 | Plesiadapiforms

With the notable exception of *Carpolestes simpsoni* (Bloch and Boyer, 2002), plesiadapiforms are generally reconstructed as specialists for large diameter vertical supports (Beard, 1991; Bloch et al., 2007; Boyer and Bloch, 2008; Szalay and Dagosto, 1980). Given our conclusion that abducted foot postures on large diameter supports can select for a lateral FHLG position, our finding that plesiadapiforms have strongly lateral FHLGs supports these behavioral reconstructions. Although several other plesiadapiforms likely had prehensile halluces (Sargis et al., 2007), *Carpolestes* is unique among known plesiadapiform taxa due to its divergent, nail-bearing hallux (Bloch and Boyer, 2002), and has consequently been reconstructed as a small branch specialist. Among the plesiadapiforms of our sample, the medially positioned FHLG of *Carpolestes* is also unique, and the species plots distantly from plesiadapids, *Cynocephalus*, and *Ptilocercus* (Figure 12). Furthermore, *Carpolestes* is quite dissimilar from the predicted mean ancestral euprimate values of both FFa and FHLG Position (Figure 8). In their original description, Bloch and Boyer (2002) suggested that the divergent, nail-bearing hallux of *Carpolestes* represented either a sympleisomorphy shared by plesiadapoids and euprimates or that the feature evolved in parallel in these two closely related clades. In their analysis of *Carpolestes*' first metatarsal torsion and hallucal physiological abduction angle, Goodenberger et al. (2015) argued that the hallucal features observed in *Carpolestes* were likely acquired in parallel to those observed in euprimates (dependent on the polarity of these hallucal morphologies). On the basis of the results of this study, we favor the same interpretation as Goodenberger et al. (2015), but emphasize that the parallel acquisition of a divergent, nail-bearing hallux remains relevant for understanding the ecological context of euprimate origins (as argued by Bloch and Boyer [2003]).

5.4.2 | Adapiforms

Our results reveal that the tali of adapiforms are generally strepsirrhine-like, with strongly lateral FHLG positions, and plot among living strepsirrhines in the multivariate space ascribed by FHLG Position, FFa, and MTF morphology (Figure 12). Earliest Eocene *Cantius ralstoni* plots remarkably close to the predicted mean ancestral euprimate values of FFa and FHLG Position (Figure 8); the only other living or extinct primates falling with the 95% HPD for these values are extinct *Eosimias*, *Asiadapis*, and *Cantius abditus*, and extant *Microcebus*. Within notharctines, it is notable that *Smilodectes* has a relatively haplorhine-like placement of the FHLG (even more medial than *Eosimias* and the basal stem catarrhine *Catopithecus*). This might indicate that members of this genus used horizontal supports more frequently than other notharctines. *Smilodectes* and other notharctines with relatively medially placed FHLGs (*Cantius trigonodus* and *Notharctus venticolus*) effectively overlap with omomyiforms in multivariate space (Figure 12), presumably due to parallel evolution.

Intriguingly, caenopithecines [large-bodied, middle Eocene adapiforms from localities in Africa, Europe, and possibly Asia (*Adapoides*) and North America (*Mahgarita* and *Mescalerolemur*, neither known from tarsal remains)] and asiadapids (small-bodied, early Eocene adapiforms from India) plot in the multivariate space distinctly occupied by extant lorisids (Figure 12). While this may not be too surprising for the caenopithecines *Afradapis* and *Caenopithecus*, whose anatomy has been interpreted as lorisid-like (Boyer et al., 2010; Seiffert et al. 2015), there has been substantial debate about asiadapids. Initial descriptions of asiadapid postcrania proposed that asiadapids were agile quadrupeds with frequent leaping (Rose et al., 2009), largely based on phenetic similarities to the postcrania of *Cantius*. More recently, Dunn et al. (2016) suggested asiadapids were generalized arboreal quadrupeds based on several postcranial features (i.e., a low humerofemoral index, a well-defined patellar groove, retroflexion of the tibial plateau). Boyer et al. (2013a) noted that asiadapid femora do not suggest a propensity for acrobatic leaping and emphasized that, due to allometric trends in calcaneal elongation, similar calcaneal morphologies require different interpretations of locomotor behavior due to the three to fourfold size differences between asiadapids and *Cantius*. In light of these allometric relationships, Boyer et al. (2013a) argued that asiadapids fit a lorisid-like pattern of calcaneal elongation and were more likely to have been slow climbers. Our study provides additional evidence from the talus that asiadapids may have been more cautious climbers. Unlike the argument of Boyer et al. (2013a), our argument does not rely on a causal relationship of absolute size on morphology independent of behavior. We expect that more detailed understanding of allometric trends in talar morphology would magnify the slow climbing signal in asiadapids.

5.4.3 | Omomyiforms

Many implications of this study for omomyiforms were discussed in previous sections. However, it should be noted that phylogenetically basal omomyiforms such as *Teilhardina belgica* and *T. brandti* appear to have retained a more laterally positioned FHLG than more derived omomyiforms. We interpret this as a plesiomorphic feature within primates that is shared with basal adapiforms. Furthermore, while most cladistic studies have assigned separate character states to omomyiforms and adapiforms, our measurements show broad overlap between the two groups (not unlike Boyer and Seiffert's [2013] results for fibular facet angle). Additionally, omomyiforms generally have shallower FHLGs than those of adapiforms. If leaping propensity affects groove depth, as it appears to in strepsirrhines, this pattern suggests generally greater emphasis on leaping in omomyiforms than adapiforms. Boyer et al. (2013a) recovered a similar signal with omomyiforms generally exhibiting greater body-mass-corrected distal calcaneal elongation than adapiforms (with the exception of *Teilhardina*).

5.4.4 | *Eosimias*

Two of the more surprising results of this study are that 1) *Eosimias* has a laterally positioned FHLG and 2), it is most similar to plesiadapiforms, dermopterans, and *Ptilocercus* in the talar features that we have quantified in this and other recent studies (Boyer and Seiffert, 2013; Boyer et al., 2015). Ancestral state reconstructions of this study support Gebo et al.'s (2000, 2001) assessment that non-euprimate outgroups tend to exhibit laterally positioned FHLGs, though we would argue that the differences between these taxa are significant. Results of our analyses suggest a lateral FHLG position is plesiomorphic for euarchontans, and while retention of the plesiomorphic FHLG position does not impact *Eosimias*' hypothesized phylogenetic position as the most basal known stem anthropoid, combining FHLG position with other quantified talar morphological features (i.e., fibular facet angle and medial tibial facet morphology) has interesting implications for interpreting eosimiid anatomy and understanding the primitive condition of anthropoids.

Previous descriptions of *Eosimias* have argued that the taxon is anatomically "intermediate" between crown anthropoids and more basal haplorhines (Gebo et al., 2000, 2001). Previous order-wide quantitative assessments of talar morphology have shown that while *Eosimias* is similar to anthropoids (and plesiadapiforms) in fibular facet angle (Boyer and Seiffert, 2013) and medial tibial facet form (Boyer et al., 2015), it is strongly distinguished from crown anthropoids and plots with plesiadapiforms, dermopterans, and ptilocercids when FHLG position data is incorporated (Figure 12). On the basis of its position in the morphospace characterized by these three talar features, the talus of *Eosimias* is much more similar to the talus of *Ptilocercus* than to any other living or extinct euprimate. Informed by the talus alone, *Eosimias* would seem a poor intermediary between crown anthropoids and more basal haplorhines. Given the absence of associated dental and postcranial material attributed to *Eosimias*, it is possible that this material does not all represent the same euarchontan taxon. However, even if the phylogenetic position of *Eosimias* were changed, ASR results for FHLG position would not be substantially affected, as other early anthropoids (*Catopithecus*, *Aegyptopithecus*, *Dolichocebus*) exhibit FHLGs that are more lateral than those observed among later anthropoids, and the earliest known euprimates (*Cantius* and *Teilhardina*) exhibit laterally positioned FHLGs. We find it more intriguing that recent results generated by automated geometric morphometric

methods recover strong phenetic similarities between *Eosimias* and non-primate euarchontans (including *Ptilocercus*) in the second mandibular molar (Gao, Yapuncich, Daubechies, Mukherjee, & Boyer, 2016). Phenetic similarities in both the dentition and postcrania may indicate that *Eosimias* is phylogenetically more basal than even stem Anthropoidea.

Functionally, talar features observed in *Eosimias* (steep fibular facet, relatively small MTF, and laterally positioned FHLG), combined with its small body size (~100g, Gebo et al., 2001), are similar to those observed in *Microcebus* and *Ptilocercus*. We interpret this suite of features to reflect an increased use of abducted foot postures and a decreased use of inverted foot postures, which may correspond with the use of relatively large diameter supports.

Unlike *Eosimias*, the co-occurring "protoanthropoid" (IVPP 12306) from the Shanghuang fissure fillings is much more similar to living and extinct small-bodied anthropoids in its FHLG placement and overall morphology. Because the specimen exhibits a more transitional morphology (e.g., a steep fibular facet, a reduced MTF, and a medially positioned FHLG), it plots very close to the late Eocene *Proteopithecus sylviae* from Egypt and between omomyiforms and extant platyrrhines (Figures 8 and 12). The functional suite observed in IVPP 12306 suggests a decreased use of abducted and inverted foot postures. Furthermore, this combination of features implies that fundamental changes in anthropoid talar morphology might have occurred in the Eocene of Asia, prior to the trans-Tethyan dispersal that gave rise to crown anthropoids and parapithecoids. This would also imply either that omomyiforms and tarsiers are largely monophyletic (rather than paraphyletic) with respect to anthropoids (as in the phylogeny used in this study), or that a more medial FHLG evolved multiple times, which is also consistent with our results (given that it appears to have occurred in the haplorhine and tupaiid lineages).

As Boyer et al. (2015) noted, the *bauplan* and ecological tendencies of basal anthropoids might not have differed drastically from the inferred euprimate condition. We restate this hypothesis to highlight the new observation that the talus of *Eosimias* presents the same constellation of features as the talus of *Ptilocercus* and as inferred for the talus of the ancestral euprimate. Ultimately, this may suggest that prosimian postcranial traits that have been associated with powerful pedal grasping (e.g., a widely divergent hallux, a large peroneal process on the first metatarsal, a relatively large medial tibial facet, a tarsifulcrumating foot, etc.) uniting strepsirrhines and tarsiers evolved in parallel.

5.4.5 | Subfossil lemurs

Among strepsirrhines, subfossil lemurs are the only taxa that deviate from exhibiting a lateral FHLG position. Dagosto (1986) made this observation qualitatively for *Megaladapis*, but it has not been recognized in other subfossil lemurs to our knowledge, nor have the behavioral implications been addressed. This pattern can be most easily interpreted for *Archaeolemur*, which has previously been described as having a semi-terrestrial, baboon-like locomotor profile (Jungers et al., 2005), which would imply the use of everted, adducted foot postures and a medially positioned FHLG. In *Megaladapis*, FHLG anatomy would, given our functional interpretations, imply that the use of abducted foot postures on large diameter vertical supports was less frequent than previously suggested (Jungers et al., 2002; Wunderlich et al., 1996), calling into question the appropriateness of the term "koala lemur." Finally, the medially positioned FHLG of *Babakotia* and *Palaeopropithecus* does not have strong implications for their previous behavioral assessments since expectations for FHLG position have not been established in specialized quadrumanual suspensory taxa.

5.4.6 | *Pondaungia?* NMMP 39

By our metric, the amphipithecid talus described by Marivaux et al. (2003) does exhibit a medially positioned FHLG. However, given that a medially positioned FHLG have evolved in multiple lineages, we do not feel this particular feature suggests anthropoid affinities for this specimen. Our ancestral state reconstructions suggest that medially positioned FHLGs have evolved in four euarchontan clades: haplorhines, tupaiids, palaeopropithecids, and *Megaladapis*. For the subfossil lemurs, the negative allometric relationship between FHLG Position and body mass may partly explain their medial groove position (i.e., reduced use of abducted foot postures as body size increases). Because NMMP-39 belonged to a fairly large-bodied animal [2-6.5 kg based on tarsal measurements (Marivaux et al., 2003)], allometry should also be considered when evaluating its morphology. *Pondaungia*? NMMP-39 plots on the margins of the PCA morphospace (Figure 12), closer to haplorhines than strepsirrhines, but the unique talar morphology of amphipithecids makes it difficult to place them phylogenetically with a high degree of certainty.

5.5 | Patterns of evolution and behavioral change

On the basis of quantitative data describing the medial tibial facet and fibular facet angle, Boyer et al. (2015) proposed the common ancestor of euprimates might not have been a small branch specialist. Their ancestral state reconstructions suggest that the ancestral euprimate exhibited a small medial tibial facet (Boyer et al., 2015) and a steep fibular facet angle (Boyer and Seiffert, 2013). This trait combination led Boyer et al. (2015) to conclude that stem and basal euprimates were less reliant on small diameter supports and inverted foot postures than extant strepsirrhines. The ancestral state reconstructions for FHLG Position (Figure 10a) presented in this study also indicate large diameter supports for the ancestral euprimate and therefore largely support Boyer et al.'s (2015) proposal. Our finding that the FHLG was strongly laterally positioned in the ancestral euprimate indicates that the foot was typically strongly abducted when dorsiflexed, which is expected for an animal clinging on relatively large diameter supports. Furthermore, ASRs indicate that the ancestral euprimate had a shallower FHLG than the ancestral euarchontan (Figure 10b), which is consistent with calcaneal elongation data (Boyer et al., 2013a) in suggesting that more acrobatic leaping evolved prior to small branch specialization in euprimates.

Combining ancestral state reconstructions from Boyer and Seiffert (2013), Boyer et al. (2015), and this study, the euarchontan common ancestor likely possessed a small medial tibial facet, a steep fibular facet angle, and a strongly laterally positioned and deep FHLG. Among extant taxa, this trait combination is best exemplified by *Ptilocercus* (a

very small-bodied arborealist that likely often encounters relatively large diameter supports). With the exception of *Carpolestes* (which has a much more medially positioned FHLG), all examined plesiadapiforms share these talar features, and have previously been argued to utilize large diameter vertical supports (Beard, 1991; Bloch et al., 2007; Boyer and Bloch, 2008; Szalay and Dagosto, 1980).

In the euprimate stem lineage, the inferred morphological changes and functional interpretations of FHLG features imply the following behavioral changes: (a) a slight reduction in abducted foot postures, reflected by a slightly more medially positioned FHLG (though the FHLG position of the ancestral euprimate is still more lateral than those of extant primates); and (b) an increase in leaping propensity, reflected by a decrease in FHLG depth. These findings compliment those of Boyer et al. (2013a), who linked increasing calcaneal elongation (relative to body mass) to an increasing propensity for leaping along the euprimate stem lineage. While Boyer et al. (2015) argued talar morphology did not indicate a transition to a small branch niche prior to the radiation of crown primates (on the basis of the retention of a small MTF and a steep fibular facet), the medial shift in FHLG position in the euprimate stem lineage does suggest a slight reduction in the use of highly abducted foot postures. According to our functional interpretations, the slight medial shift in FHLG position along the euprimate stem lineage suggests either a reduction in vertical support use, a reduction in relative support diameter, or potentially both. As a result of this evolutionary sequence, we might expect the talar morphology of the ancestral euprimate to be similar to *Ptilocercus*, a similarity that has previously been emphasized by Sargis (2002, 2004). The inferred positional behavior for the ancestral euprimate combines the use of abducted foot postures on large diameter (potentially vertical) supports and an increased propensity for leaping.

While the talar morphology of *Ptilocercus* may resemble the ancestral euprimate, the postcrania of *Ptilocercus* lacks other morphological innovations that are evident in the earliest known euprimates. First, though *Ptilocercus* has a divergent hallux, the digit is not widely divergent and opposable as observed in early euprimates such as *Archicebus achilles* (Ni et al., 2013) and *Teilhardina belgica* (Gebo et al., 2015). Second, *Ptilocercus* retains claws on all its digits, while the early euprimate *Teilhardina brandti* has nails on its digits (Rose et al., 2011). Third, our ancestral state reconstructions of FHLG depth suggest that the ancestral euprimate had a shallower FHLG than *Ptilocercus*. Finally, *Ptilocercus* exhibits less calcaneal elongation relative to its body mass than all fossil euprimates (with the exception of subfossil lemurs) analyzed by Boyer et al. (2013a). The first two of these features have been associated with pedal grasping and potentially the occupation of the terminal branch niche, while the latter two may be associated with leaping. Thus, the set of postcranial differences between *Ptilocercus* and the ancestral euprimate combines features that are prominently involved in multiple hypotheses for the adaptive origins of euprimates, including the vertical clinging and leaping hypothesis (Napier and Walker, 1967), the grasp-leaping hypothesis (Dagosto, 2007; Szalay, 2007; Szalay and Dagosto, 1980, 1988), the angiosperm coevolution hypothesis (Sussman, 1991; Sussman, Rasmussen, & Raven, 2013), and the nocturnal visual predation hypothesis (Cartmill, 1972, 1974a, 1974b). The results of this study certainly do not resolve the conflicts between these adaptive scenarios, but they do suggest the continued use of relatively large diameter supports and an increased propensity for leaping within the euprimate stem lineage. These observations complicate proposals that the ancestral euprimate was a relatively slow-moving generalized quadruped (i.e., Cartmill, 1972, 1974a, 1974b) or that improving pedal grasping for exploitation of the terminal branch niche was the primary postcranial change in the euprimate stem lineage (i.e., Sussman, 1991; Sussman et al., 2013). Quantifying and evaluating other osteological features that potentially facilitate pedal grasping and/or leaping (e.g., development of the posterior trochlear shelf of the talus, retroflexion of the tibial plateau, prominence of the intercondylar spines of the tibial plateau, depth of the patellar groove, and other features summarized by Dagosto [2007]) would help to distinguish the relative strengths of these adaptive scenarios.

Other recent evidence provides independent support for the perspective that the ancestral euprimate may have utilized relatively large diameter supports and emphasized leaping prior to a transition to the terminal branch niche. First, the low intermembral index in the basal haplorhine *Archicebus achilles* (Ni et al., 2013) implies a strong propensity for leaping. Second, both *Archicebus* (Ni et al., 2013) and *Teilhardina belgica* (Gebo et al., 2015) have elongated metatarsals (matching treeshrews and anthropoids in relative length), which may reflect relatively recent metatarsifulcrimating ancestry for these taxa. If prehensility is defined as phalangeal length relative to metapodial length (as in Boyer, Yapuncich, Chester, Bloch, & Godinot, 2013b, 2016), then both *Archicebus* and *T. belgica* have a relatively low degree of pedal prehensility (though both species exhibit long, robust, and divergent halluces and were capable of hallucal grasping). Transitioning to a terminal branch niche may have increased the selective pressure to improve pedal prehensility, necessitating a shift to a tarsifulcrumating foot through the reduction of non-hallucal metatarsals. Though the lack of claws seems a clear indicator of terminal branch use in *Archicebus* and *Teilhardina*, the fact that they had not yet developed metatarsal reduction could indicate this transition was recent. Additionally, comparative studies of fossil primate hands (Boyer et al., 2013b, 2016; Gebo et al., 2015) suggest that the ancestral euprimate likely had exceptionally elongate fingers similar to modern tarsiers or *Daubentonia*, which would facilitate clinging to, and grasping of, proportionally larger supports, rather than small, terminal branches. Finally, Gebo et al. (2012) noted that both *Tarsius* and *Teilhardina brandti* have circular and expanded apical tufts on their distal phalanges, a morphological similarity that may indicate *Teilhardina* used smooth and vertical supports similar to *Tarsius* (Anemone and Nachman, 2003; Day and Iliffe, 1975; Niemitz, 1984).

Our proposed scenario for euprimate postcranial evolution, in which terminal branch adaptations lag behind other specializations, is atypical compared to many previous proposals. However, it is based on consistent and complementary signals in multiple supraordinally comprehensive datasets. Furthermore, the scenario is not unprecedented in the literature, as it aligns well with that presented by Beard (1991), who proposed that adaptations for large diameter vertical support use (including a lateral FHLG) in plesiadapiforms and dermopterans were "retained" by the earliest euprimates and canalized in later primate

evolution in significant ways. Presumably, if the ancestral euprimates were specialized for vertical postures and leaping, this could explain why vertical clinging and leaping behaviors are observed in many primate lineages (Napier and Walker, 1967). Beard (1991) published his scenario at a time when many researchers were expanding and solidifying the terminal branch niche as fundamental to euprimate origins (Cartmill, 1992; Sussman, 1991), and gained relatively little notice as a result. The view that adaptation to the terminal branch niche was the primary causal factor in euprimate origins was bolstered by plesiadapiform-focused work (e.g., Bloch and Boyer, 2002; Bloch et al., 2007; Boyer and Bloch, 2008) that conceived the ancestral euprimate as a small branch specialist given the conclusion that small branch adaptations (e.g., a divergent hallux) in the plesiadapiform *Carpolestes simpsoni* were homologous synapomorphies with euprimates. However, we feel the growing body of detailed comparative anatomical data and functional inferences discussed here now lend stronger support to Beard's (1991) hypothesis that the ancestral euprimate retained adaptations for relatively large diameter vertical support use.

ACKNOWLEDGMENTS

The authors thank J. Thostenson at the SMIF lab at Duke University and M. Hill at the AMNH microscopy lab for help with CT-scanning. I. Wallace executed and processed scans at Stony Brook University's Center for Biotechnology. R. Neu helped develop measurement protocols as a part of an undergraduate research project. They thank the staff at the AMNH and USNM mammalogy and paleontology departments for access to specimens. They are sincerely grateful to K. C. Beard, S. Chester, E. Delson, D. Gebo, G. Gunnell, W. Harcourt-Smith, B. Patel, K. Rose, T. Smith, A. Su, and L. Tallman for access to additional specimens. S. Chester's scans were funded by NSF DDIG SBE 1028505 to S. Chester and E. J. Sargis. B. Patel's scans were funded by a Leakey grant to B. Patel and a Wenner-Gren grant to C. Orr. This research was supported by NSF grants to GSY and DMB (BCS 1540421), DMB and ERS (BCS 1317525 and BCS 1231288), DMB and GFG (BCS 1440742), DMB (BCS 1552848), J. Bloch (BCS 1440558), and an AAPA Professional Development Grant in 2009 to DMB. This is Duke Lemur Center publication #1347.

NOTES

[1] Both the bone bearing the FHLG and the muscle whose tendon passes through the FHLG have different names in human (talus and *flexor hallucis longus*) and vertebrate (astragalus and *flexor digitorum fibularis*) anatomy. Given this journal's primary subject, we use terms associated with human anatomy.

[2] It is important to note that pedal grasping does not require the divergent and opposable hallux that characterizes euprimates (Sargis et al., 2007). The scandentian *Ptilocercus lowii*, which has a divergent but non-opposable hallux, is capable of pedal grasping (Sargis, 2002), and has served as a modern analogue for several plesiadapiforms that lack a strongly divergent and opposable hallux (Bloch and Boyer, 2007; Sargis, 2002; Sargis, 2004; Szalay and Dagosto, 1988).

[3] FHLG Ellipse is an asymmetrical index that can generate very high values as FHLGDepth approaches zero. However, FHLG Ellipse is normally distributed.

[4] Though the sample size is limited ($n = 5$ "prosimian" taxa), regressions of FHL mass∼body mass using data from Demes et al. (1998) suggest FHL scales with greater positive allometry than total muscle mass.

[5] In a tarsifulcrumating foot, push-off occurs at the distal margin of the tarsals during saltation. In contrast, in a metatarsifulcrimating foot, push-off occurs at the distal margin of the metatarsals (Morton, 1924).

REFERENCES

Anemone, R. L. (1990). The VCL hypothesis revisited: Patterns of femoral morphology among quadrupedal and saltatorial prosimian primates. *American Journal of Physical Anthropology*, *83*, 373–393.

Anemone, R. L., & Covert, H. H. (2000). New skeletal remains of *Omomys* (primates, omomyidae): Functional morphology of the hindlimb and locomotor behavior of a Middle Eocene primate. *Journal of Human Evolution*, *38*, 607–633.

Anemone, R. L., & Nachman, B. A. (2003). Morphometrics, functional anatomy, and the biomechanics of locomotion among tarsiers. In P. C. Wright, E. L. Simons, & S. Gursky (Eds.), *Tarsiers—past, present, and future* (pp. 97–120). New Brunswick, NJ: Rutgers University Press.

Argot, C. (2002). Functional-adaptive analysis of the hindlimb anatomy of extant marsupials and the paleobiology of the Paleocene marsupials *Mayulestes ferox* and *Pucadelphys andinus*. *Journal of Morphology*, *253*, 76–108.

Arnold, C., Matthews, L. J., & Nunn, C. L. (2010). The 10kTrees website: A new online resource for primate phylogeny. *Evolutionary Anthropology: Issues, News, and Reviews*, *19*, 114–118.

Beard, K. C. (1991). Vertical postures and climbing in the morphotype of Primatomorpha: Implications for locomotor evolution in primate history. In: Y. Coppens & B. Senut (Eds.), *Origine(s) de la bipédie chez lez hominidés* (pp. 79–87). Paris: Cahiers de Paléoanthropologie, CNRS.

Beard, K. C., Dagosto, M., Gebo, D. L., & Godinot, M. (1988). Interrelationships among primate higher taxa. *Nature*, *331*, 712–714.

Bloch, J. I., & Boyer, D. M. (2002). Grasping primate origins. *Science*, *298*, 1606–1610.

Bloch, J. I., & Boyer, D. M. (2003). Response to comment on "Grasping primate origins." *Science*, *300*, 741c.

Bloch, J. I., & Boyer, D. M. (2007). New skeletons of Paleocene-Eocene plesiadapiformes: A diversity of arboreal positional behaviors in early primates. In: M. Dagosto & M. J. Ravosa (Eds.), *Primate origins: Adaptations and evolution* (pp. 535–581). New York: Plenum Press.

Bloch, J. I., Silcox, M. T., Boyer, D. M., & Sargis, E. J. (2007). New Paleocene skeletons and the relationships of plesiadapiforms to crown-clade primates. *Proceedings of the National Academy of Sciences USA*, *104*, 1159–1164.

Boyer, D. M., & Bloch, J. I. (2008). Evaluating the mitten-gliding hypothesis for Paromomyidae and Micromomyidae (Mammalia, "Plesiadapiformes") using comparative functional morphology of new Paleogene skeletons. In: E. J. Sargis & M. Dagosto (Eds.), *Mammalian evolutionary morphology: A tribute to Frederick S. Szalay* (pp. 233–284). Dordrecht, Netherlands: Springer.

Boyer, D. M., Gunnell, G. F., Kaufman, S., & McGeary, T. (2017). MorphoSource—Archiving and sharing 3D digital specimen data. *Journal of Paleontology*. DOI:10.1017/scs.2017.13

Boyer, D. M., Patel, B. A., Larson, S. G., & Stern, Jr, J. T. (2007). Telemetered electromyography of peroneus longus in Varecia variegata and *Eulemur rubriventer*: Implications for the functional significance of a large peroneal process. *Journal of Human Evolution*, *53*, 119–134.

Boyer, D. M., Scott, C. S., & Fox, R. C. (2012). New craniodental material of *Pronothodectes gaoi* Fox (Mammalia, "Plesiadapiformes") and relationships among members of Plesiadapidae. *American Journal of Physical Anthropology*, *147*, 511–550.

Boyer, D. M., & Seiffert, E. R. (2013). Patterns of astragalar fibular facet orientation in extant and fossil primates and their evolutionary implications. *American Journal of Physical Anthropology*, *151*, 420–447.

Boyer, D. M., Seiffert, E. R., Gladman, J. T., & Bloch, J. I. (2013a). Evolution and allometry of calcaneal elongation in living and extinct primates. *PLoS One*, *8*, e67792.

Boyer, D. M., Seiffert, E. R., & Simons, E. L. (2010). Astragalar morphology of *Afradapis*, a large adapiform primate from the earliest late Eocene of Egypt. *American Journal of Physical Anthropology*, *143*, 383–402.

Boyer, D. M., Yapuncich, G. S., Butler, J. E., Dunn, R. H., & Seiffert, E. R. (2015). Evolution of postural diversity in primates as reflected by the size and shape of the medial tibial facet of the talus. *American Journal of Physical Anthropology*, *157*, 134–177.

Boyer, D. M., Yapuncich, G. S., Chester, S. G. B., Bloch, J. I., & Godinot, M. (2013b). Hands of early primates. *American Journal of Physical Anthropology*, *152*, 33–78.

Boyer, D. M., Yapuncich, G. S., Chester, S. G. B., Bloch, J. I., & Godinot, M. (2016). Hands of Paleogene primates. In: T. L. Kivell, P. Lemelin, B. G. Richmond, & D. Schmitt (Eds.), *The evolution of the primate hand* (pp. 373–419), New York: Springer.

Cartmill, M. (1972). Arboreal adaptations and the origin of the order Primates. In: R. Tuttle (Ed.), *The functional and evolutionary biology of primates* (pp. 97–122). Chicago: Aldine-Atherton Press.

Cartmill, M. (1974a). Pads and claws in arboreal locomotion. In: F. Jenkins (Ed.), *Primate locomotion* (pp. 45–83). New York: Plenum Press.

Cartmill, M. (1974b). Rethinking primate origins. *Science*, *184*, 436–443.

Cartmill, M. (1975). *Primate origins*. Minneapolis: Burgess Publishing.

Cartmill, M. (1985). Climbing. In: M. Hildebrand, D. M. Bramble, K. F. Liem, & D. B. Wake (Eds.), *Functional vertebrate morphology* (pp. 73–88). Cambridge, UK: Belknap Press.

Cartmill, M. (1992). New views on primate origins. *Evolutionary anthropology: Issues, news, and reviews*, *1*, 105–111.

Charles-Dominique, P. (1977). *Ecology and behavior of nocturnal primates*. London: Duckworth.

Chester, S. G. B., Bloch, J. I., Boyer, D. M., & Clemens, W. A. (2015). Oldest known euarchontan tarsals and affinities of Paleocene *Purgatorius* to Primates. *Proceedings of the National Academy of Sciences USA*, *122*, 1487–1492.

Covert, H. H. (1988). Ankle and foot morphology of *Cantius mckennai*: Adaptations and phylogenetic implications. *Journal of Human Evolution*, *17*, 57–70.

Covert, H. H., & Williams, B. A. (1994). Recently recovered specimens of North American Eocene omomyids and adapids and their bearing on debates about anthropoid origins. In: J. G. Fleagle & R. F. Kay (Eds.), *Anthropoid origins* (pp. 29–54). New York: Plenum Press.

Dagosto, M. (1983). Postcranium of *Adapis parisiensis* and *Leptadapis magnus* (Adapiformes, Primates). *Folia Primatologica*, *41*, 49–101.

Dagosto, M. (1986). *The joints of the tarsus in the strepsirhine primates: functional, adaptive, and evolutionary implications [dissertation]*. New York: City University of New York.

Dagosto, M. (1988). Implications of postcranial evidence for the origin of euprimates. *Journal of Human Evolution*, *17*, 35–56.

Dagosto, M. (1990). Models for the origin of the anthropoid postcranium. *Journal of Human Evolution*, *19*, 121–139.

Dagosto, M. (2007). The postcranial morphotype of primates. In: M. J. Ravosa & M. Dagosto (Eds.), *Primate origins—adaptations and evolution* (pp. 489–534). New York: Springer.

Dagosto, M., & Gebo, D. L. (1994). Postcranial anatomy and the origin of the Anthropoidea. In: J. G. Fleagle & R. F. Kay (Eds.), *Anthropoid origins* (pp. 567–593). New York: Plenum Press.

Dagosto, M., Gebo, D. L., & Beard, K. C. (1999). Revision of the Wind River faunas, early Eocene of central Wyoming. Part 14. Postcranium of *Shoshonius cooperi* (Mammalia: Primates). *Annals of Carnegie Museum*, *68*, 175–211.

Dagosto, M., Marivaux, L., Gebo, D. L., Beard, K. C., Chaimanee, Y., Jaeger, J. J., ... Kyaw, A. A. (2010). The phylogenetic affinities of the Pondaung tali. *American Journal of Physical Anthropology*, *143*, 223–234.

Day, M. H., & Iliffe, S. R. (1975). The contrahens muscle layer in *Tarsius*. *Folia Primatologica*, *24*, 241–249.

Demes, B., Fleagle, J. G., & Lemelin, P. (1998). Myological correlates of prosimian leaping. *Journal of Human Evolution*, *34*, 385–399.

Demes, B., & Günther, M. M. (1989). Biomechanics and allometric scaling in primate locomotion and morphology. *Folia Primatologica*, *53*, 125–141.

Demes, B., Jungers, W. L., Fleagle, J. G., Wunderlich, R. E., Richmond, B. G., & Lemelin, P. (1996). Body size and leaping kinematics in Malagasy vertical clingers and leapers. *Journal of Human Evolution*, *31*, 367–388.

Dunn, R. H., Rose, K. D., Rana, R. S., Kumar, K., Sahni, A., & Smith, T. (2016). New euprimate postcrania from the early Eocene of Gujarat, India, and the strepsirrhine-haplorhine divergence. *Journal of Human Evolution*, *99*, 25–51.

Dunn, R. H., Sybalsky, J. M., Conroy, G. C., & Rasmussen, D. T. (2006). Hindlimb adaptations in *Ourayia* and *Chipetaia*, relatively large-bodied omomyine primates from the middle Eocene of Utah. *American Journal of Physical Anthropology*, *131*, 303–310.

Gao, T., Yapuncich, G. S., Daubechies, I., Mukherjee, S., & Boyer, D. M. (2016). Development and assessment of fully automated and globally transitive geometric morphometric methods, with application to a biological comparative dataset with high interspecific variation. *bioRxiv*, Available at: https://doi.org/10.1101/086280

Gebo, D. L. (1986a). Anthropoid origins—the foot evidence. *Journal of Human Evolution*, *15*, 421–430.

Gebo, D. L. (1986b). *The anatomy of the prosimian foot and its application to the primate fossil record [dissertation]*. Durham, NC: Duke University.

Gebo, D. L. (1987a). Functional anatomy of the tarsier foot. *American Journal of Physical Anthropology*, *73*, 9–31.

Gebo, D. L. (1987b). Locomotor diversity in prosimian primates. *American Journal of Primatology*, *13*, 271–281.

Gebo, D. L. (1988). Foot morphology and locomotor adaptation in Eocene primates. *Folia Primatologica*, *50*, 3–41.

Gebo, D. L. (1989). Postcranial adaptation and evolution in Lorisidae. *Primates*, *30*, 347–367.

Gebo, D. L. (1993). Functional morphology of the foot in Primates. In: D. L. Gebo (Ed.), *Postcranial adaptation in nonhuman primates* (pp. 175–196). DeKalb, IL: Northern Illinois University Press.

Gebo, D. L. (2004). A shrew-sized origin for primates. *Yearbook of Physical Anthropology*, *47*, 40–62.

Gebo, D. L. (2011). Vertical clinging and leaping revisited: Vertical support use as the ancestral condition of strepsirrhine primates. *American Journal of Physical Anthropology*, *146*, 323–335.

Gebo, D. L., & Dagosto, M. (1988). Foot anatomy, climbing, and the origin of the Indriidae. *Journal of Human Evolution*, *17*, 135–154.

Gebo, D. L., Dagosto, M., Beard, K. C., & Ni, X. (2008). New primate hind limb elements from the middle Eocene of China. *Journal of Human Evolution*, *55*, 999–1014.

Gebo, D. L., Dagosto, M., Beard, K. C., & Qi, T. (2001). Middle Eocene primate tarsals from China: Implications for haplorhine evolution. *American Journal of Physical Anthropology*, *116*, 83–107.

Gebo, D. L., Dagosto, M., Beard, K. C., Qi, T., & Wang, J. (2000). The oldest known anthropoid postcranial fossils and the early evolution of higher primates. *Nature*, *404*, 276–278.

Gebo, D. L., Dagosto, M., & Rose, K. D. (1991). Foot morphology and evolution in early Eocene *Cantius*. *American Journal of Physical Anthropology*, *86*, 51–73.

Gebo, D. L., & Simons, E. L. (1987). Morphology and locomotor adaptations of the foot in early Oligocene anthropoids. *American Journal of Physical Anthropology*, *74*, 83–101.

Gebo, D. L., Smith, T., & Dagosto, M. (2012). New postcranial elements for the earliest Eocene fossil primate *Teilhardina belgica*. *Journal of Human Evolution*, *63*, 205–218.

Gebo, D. L., Smith, R., Dagosto, M., & Smith, T. (2015). Additional postcranial elements of *Teilhardina belgica*: The oldest European primate. *American Journal of Physical Anthropology*, *156*, 388–406.

Goodenberger, K. E., Boyer, D. M., Orr, C. M., Jacobs, R. L., Femiani, J. C., & Patel, B. A. (2015). Functional morphology of the hallucal metatarsal with implications for inferring grasping ability in extinct primates. *American Journal of Physical Anthropology*, *156*, 327–348.

Grand, T. I. (1967). The functional anatomy of the ankle and foot of the slow loris. *American Journal of Physical Anthropology*, *26*, 207–218.

Gunnell, G. F. (2002). Notharctine primates (Adapiformes) from the early to middle Eocene (Wasatchian-Bridgerian) of Wyoming: transitional species and the origins of *Notharctus* and *Smilodectes*. *Journal of Human Evolution*, *43*, 353–380.

Gunnell, G. F., & Rose, K. D. (2002). Tarsiiforms: Evolutionary history and adaptation. In: W. C. Hartwig (Ed.), *The primate fossil record* (pp. 45–82). Cambridge: Cambridge University Press.

Hall-Craggs, E. C. B. (1965). An osteometric study of the hind limb of the Galagidae. *Journal of Anatomy*, *99*, 119–126.

Hammer, Ø., Harper, D. A. T., & Ryan, P. D. (2001). PAST: paleontological statistics software package for education and data analysis. *Paleontologica Electronica*, *4*, 1–9.

Janečka, J. E., Miller, W., Pringle, T. H., Wiens, F., Zitzmann, A., Helgen, K. M., … Murphy, W. J. (2007). Molecular and genomic data identify the closest living relative of Primates. *Science*, *318*, 792–794.

Jouffroy, F. K., Berge, C., & Niemitz, C. (1984). Comparative study of the lower extremity in the genus *Tarsius*. In: C. Niemitz (Ed.), *Biology of the tarsiers* (pp. 167–190). New York: Gustav Fischer.

Jungers, W. L., Godfrey, L. R., Simons, E. L., Wunderlich, R. E., Richmond, B. G., & Chatrath, P. S. (2002). Ecomorphology and behavior of giant extinct lemurs from Madagascar. In *Reconstructing behavior in the primate fossil record* (pp. 371–411). Springer US.

Jungers, W. L., Lemelin, P., Godfrey, L. R., Wunderlich, R. E., Burney, D. A., Simons, E. L., … Randria, G. F. N. (2005). The hands and feet of *Archaeolemur*: Metrical affinities and their functional significance. *Journal of Human Evolution*, *49*, 36–55.

Kay, R. F. (2015). Biogeography in deep time—What do phylogenetics, geology, and paleoclimate tell us about early platyrrhine evolution? *Molecular Phylogenetics and Evolution*, *82*, 358–374.

Kay, R. F., Fleagle, J. G., Mitchell, T. R. T., Colbert, M., Bown, T., & Powers, D. W. (2008). The anatomy of *Dolichocebus gaimanensis*, a stem platyrrhine monkey from Argentina. *Journal of Human Evolution*, *54*, 323–382.

Kay, R. F., Ross, C. F., & Williams, B. A. (1997). Anthropoid origins. *Science*, *275*, 797–804.

Langdon, J. H. (1990). Variations in cruropedal musculature. *International Journal of Primatology*, *11*, 575–606.

Le Gros Clark, W. E. (1927). Exhibition of photographs of the tree shrew (*Tupaia minor*). Remarks on the tree shrew *Tupaia minor*, with photographs. *Proceedings of the Zoological Society of London*, *1927*: 254–256.

Lewis, O. J. (1980a). The joints of the evolving foot. Part I. The ankle joint. *Journal of Anatomy*, *130*, 527–543.

Lewis, O. J. (1980b). The joints of the evolving foot. Part II. The intrinsic joints. *Journal of Anatomy*, *130*, 833–857.

Lewis, O. J. (1980c). The joints of the evolving foot. Part III. The fossil evidence. *Journal of Anatomy*, *131*, 275–298.

Maddison, W. P., & Maddison, D. R. (2011). Mesquite: a modular system for evolutionary analysis. Version 2.75. Available at: http://mesquiteproject.org.

Marigó, J., Roig, I., Seiffert, E. R., Moyà-Solà, S., & Boyer, D. M. (2016). Astragalar and calcaneal morphology of the middle Eocene primate *Anchomomys frontanyensis* (Anchomomyini): implications for early primate evolution. *Journal of Human Evolution*, *91*, 122–143.

Marivaux, L., Beard, K. C., Chaimanee, Y., Dagosto, M., Gebo, D. L., Guy, F., … Jaeger, J. J. (2010). Talar morphology, phylogenetic affinities, and locomotor adaptation of a large-bodied amphipithecid primate from the late middle Eocene of Myanmar. *American Journal of Physical Anthropology*, *143*, 208–222.

Marivaux, L., Chaimanee, Y., Ducrocq, S., Marandat, B., Sudre, J., Soe, A. N., … Jaeger, J. J. (2003). The anthropoid status of a primate from the late middle Eocene Pondaung Formation (central Myanmar): Tarsal evidence. *Proceedings of the National Academy of Sciences USA*, *100*, 13173–13178.

Marivaux, L., Tabuce, R., Lebrun, R., Ravel, A., Adaci, M., Mahboubi, M., & Bensalah, M. (2011). Talar morphology of azibiids, strepsirrhine-related primates from the Eocene of Algeria: Phylogenetic affinities and locomotor adaptation. *Journal of Human Evolution*, *61*, 447–457.

Meldrum, D. J., Dagosto, M., & White, J. (1997). Hindlimb suspension and hind foot reversal in *Varecia variegata* and other arboreal mammals. *American Journal of Physical Anthropology*, *103*, 85–102.

Morton, D. J. (1922). Evolution of the human foot. I. *American Journal of Physical Anthropology*, *5*, 305–336.

Morton, D. J. (1924). Evolution of the human foot. II. *American Journal of Physical Anthropology*, *7*, 1–52.

Moyà-Solà, S., Köhler, M., Alba, D. M., & Roig, I. (2012). Calcaneal proportions in primates and locomotor inferences in *Anchomomys* and other Palaeogene Euprimates. *Swiss Journal of Palaeontology*, *131*, 147–159.

Muchlinski, M. N., Snodgrass, J. J., & Terranova, C. J. (2012). Muscle mass scaling in primates: an energetic and ecological perspective. *American Journal of Primatology*, *74*, 395–407.

Napier, J. R., & Walker, A. C. (1967). Vertical clinging and leaping—A newly recognized category of locomotor behavior of primates. *Folia Primatologica*, *6*, 204–219.

Ni, X., Gebo, D. L., Dagosto, M., Meng, J., Tafforeau, P., Flynn, J. J., & Beard, K. C. (2013). The oldest known primate skeleton and early haplorhine evolution. *Nature*, *498*, 60–64.

Niemitz, C. (1984). Locomotion and posture of *Tarsius bancanus*. In: C. Niemitz (Ed.), *Biology of tarsiers* (pp. 191–225). Stuttgart, Germany: Gustav Fischer Verlag.

Orme, C. D. L., Freckleton, R. P., Thomas, G. H., Petzoldt, T., Fritz, S. A., Isaac, N., & Pearse, W. (2012). caper: Comparative analysis of phylogenetics and evolution in R. R package version 0.5.

Pagel, M., & Meade, A. (2013). BayesTraits v2 manual. Reading: Department of Animal and Microbial Sciences, University of Reading.

Pozzi, L., Hodgson, J. A., Burrell, A. S., Sterner, K. N., Raaum, R. L., & Disotell, T. R. (2014). Primate phylogenetic relationships and divergence dates inferred from complete mitochondrial genomes. *Molecular Phylogenetics and Evolution*, *75*, 165–183.

Rambaut, A., & Drummond, A. (2009). Tracer, version 1.6, MCMC trace analysis package.

Rasoazanabary, E. (2010). *The human factor in mouse lemur (Microcebus griseorufus) conservation: Local resource utilization and habitat*

disturbance at Beza Mahafaly, SW Madagascar [dissertation]. Amherst: University of Massachusetts.

Roberts, M., & Cunningham, B. (1986). Space and substrate use in captive Western tarsiers (*Tarsius bancanus*). *International Journal of Primatology*, *7*, 113–130.

Roberts, T. E., Lanier, H. C., Sargis, E. J., & Olson, L. E. (2011). Molecular phylogeny of treeshrews (Mammalia: Scandentia) and the timescale of diversification in Southeast Asia. *Molecular Phylogenetics and Evolution*, *60*, 358–372.

Rose, K. D., Chester, S. G. B., Dunn, R. H., Boyer, D. M., & Bloch, J. I. (2011). New fossils of the oldest North American euprimate *Teilhardina brandti* (Omomyidae) from the Paleocene-Eocene Thermal Maximum. *American Journal of Physical Anthropology*, *146*, 281–305.

Rose, K. D., Rana, R. S., Sahni, A., Kumar, K., Missiaen, P., Singh, L., & Smith, T. (2009). Early Eocene primates from Gujarat, India. *Journal of Human Evolution*, *56*, 366–404.

Sargis, E. J. (2002). The postcranial morphology of *Ptilocercus lowii* (Scandentia, Tupaiidae): an analysis of primatomorphan and volitantian characters. *Journal of Mammalian Evolution*, *9*, 137–160.

Sargis, E. J. (2004). New views on tree shrews: The role of tupaiids in primate supraordinal relationships. *Evolutionary Anthropology: Issues, News, and Reviews*, *13*, 56–66.

Sargis, E. J., Boyer, D. M., Bloch, J. I., & Silcox, M. T. (2007). Evolution of pedal grasping in Primates. *Journal of Human Evolution*, *53*, 103–107.

Schultz, A. (1963). Relations between the lengths of the main parts of the foot skeleton in primates. *Folia Primatologica*, *1*, 150–171.

Seiffert, E. R., Costeur, L., & Boyer, D. M. (2015). Primate tarsal bones from Egerkingen, Switzerland, attributable to the middle Eocene adapiform *Caenopithecus lemuroides*. *PeerJ*, *3*, e1036.

Seiffert, E. R., & Simons, E. L. (2001). Astragalar morphology of late Eocene anthropoids from the Fayum Depression (Egypt) and the origin of catarrhine primates. *Journal of Human Evolution*, *41*, 577–605.

Shapiro, L. J., Kemp, A. D., & Young, J. W. (2016). Effects of substrate size and orientation on quadrupedal gait kinematics in mouse lemurs (*Microcebus murinus*). *Journal of Experimental Zoology*, *325*, 329–343.

Smith, F. A., Lyons, S. K., Ernest, S. K. M., Jones, K. E., Kaufman, D. M., Dayan, T., … Haskell, J. P. (2003). Body mass of Quaternary mammals. *Ecology*, *84*, 3403.

Smith, R. J., & Jungers, W. L. (1997). Body mass in comparative primatology. *Journal of Human Evolution*, *32*, 523–559.

Springer, M. S., Meredith, R. W., Gatesy, J., Emerling, C. A., Park, J., Rabosky, D. L., … Murphy, W. J. (2012). Macroevolutionary dynamics and historical biogeography of primate diversification inferred from a species supermatrix. *PLoS One*, *7*, e49521.

Stevens, N. (2008). The effect of branch diameter on primate gait sequence pattern. *American Journal of Primatology*, *70*, 356–362.

Strait, D. S., & Grine, F. E. (2004). Inferring hominoid and early hominid phylogeny using craniodental characters: The role of fossil taxa. *Journal of Human Evolution*, *47*, 399–452.

Sussman, R. W. (1991). Primate origins and the evolution of angiosperms. *American Journal of Primatology*, *23*, 209–223.

Sussman, R. W., Rasmussen, D. T., & Raven, P. H. (2013). Rethinking primate origins again. *American Journal of Primatology*, *75*, 95–106.

Szalay, F. S. (1976). Systematics of the Omomyidae (Tarsiiformes, Primates) taxonomy, phylogeny, and adaptations. *Bulletin of the American Museum of Natural History*, *156*, 1–294.

Szalay, F. S. (2007). Ancestral locomotor modes, placental mammals, and the origin of euprimates: Lessons from history. In: M. J. Ravosa & M. Dagosto (Eds.), *Primate origins—adaptations and evolution* (pp. 457–487). New York: Springer.

Szalay, F. S., & Dagosto, M. (1980). Locomotor adaptations as reflected on the humerus of Paleogene primates. *Folia Primatologica*, *34*, 1–45.

Szalay, F. S., & Dagosto, M. (1988). Evolution of hallucial grasping in the primates. *Journal of Human Evolution*, *17*, 1–33.

Szalay, F. S., & Decker, R. L. (1974). Origins, evolution, and function of the tarsus in the late Cretaceous Eutheria and Paleocene Primates. In: F. A. Jenkins (Ed.), *Primate locomotion* (pp. 223–259). New York: Academic Press.

Szalay, F. S., & Drawhorn, G. (1980). Evolution and diversification of the Archonta in an arboreal milieu. In: W. P. Luckett (Ed.), *Comparative biology and evolutionary relationships of tree shrews* (pp. 133–169). New York: Plenum Press.

Tacutu, R., Craig, T., Budovsky, A., Wuttke, D., Lehmann, G., Taranukha, D., … de Magalhães, J. P. (2013). Human ageing genomic resources: Integrated databases and tools for the biology and genetics of ageing. *Nucleic Acid Research*, *41*, D1027–D1033.

Tornow, M. A. (2008). Systematic analysis of the Eocene primate family Omomyidae using gnathic and postcranial data. *Bulletin of the Peabody Museum of Natural History*, *49*, 43–129.

Toussaint, S., Herrel, A., Ross, C. F., Auard, F., & Pouydebat, E. (2015). Substrate diameter and orientation in the context of food type in the gray mouse lemur, *Microcebus murinus*: Implications for the origins of grasping in primates. *International Journal of Primatology*, *36*, 583–604.

Visualization Sciences Group. (2014). Avizo 8.1. Burlington, MA: Mercury Computer Systems.

White, J. L., & Gebo, D. L. (2004). Unique proximal tibial morphology in strepsirrhine primates. *American Journal of Primatology*, *64*, 293–308.

White, T. D., & Folkens, P. A. (2010). *The human bone manual*. Amsterdam: Elsevier.

Winchester, J. M., Boyer, D. M., Cooke, S. E., St. Clair, E. M., Ledogar, J. A., & Gosselin-Ildari, A. D. (2014). Dental topography of platyrrhines and prosimians: Convergence and contrasts. *American Journal of Physical Anthropology*, *153*, 29–44.

Wunderlich, R. E., Simons, E. L., & Jungers, W. L. (1996). New pedal remains of Megaladapis and their functional significance. *American Journal of Physical Anthropology*, *100*, 115–138.

Yapuncich, G. S., & Boyer, D. M. (2014). Interspecific scaling patterns of talar articular surfaces within Euarchonta. *Journal of Anatomy*, *224*, 150–172.

Yapuncich, G. S., Gladman, J. T., & Boyer, D. M. (2015). Predicting euarchontan body mass: A comparison of tarsal and dental variables. *American Journal of Physical Anthropology*, *157*, 472–506.

SUPPORTING INFORMATION

Additional Supporting Information may be found in the online version of this article.

How to cite this article: Yapuncich GS, Seiffert ER, Boyer DM. Quantification of the position and depth of the *flexor hallucis longus* groove in euarchontans, with implications for the evolution of primate positional behavior. *Am J Phys Anthropol*. 2017;00:000–000. https://doi.org/10.1002/ajpa.23213